UNIVERSITY OF CALIFORNIA, SAN DIEGO

Regulation of Mammalian Metabolism by Facilitated Transport Across the Inner Mitochondrial Membrane

A dissertation submitted in partial satisfaction of the requirements for the degree of Doctor of Philosophy

in

Bioengineering

by

Nathaniel Martin Vacanti

Committee in charge:

Professor Christian M. Metallo, Chair
Professor Pedro Cabrales
Professor Terence Hwa
Professor Anne N. Murphy
Professor Shankar Subramaniam

2015

The dissertation of Nathaniel Martin Vacanti is approved, and it is acceptable in quality and form for publication on microfilm and electronically:

Chair

University of California, San Diego

2015

DEDICATION

I dedicate this dissertation to my father, Martin; my mother, Elizabeth; my sister, Bridgette; and my brother Lucas.

I cannot thank my parents enough for the work they have done and the sacrifices they have made to give me this opportunity; I can only hope to make the most of it.

I am blessed to have an older sister who has always been there for me and I know always will be. I aspire to become as tough and insightful as Bridgette.

Lucas is unwavering in his loyalty and commitment. I am proud to call him my brother.

They are all role models and inspirations.

TABLE OF CONTENTS

LIST OF FIGURES

LIST OF TABLES

ACKNOWLEDGEMENTS

I thank the chair of my dissertation committee, Professor Christian M. Metallo, for his guidance throughout my career as a Ph.D. student. I owe all of my success at UCSD to his mentorship and will take the lessons learned in his laboratory wherever I go. I thank the members of the Metallo Lab including, Dr. Hui "Sunny" Zhang, Dr. Martina Wallace, Dr. Thekla Cordes, Dr. Le You, Seth J. Parker, Mehmet G. Badur, Courtney R. Green, and Christopher S. Ahn for their help and support. I also thank Dr. Anne N. Murphy and Dr. Ajit S. Divakaruni for their invaluable guidance.

Chapter 1, in full, is a reprint of the material as it appears in "Exploring metabolic pathways that contribute to the stem cell phenotype", Biochimica et Biophysica Acta, vol. 1830, 2013. Nathaniel M. Vacanti is the primary author of this publication. The material in Chapter 2 is currently being prepared for submission for publication. Nathaniel M. Vacanti is the primary author and Christian M. Metallo is a co-author of this material. Chapter 3, in full, is a reprint of the material as it appears in "Regulation of Substrate Utilization by the Mitochondrial Pyruvate Carrier", Molecular Cell, vol. 56, 2014. Nathaniel M. Vacanti is the primary author of this publication. The material in Chapter 4 is currently being prepared for submission for publication. Nathaniel M. Vacanti is the primary author and Ajit S. Divakaruni, Anne N. Murphy, and Christian M. Metallo are co-authors of this material.

VITA

Education

University of California, San Diego
La Jolla, CA
Ph.D. Bioengineering
September, 2015

Massachusetts Institute of Technology
Cambridge, MA
M.S. Chemical Engineering
June, 2010

University of Connecticut
Storrs, CT
B.S. Chemical Engineering
Minor Biomedical Engineering
May, 2008

Peer-Reviewed Publications

Vacanti NM, Divakaruni AS, Green CR, Parker SJ, Henry RR, Ciaraldi TP, Murphy AN, Metallo CM, Regulation of Substrate Utilization by the Mitochondrial Pyruvate Carrier. Molecular Cell. 2014.

Vacanti NM, Metallo CM, Exploring Metabolic Pathways that Contribute to the Stem Cell Phenotype, Biochimica et Biophysica Acta - General Subjects. 2012.

Vacanti NM, Cheng H, Hill PS, Guerreiro JD, Dang TT, Ma M, Watson S, Hwang NS, Langer RS, Anderson DG, Localized Delivery of Dexamethasone From Electrospun Fibers Reduces the Foreign Body Response. Biomacromolecules. 2012.

Cheng H, Hill PS, Siegwart DJ, Vacanti N, Lytton-Jean AK, Cho SW, Ye A, Langer R, Anderson DG, A Novel Family of Biodegradable Poly(ester amide) Elastomers. Advanced Materials. 2011.

Ditlev JA, Vacanti NM, Novak IL, Loew LM, An Open Model of Actin Dendritic Nucleation. Biophysical Journal. 2009.

Oral Presentations

Vacanti NM (speaker), Divakaruni AS, Green CR, Murphy AN, Metallo CM. Mitochondrial Transport Regulates Nutrient Utilization. Science for Life Laboratories Special Seminar, Invited

Speaker. Karolinska Institutet, Stockholm, Sweden. June 9th, 2015.

Vacanti NM (speaker), Divakaruni AS, Green CR, Murphy AN, Metallo CM. Mitochondrial Transport Regulates Nutrient Utilization. Friends of Cells Data Club. University of California, San Diego. La Jolla, CA. March 20th, 2015.

Divakaruni AS (speaker), Vacanti NM, Andreyev AY, Ciaraldi TP, Metallo CM, Murphy AN. Inibition of the Mitochondrial Pyruvate Carrier Potentiates Metabolic Flexibility. Abcam Mitochondria, Energy Metabolism and Cancer Meeting. University College London, England. February 26, 2014.

Vacanti NM (speaker), Divakaruni AS, Murphy AN, Metallo CM. Control of Mitochondrial Substrate Utilization by the Mitochondrial Pyruvate Carrier. American Institute of Chemical Engineers Annual Meeting. San Francisco, CA. November 3-8, 2013.

Poster Presentations

Divakaruni AS, Andreyev AY, Vacanti NM, Ciaraldi TP, Metallo CM, Murphy AN. Mild Inhibition of the Mitochondrial Pyruvate Carrier is Neuroportective and Potentiates Metabolic Flexibility. Society for Neuroscience Annual Meeting. San Diego, CA. November 9-13, 2013.

Vacanti NM, Metallo CM. Regulation of Metabolism in Heart Disease. UCSD Jacobs School of Engineering Research Expo. La Jolla, CA. April 18, 2013.

Vacanti NM, Parker SJ, Metallo CM. Understanding Metabolic Function and Regulation in Stem Cells and Tumors. UCSD Jacobs School of Engineering Research Expo. La Jolla, CA. April 12, 2012.

ABSTRACT OF THE DISSERTATION

Regulation of Mammalian Metabolism by Facilitated Transport Across the Inner Mitochondrial Membrane

by

Nathaniel Martin Vacanti

Doctor of Philosophy in Bioengineering

University of California, San Diego, 2015

Professor Christian M. Metallo, Chair

The enzymes and reactions of the metabolic network provide cells with a means to utilize the energy stored in substrate chemical bonds and to rearrange those bonds to form biosynthetic building blocks. The chapters of this dissertation are all independent bodies of work exploring how the metabolic network influences and regulates cellular function or dysfunction. Chapter 1, titled "Exploring Metabolic Pathways that Contribute to the Stem Cell Phenotype", is a case study on how the metabolic network exerts control over, or is perturbed by the cellular phenotype, specifically the stem cell phenotype. Substrate and pathway utilization along with molecular signals altering metabolism are key regulators of the stem cell phenotype and influence differentiation status. Chapter 2, titled "Inner Mitochondrial Membrane Transport

Regulates Cellular Function" explores an under-appreciated node of metabolic regulation: substrate transport across the inner mitochondrial membrane. Mitochondria are the powerhouses of cells, supplying energy in the form of adenosine triphosphate and crucial building blocks for biosynthesis. Therefore communication with the cytosol *via* molecular transport exerts exquisite control over the metabolic network. This chapter examines the proteins responsible for molecular exchange across the inner mitochondrial membrane with a focus on their regulatory effects and the methodologies used to investigate them. Many of the highlighted studies examine these transport proteins in isolation, and much work remains on elucidating their full influence over cellular function. Chapter 3, titled "Regulation of Substrate Utilization by the Mitochondrial Pyruvate Carrier" examines how mitochondrial pyruvate transport across the inner mitochondrial membrane influences substrate and pathway utilization. Employing ^{13}C tracing allows the regulatory effects of the mitochondrial pyruvate carrier to be examined in whole-cell systems, elucidating their altered reliance on fatty acids and amino acids as fuels and biosynthetic precursors. Finally, Chapter 4, titled "Identification of a Mitochondrial Glutamine Carrier" applies ^{13}C tracing to solve the inverse problem. The effects on the metabolic network of inhibiting a mitochondrial carrier are used to deduce its substrate. This previously unannotated carrier is found to transport glutamine across the inner mitochondrial membrane.

Chapter 1

Exploring Metabolic Pathways that Contribute to the Stem Cell Phenotype

Abstract

Background: Stem cells must negotiate their surrounding nutritional and signaling environment and respond accordingly to perform various functions. Metabolic pathways enable these responses, providing energy and biosynthetic precursors for cell proliferation, motility, and other functions. As a result, metabolic enzymes and the molecules which control them are emerging as attractive targets for the manipulation of stem cells. To exploit these targets a detailed characterization of metabolic flux regulation is required.

Scope of Review: Here we outline recent advances in our understanding of metabolism in pluripotent stem cells and adult progenitors. We describe the regulation of glycolysis, mitochondrial metabolism, and the redox state of stem cells, highlighting key enzymes and transcription factors involved in the control of these pathways.

Major Conclusions: A general description of stem cell metabolism has emerged, involving increased glycolysis, limited oxidative metabolism, and resistance to oxidative damage. Moving forward, the application of systems-based approaches to stem cells will help shed light on metabolic pathway utilization in proliferating and quiescent stem cells.

General Significance: Metabolic flux contributes to the unique properties of stem cells and progenitors. This review provides a detailed overview of how stem cells metabolize their surrounding nutrients to proliferate and maintain lineage homeostasis.

Introduction

Over the last several decades our view of cellular phenotypes within tissues has changed dramatically. With the identification and characterization of stem cells and progenitors, we now appreciate the heterogeneity that exists within a specific tissue, organ, or tumor. While individual cell types interact and support one another (*e.g.*, stroma and epithelia, glia and neurons), cells within the same lineage can also exhibit varied marker and gene expression patterns. For example, mammary cells can be sorted from normal tissue based on their $CD29^{lo}CD24^{+}$ or $CD24^{+}CD49^{+}$ expression status to obtain progenitors capable of regenerating mammary glands (Stingl et al., 2006; Shackleton et al., 2006). In the hematopoietic system, clusters of differentiation have been studied for some time, and researchers have long been able to isolate stem cell populations capable of lineage rescue (Spangrude et al., 1988; Bhatia et al., 1997). This concept has been extended to tumors as well; whereby researchers can isolate subpopulations of cancer cells that exhibit enhanced capacity to initiate tumors (*e.g.*, breast, glioblastoma, leukemia) (Diehn et al., 2009; Li et al., 2009; Wang and Dick, 2005). Breast cancer cells which are $CD44^{+}CD24^{lo/-}$ form tumors more readily when transferred to immunocompromised mice (Al-Hajj et al., 2003), and their gene expression signature correlates with a poor prognosis (Liu et al., 2007). Alternatively, aldehyde dehydrogenase (ALDH) enzyme activity or ALDH1 expression are associated with stem cell populations (Ginestier et al., 2007), though the metabolic consequences of this property are unclear. Finally, the ability to maintain embryonic stem cells (ESCs) in culture and induce pluripotency in somatic cells has provided researchers new tools to examine stem cell behavior (Thomson et al., 1998; Takahashi et al., 2007), as these cells can be studied effectively *in vitro* and share some (though not all) characteristics of progenitors *in vivo*. These systems are now helping us elucidate the metabolic phenotype of stem cells.

In the body, progenitor cells may take one of several fates: quiescence, proliferation

and self-renewal, transit amplification and terminal differentiation, or programmed cell death (Figure 1.1). The metabolic needs of cells change significantly as a function of their fate and function. This is particularly true for cells proliferating rapidly in culture, which require adenosine triphosphate (ATP), reducing equivalents, and biosynthetic intermediates to grow and divide (Vander Heiden et al., 2009). These requirements must be continually met through various metabolic pathways. The energetic and biosynthetic demands of quiescent cells are expected to be much lower than those of proliferating cells, though evidence suggests that these populations remain metabolically active (Lemons et al., 2010).

In addition to the internal needs of cells, exogenous cues influence both cellular fate and metabolic processes. The tissue microenvironment strongly influences the self-renewal and differentiation of stem cells of various origins. Indeed, the *in vivo* stem cell niche is thought to lie in regions of low oxygen (*i.e.*, hypoxia) (Mohyeldin et al., 2010). Such conditions induce stem cell-like gene expression patterns in cells and can improve the efficiency of induced pluripotent stem cell (iPSC) generation (Yoshida et al., 2009). Hypoxia itself is a profound regulator of metabolism (Metallo et al., 2012; Wise et al., 2011; Papandreou et al., 2006; Kim et al., 2006; Semenza, 2009). Alternatively, the physical and biochemical properties of extracellular matrices can influence the fate of mesenchymal stem cells (MSCs) and pluripotent stem cells (PSCs) (Saha et al., 2011; Anderson et al., 2004; Brafman et al., 2010). In other cell types loss of matrix contact results in significant metabolic defects that can result in cell death (Grassian et al., 2011; Schafer et al., 2009). Finally, growth factor signaling is required to maintain stem cells in the undifferentiated state *in vitro* (Feng et al., 2009; Dang et al., 2008; Maherali and Hochedlinger, 2008), and the pathways activated in stem cells are interconnected with metabolism, regulating nutrient uptake and driving flux through glycolysis (Rathmell et al., 2000; Vander Heiden et al., 2001). Therefore, the metabolic phenotype of a cell is intimately related to the functional programs it executes, both by necessity and as a result of extracellular signals.

As most *in vitro* model systems of stem cells are highly proliferative, the general characteristics of progenitors are bearing remarkable similarity to cancer cells and cancer stem cells (Ben-Porath et al., 2008; Wong et al., 2008). Given the metabolic needs of actively

dividing cells, these results are not surprising. These similarities are also likely due, in part, to regulatory molecules like hypoxia inducible factors (HIFs) and c-Myc, which are commonly activated in stem cells and tumors (see "Molecular Regulators of Metabolism and the Stem Cell Phenotype" section below). However, metabolic analyses must go deeper, and more detailed characterizations of stem cell metabolism are required to identify differentially regulated metabolic nodes for therapeutic targeting of "good" and "bad" stem cell populations. Such characterizations will require a combination of molecular and systems-based approaches (Quek et al., 2010; Zamboni, 2011). Additionally, as we attempt to engineer and cultivate stem cells for clinical use (King and Miller, 2007), a clearer understanding of how cell fate and metabolic processes are intertwined is required.

Here we review recent advances in our understanding of metabolic pathway utilization, or "flux", in progenitor cells and their derivatives. Using a collection of different methods and approaches, significant insights have been made regarding the function and regulation of glucose metabolism, mitochondrial function, redox metabolism, and lipid biology in stem cells. Where possible we highlight findings in pluripotent cell systems or *in vivo* stem cell populations, though some interesting and seemingly applicable metabolic traits of rapidly proliferating cells have been uncovered in cancer cell lines. Common threads also emerge between stem cells and cancer when considering the dual role of regulatory proteins such as c-Myc and HIFs in controlling properties of "stemness" and metabolic pathways. Much less attention has been paid to non-proliferating, quiescent cells, as the sorting required to access such populations complicates application of the most advanced methods for metabolic characterization. Such slow-cycling cells represent an interesting area of future study. Nevertheless, a picture is emerging which describes the metabolic phenotype of proliferating stem cells. While this image is likely to evolve significantly over the next decade, key discoveries discussed herein will frame the directions of future investigations.

Glucose Metabolism

The most commonly cited feature describing the metabolism of stem cells and most proliferating cells is their glycolytic phenotype. This designation stems from Otto Warburg's

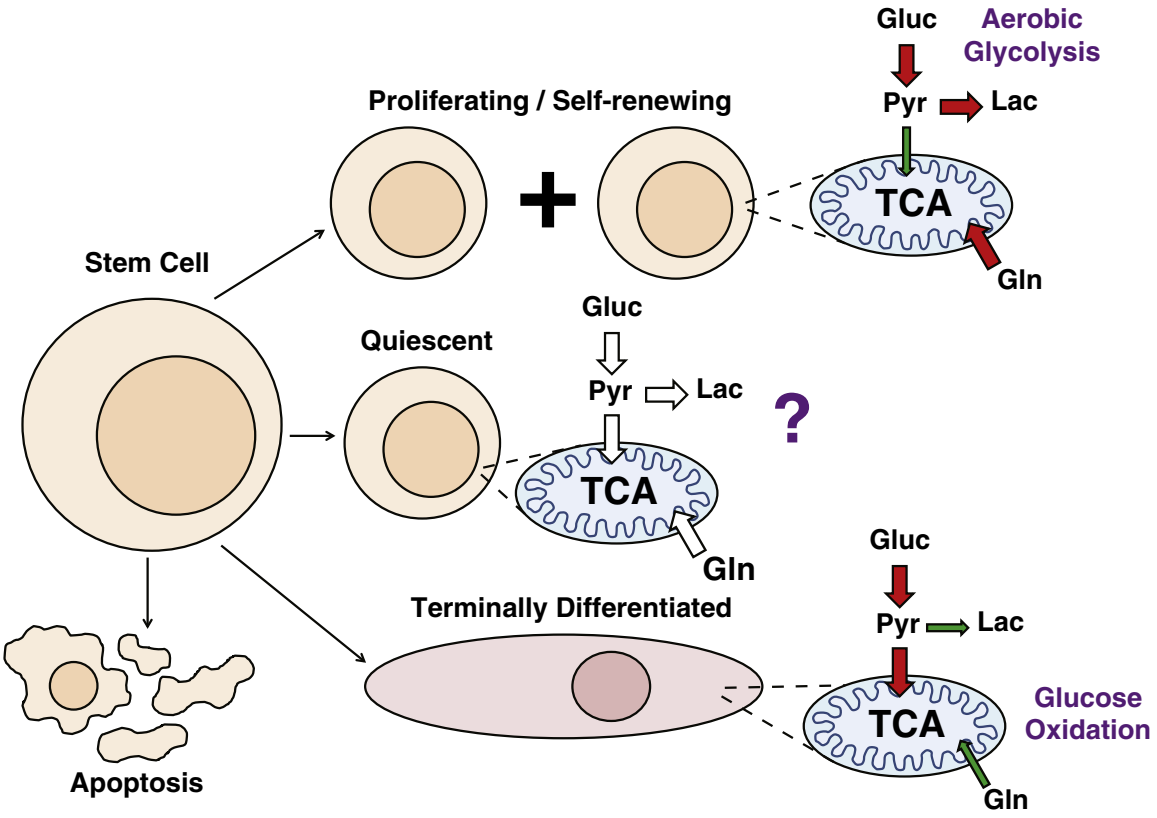

Figure 1.1: Stem Cell Fate Choices and Metabolic Phenotypes. In response to stimuli and cues, stem cells can enter a state of proliferation or self-renewal where they maintain a high glycolytic flux to support biosynthesis. Cells may also be directed to terminally differentiate where glucose oxidation supports energy generation in mitochondria. Alternatively, cells may undergo programmed cell death or exit the cell cycle and remain quiescent, a state where the relative metabolic fluxes are largely uncharacterized.

work in the early 20th century when he demonstrated that tumors and proliferating tissues undergo aerobic glycolysis, consuming high levels of glucose and diverting much of this carbon to lactate (Hsu and Sabatini, 2008). This phenomenon seems to apply to pluripotent cells in culture, which are typically maintained in a state of constant proliferation. Direct evidence of this glycolytic phenotype in stem cells has come in the form of enzyme levels and activities. Increased levels of hexokinase II were detected in human embryonic stem cells (hESCs) and iPSCs relative to teratoma-derived fibroblasts and the parental IMR90 fibroblasts used for reprogramming (Varum et al., 2011). The product of this reaction, glucose-6-phosphate (G6P), was present at elevated levels in human pluripotent cells relative to human foreskin fibroblasts when analyzed by tandem mass spectrometry (Prigione et al., 2011), providing additional evidence of increased glucose uptake and phosphorylation in stem cells.

Hexosamine Biosynthesis and the Pentose Phosphate Pathway

Upon phosphorylation by hexokinases (HKs), glucose is primarily directed toward three pathways: glycolysis, the hexosamine biosynthesis pathway (HBP), and the pentose phosphate pathway (PPP). While flux through glycolysis seems to be highest in proliferating stem cells, the latter pathways are very important for cell growth, but are less well-studied in stem cell systems. Hexosamine biosynthesis involves the acetyl coenzyme A (AcCoA) and glutamine-dependent conversion of fructose-6-phosphate to N-acetylglucosamine (GlcNAc) and other glycosaminoglycans (Figure 1.2). These metabolites serve as substrates for post-translational modification of glycoproteins and proteoglycan synthesis. In proliferating cells flux through the HBP is required to maintain glycosylation and surface expression of receptors, which in turn provide feedback signals to drive glutamine uptake (Wellen et al., 2010). Glycosylation *via* HBP is important for expression of various growth factor receptors, the activation of signaling cascades, and cellular differentiation (Lau et al., 2007). Flux through this pathway is presumably critical for stem cell populations which depend upon these signaling pathways to stimulate proliferation and regulate cell fate choices. Some studies have explored the role of glycobiology in ESCs, observing changes in levels of hyaluronan, chondroitin sulfate, and heparin sulfate (Nairn et al., 2007). Alternatively, forced induction of O-GlcNAcylation impaired the cardiac differentiation

of ESCs (Kim et al., 2009a). How the HBP contributes to undifferentiated stem cell growth and maintenance has yet to be investigated in detail.

The oxidative PPP is critical for supplying ribose to synthesize nucleotides and reducing equivalents in the form of nicotinamide adenine dinucleotide phosphate (NADPH) in proliferating cells (Figure 1.2). While flux through the non-oxidative PPP can also generate ribose carbon, NADPH is regenerated in the cytosol for reductive biosynthesis by glucose-6-phosphate dehydrogenase (G6PD) and phosphogluconate dehydrogenase (PGD) in the oxidative pathway only. As discussed in the "Redox Metabolism" section, the redox state is particularly important in stem cell populations, and NADPH helps regulate the abundance of oxidative species by maintaining glutathione (GSH) in the reduced state (*via* glutathione reductase). Cells from G6PD-deficient patients and mouse embryonic stem cells (mESCs) with *G6PD*-deleted are viable, but exhibit increased sensitivity to oxidative treatments (Fico et al., 2004; Efferth et al., 1995). Interestingly, this deficiency seems to influence ESC differentiation, preferentially inducing cells toward the endodermal lineage (Manganelli et al., 2012). While the high glycolytic flux described in pluripotent cells would be expected to enhance flux through the PPP, few direct investigations on regulation of this pathway in stem cells have been completed. Given the growing importance of redox metabolism in stem cells and progenitors, analysis of PPP regulation is expected to be a high priority.

Glycolysis

The majority of glucose carbon which enters proliferating cells is secreted as lactate, and this phenomenon occurs in human pluripotent cells as well. hESCs and iPSCs exhibit decreased oxygen consumption and increased acidification of media (used as a surrogate for lactate production) relative to their more differentiated counterparts (Varum et al., 2011; Folmes et al., 2011; Zhang et al., 2011; Panopoulos et al., 2012), providing evidence for this phenotype. The use of mitochondrial respiratory chain inhibitors in pluripotent cells suggests that much of their ATP is derived from glycolysis (Varum et al., 2011). Elevated glycolytic flux and enzyme activities of glyceraldehyde-3-phosphate dehydrogenase (GAPDH), phosphoglycerate kinase (PGK), phosphoglycerate mutase (PGAM), and enolase (ENO), have been observed in

mESCs relative to mouse embryonic fibroblasts (MEFs) (Kondoh et al., 2007). Intriguingly, Beach and colleagues were previously able to demonstrate that overexpression of PGAM or other glycolytic enzymes (*e.g.*, phosphohexose isomerase, PHI; PGK) could increase cellular lifespan and prevent senescence in MEFs, suggesting that glycolytic flux itself can influence cell fate (Kondoh et al., 2005). However, the mechanism of this phenomenon has yet to be elucidated.

Transcriptional analyses of pluripotent cells and their derivatives support the observations described above, as numerous studies have indicated that glycolytic genes are expressed at higher levels in pluripotent stem cells compared to more differentiated cells (Varum et al., 2011; Panopoulos et al., 2012; Prigione and Adjaye, 2010). Furthermore, the gene expression profile of proliferating *versus* differentiating mESCs correlates with fluxes calculated from a stoichiometric model of central carbon metabolism (Sepúlveda et al., 2010). Notably, key transcription factors that are active in stem cell populations and cancer cells are c-Myc and HIFα proteins, both of which target glycolytic genes and promote flux through this pathway ("Molecular Regulators of Metabolism and the Stem Cell Phenotype" section) (Dang et al., 2008; Gordan et al., 2007b; Das et al., 2012). Furthermore, when comparing PSCs to somatic cell types, Panopoulos et al. (2012) identified many differentially methylated genes that encode enzymes involved in glycolysis, including several aldehyde dehydrogenases, *ENO*, *GAPDH*, *HKs*, pyruvate kinase (*PKM2*), lactate dehydrogenases (*LDHB*, *LDHC*), and others. These results suggest that the epigenetic status of cells influences metabolic gene expression and pathway activity.

The final, ATP-generating, enzymatic step in glycolysis is catalyzed by pyruvate kinase and encoded by the *PKM2* gene in cells outside of the erythroid and hepatocyte lineages (which use the *PKLR* gene). Differential splicing of *PKM2* exons 9 and 10 gives rise to the M1 (PKM1) and M2 (PKM2) isoforms, respectively; the latter of which is specifically expressed during embryonic development and in tumor cells (Mazurek et al., 2005; Jurica et al., 1998). Although expression of PKM2 is associated with higher glycolytic activity and the Warburg effect in tumors, the activity of this enzyme is lower than that of PKM1 and is decreased upon binding to phosphotyrosine peptides (Christofk et al., 2008). Some evidence suggests that decreased PKM2 activity may facilitate flux of glycolytic carbon toward biosynthetic pathways such as

the oxidative PPP and serine biosynthesis in cancer cells (Ye et al., 2012). Although PKM2 is specifically expressed in embryonic cells (Jurica et al., 1998), the role of PKM2 in maintaining or regulating stem cell function has yet to be determined.

In order for cells to maintain a high flux through glycolysis, nicotinamide adenine dinucleotide (NAD^+) must be regenerated to resupply NADH for the GAPDH reaction. Highly proliferative stem and cancer cells meet this need by converting pyruvate to lactate at high rates using lactate dehydrogenase (LDH), a tetrameric enzyme encoded by several genes (A, B, and C) expressed in different combinations in various tissues. The B and C isoforms of LDH are known to be transcribed at high levels in pluripotent cells (Folmes et al., 2011; Panopoulos et al., 2012). Meanwhile, LDH-A is highly expressed in tumors and induced by both hypoxia and c-Myc (Dang et al., 2008). How each isozyme functions differently in stem cells and cancer is not clear, though post-translational modifications of enzymes may provide a means of regulating their localization, activity, and responsiveness to exogenous signals (Fan et al., 2011). Nevertheless, high LDH expression facilitates diversion of glucose carbon away from oxidative metabolism in proliferating cells, a phenomenon observed both in pluripotent stem cells and proliferating cancer cell lines.

Serine and glycine can be taken up by cells but also synthesized from the glycolytic intermediate 3-phosphoglycerate (3PG) (Figure 1.2). These amino acids are important precursors for the biosynthesis of purines, glutathione, and lipid headgroups. Notably, metabolism of serine by serine hydroxymethyltransferases (SHMTs) generates glycine and one carbon units for the folate pool. These metabolites are critical for nucleotide synthesis and may also be used to regenerate methionine, which provides substrates for methylation *via* s-adenosyl methionine. Pathways converging on serine and glycine have received increasing attention in the cancer community due to their roles in biosynthesis, redox metabolism, and methylation (Sreekumar et al., 2009; Possemato et al., 2011; Locasale et al., 2011; Zhang et al., 2012). The enzymes and metabolites within this pathway are likely to emerge as key players that are regulated during stem cell differentiation, though specific results generated in pluripotent and multipotent cell populations are lacking.

An overriding goal in understanding the metabolic phenotype of stem cells is to exploit

this information to improve control over cell fates. To this end several groups have attempted to modulate reprogramming efficiency of human fibroblasts to iPS cells by treatment with compounds that inhibit or stimulate glycolytic metabolism. Inhibition of glucose uptake or glycolytic enzyme activity using 2-deoxyglucose or 3-bromopyruvate, respectively, decreased pluripotent cell growth and reprogramming, which is perhaps not surprising given the need for glycolysis during proliferation (Folmes et al., 2011; Panopoulos et al., 2012). Intriguingly, stimulation of glycolytic activity with fructose-6-phosphate or fructose-2,6-bisphoshate can significantly enhance iPSC colony formation (Panopoulos et al., 2012; Zhu et al., 2010). On the other hand, knockdown of PGK induces differentiation in mouse C2C12 myoblasts (Bracha et al., 2010), indicating that direct manipulation of glycolysis can modulate the stem cell phenotype. These exciting results now raise the question of how glycolytic flux or metabolites alone can mediate the stem cell phenotype, as the specific mechanism remains unknown.

Mitochondria and Tricarboxylic Acid Metabolism

Mitochondria are a hub of metabolic activity in eukaryotic cells, executing metabolic reactions which are absolutely required for autonomous cell growth. The tricarboxylic acid (TCA) cycle generates reducing equivalents which are consumed during oxidative phosphorylation (OXPHOS) to efficiently produce ATP for cellular processes. The main entry point for glycolytic carbon in the TCA cycle is the pyruvate dehydrogenase (PDH) complex, which oxidizes pyruvate to generate AcCoA and CO_2. AcCoA in the mitochondria condenses with oxaloacetate to form citrate and is subsequently metabolized further or directed to the cytosol to supply carbon for lipid biosynthesis (Figure 1.2).

As proliferating cells increase flux through glycolysis, glucose-derived carbon is directed away from oxidation by PDH (Vander Heiden et al., 2009). This enzyme complex is highly regulated by cofactors, allosteric interactions, and post-translational modifications, and PDH activity is directly controlled by PDH kinases (PDKs), which phosphorylate and inactivate the enzyme. PDH phosphorylation and PDK1 levels were observed to be elevated in human pluripotent cells compared to terminally differentiated fibroblasts (Varum et al., 2011), which is expected to de-

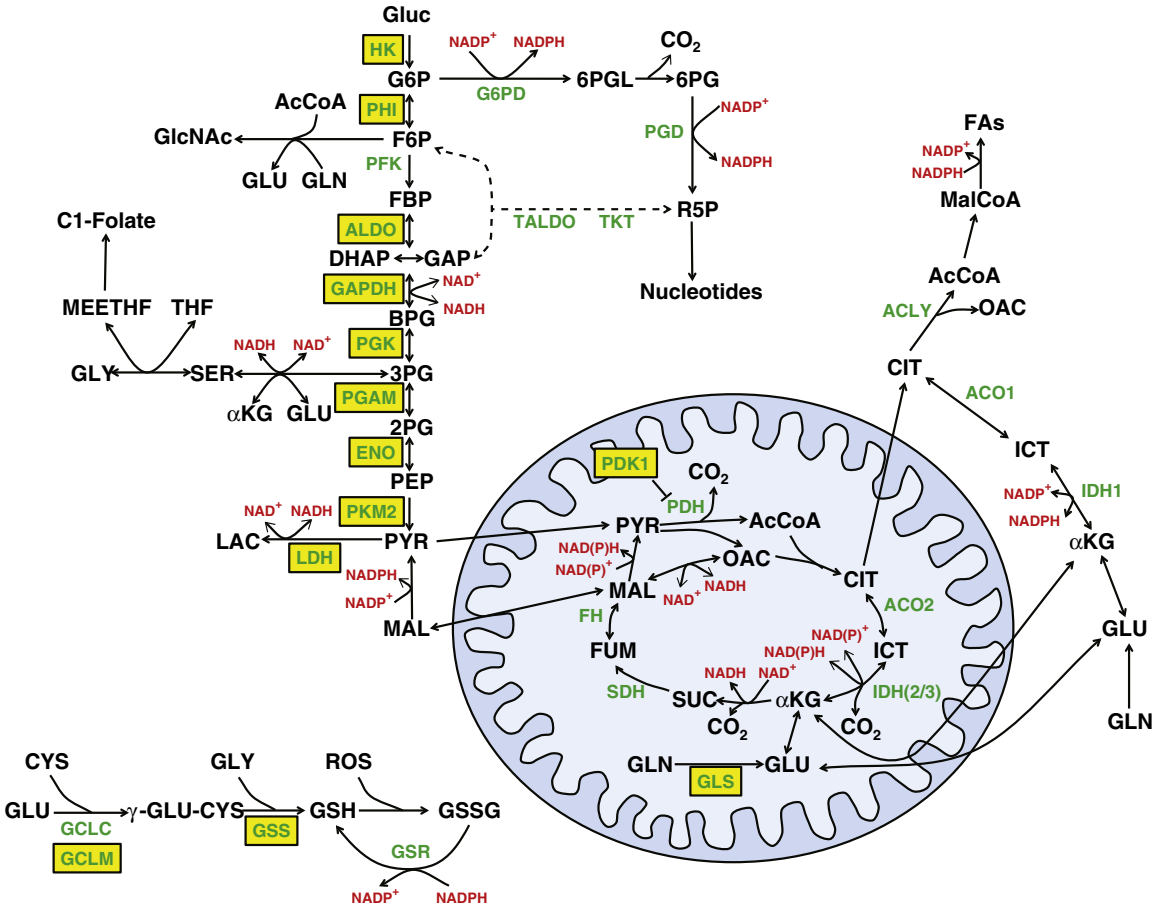

Figure 1.2: Metabolic Pathways that are Regulated to Support Stem Cell Growth. Glucose taken up by cells is phosphorylated by HKs and metabolized in glycolysis, the hexosamine biosynthesis pathway, or the pentose phosphate pathway. Glucose-derived pyruvate is either diverted to lactate or oxidize in the TCA cycle to support energy generation in mitochondria or biosynthesis in the cytosol. Reduced glutathione is synthesized from glutamate, cysteine, and glycine and protects cells from oxidative damage by reacting with ROS. Enzymes which are differentially regulated in stem cell populations are highlighted in yellow.

crease oxidation of glucose carbon in the TCA cycle. This result has led to the general conclusion that pluripotent stem cells exhibit limited oxygen consumption, which has been supported by oxygen measurements in numerous stem cell model systems (Varum et al., 2011; Zhang et al., 2011). Additionally, numerous studies have observed decreased expression of genes involved in OXPHOS, differentially methylated genes along this pathway, and lower levels of complex I subunits (Varum et al., 2011; Prigione et al., 2011; Panopoulos et al., 2012). This phenotype is also supported by metabolomics experiments in which the abundances of TCA intermediates such as AcCoA, citrate, glutamate, and malate were decreased in ESCs and iPSCs compared to somatic cells (Panopoulos et al., 2012). Additionally, reprogramming of cells in the presence of dichloroacetate, an inhibitor of PDK activity, decreases pluripotent colony formation (Folmes et al., 2011). Treatment would be expected to increase pyruvate entry into the mitochondria and downstream TCA metabolism, which seems to be antagonistic toward the pluripotent state. Anaplerotic pathways such as glutaminolysis and pyruvate carboxylase are often necessary to maintain flux through the TCA cycle, and glutamine is a particularly important substrate for proliferating mouse ESCs (Fernandes et al., 2010). However, the utilization of these pathways must be more thoroughly explored in stem cells, as cancer cells in hypoxic microenvironments or those with diminished oxidative mitochondrial activity are more reliant on glutamine consumption (Metallo et al., 2012; Wise et al., 2011; Mullen et al., 2012; Scott et al., 2011).

More recently, Zhang et al. (2011) identified a role for uncoupling protein 2 (UCP2) in maintaining the energetic state of human iPSCs. By forcing expression during differentiation or knocking down endogenous expression in undifferentiated cells, they were able to perturb the switch toward oxidative metabolism during retinoic acid-induced differentiation. In addition to measuring oxygen consumption and extracellular acidification, the authors utilized stable isotope tracers and mass spectrometry to investigate TCA metabolism. By quantifying the incorporation of uniformly ^{13}C-labeled [U-$^{13}C_6$]glucose atoms into the glutamate pool, they observed that glucose oxidation decreases in hESCs upon differentiation with retinoic acid, and this effect was exacerbated upon forced expression of UCP2 during differentiation. The authors noted that hESCs do in fact exhibit oxidative mitochondrial metabolism, an active respiratory chain, and can consume oxygen at maximum capacity.

Another means of quantifying the relative metabolic rate of mitochondria is the mitochondrial membrane potential ($\Delta\psi_m$), which can be measured *via* fluorescence of tetramethylrhodamine methyl ester (Schieke et al., 2006). To understand the functional relevance of this readout, mESCs were sorted into populations of high and low $\Delta\psi_m$, and their metabolic profile and behavior were examined. Although the two populations were indistinguishable with respect to pluripotency marker expression, cells with high $\Delta\psi_m$ exhibited both elevated oxygen consumption and lactate secretion (Schieke et al., 2008). Furthermore, sorted populations of high $\Delta\psi_m$ mESCs formed much larger teratomas when implanted into mice, suggesting that the metabolic state of the cells' mitochondria influences *in vivo* growth potential.

Other amino acid and TCA-associated metabolic reactions have also been implicated in stem cell maintenance or differentiation. Specific point mutations in $NADP^+$-dependent isocitrate dehydrogenases 1 and 2 are associated with glioblastoma and acute myeloid leukemia (Dang et al., 2009; Ward et al., 2010). These changes result in a gain-of-function phenotype, enabling the enzymes to reductively generate (R)2-hydroxyglutarate (2HG) from α-ketoglutarate (Dang et al., 2009). Recently these mutant enzymes have been shown to inhibit lineage-specific progenitor cell differentiation by modulating the activity of α-ketoglutarate-dependent demethylases (Lu et al., 2012). Along these lines, 2HG treatment has also been shown to promote iPSC colony formation during reprogramming (Zhu et al., 2010), highlighting a potential role for this metabolite in regulating stem cell differentiation. The TCA cycle also supplies AcCoA in the cytosol for lipogenesis and acetylation, and conditions of nutrient deprivation can cause this substrate to become limited. Such changes have been shown to subsequently affect differentiation processes in pre-adipocytes by perturbing histone acetylation (Wellen et al., 2009). Therefore, by regulating the supply of energy, charge, and biosynthetic precursors, mitochondria play key roles in driving and maintaining the stem cell phenotype.

Redox Metabolism

Reactive oxygen species (ROS), including hydrogen peroxide (H_2O_2), superoxide ($\cdot O_2$), and hydroxyl free radical ($\cdot OH$), are highly reactive forms of partially reduced molecular oxygen

(O_2). ROS are produced in small quantities under normal metabolic conditions, and acute inhibition of the electron transport chain or hypoxic environments lead to an increase in their generation (Chen et al., 2003; Guzy et al., 2005). Cells protect themselves from oxidative damage using various enzymes and metabolites, including GSH (Figure 1.2). *In vivo* and *in vitro* studies suggest that stem-like cells differentially regulate ROS levels and are protected from oxidative damage (Ogasawara and Zhang, 2009).

Several investigators have characterized pluripotent cells based on ROS levels, neutralizing enzymes, and oxidative damage (Prigione et al., 2010; Cho et al., 2006; Saretzki et al., 2004). hESCs and iPSCs had significantly lower levels of oxidatively modified proteins in comparison to mature fibroblasts, and these levels increased upon differentiation. Treatment of foreskin fibroblasts with H_2O_2 significantly increased levels of 8-hydroxy-2'-deoxyguanosine (8-OHdG), an oxidized derivative of the nucleotide guanosine, while 8-OHdG staining was nearly undetectable in both untreated and H_2O_2-treated iPSCs and ESCs. These results indicate that iPSCs and ESCs are more resistant to DNA damage by ROS than more differentiated cell types (Prigione et al., 2010). Additionally, lipid hydroperoxides, which are generated upon reaction of ROS with unsaturated fatty acids (Blair, 2001), were significantly lower in iPSCs and ESCs compared to fibroblasts, consistent with previous observations that the stem cells were subjected to less oxidative damage than the differentiated fibroblasts (Prigione et al., 2010). Interestingly, expression levels of antioxidant enzymes, including superoxide dismutase and glutathione peroxidase, were reduced in iPSCs and ESCs compared to differentiated fibroblasts supporting the hypothesis that ROS levels are lower due to decreased mitochondrial activity in the undifferentiated cells (Prigione et al., 2010). However the underlying mechanisms resulting in the added resistance of pluripotent cells to oxidative stress remain unclear.

The regulation of ROS influences both embryonic (Cho et al., 2006; Guo et al., 2004; Sauer et al., 2000) and adult (Vieira et al., 2011; Owusu-Ansah and Banerjee, 2009; Wang et al., 2007; Kanda et al., 2011; Tormos et al., 2011) stem cell differentiation. In ESCs the DNA binding affinity of Oct-4 was reduced by the oxidizing agent, diamide, and restored by the antioxidant enzyme, thioredoxin (Guo et al., 2004). Embryoid body differentiation to cardiomyocytes was enhanced by incubation with H_2O_2, while antioxidants had the opposite effect (Sauer et al.,

2000). In adult progenitors, differentiation of human (Tormos et al., 2011) and rat (Kanda et al., 2011) MSCs into adipocytes was inhibited by the presence of antioxidants, but these effects were reversed in human MSCs by addition of H_2O_2 (Tormos et al., 2011). Additionally, neuronal differentiation of rat MSCs was mediated by phosphatidylcholine-specific phospholipase C through elevation of ROS derived from NADPH oxidase activity (Wang et al., 2007). These results collectively support the concept that ROS are important for differentiation and a reduced environment is conducive to "stemness".

Tumors contain cell populations which exhibit some similarities to adult progenitors and ESCs (Al-Hajj et al., 2003). Indeed, the redox status of "tumor-initiating cell" or "cancer stem cell" populations seems to play a role in the sensitivity of tumors to oxidative therapies (Ogasawara and Zhang, 2009). Diehn et al. (2009) isolated stem-like cell populations from human and murine mammary tumors using the $Lin^-CD44^+CD24^{-/low}$ marker. These cells exhibited decreased ROS levels and reduced levels of DNA damage after radiation treatment. More importantly, these cells preferentially survived irradiation in intact tumors. Gene expression analysis of the sorted population indicated that these cells expressed higher levels of mRNA encoding glutamate-cysteine ligase (GCLM) and glutathione synthetase (GSS). These enzymes mediate the synthesis of reduced GSH, which helps maintain the reduced state of cells and mitigates oxidative damage (Figure 1.2). A similar radioresistance phenotype has been demonstrated in $CD133^+$ glioma stem cells; in this case due to an enhanced DNA-damage response (Bao et al., 2006). Altogether, these results suggest that the ability to tightly control ROS levels and oxidative reactions is an important property of pluripotent cells, adult progenitors, and cancer stem cells.

Lipid Metabolism

To more generally characterize the metabolome of ESCs, Yanes et al. (2010) performed a non-targeted analysis of metabolites present in ESCs and more mature cell types. They detected many lipid molecules present at different levels in the ESCs compared to neurons and cardiomyocytes, and lipids upregulated in ESCs tended to be more oxidized. Additionally, inhibi-

tion of enzymes which metabolize unsaturated fatty acids to more complex eicosanoids (*e.g.*, Δ5 and Δ6 desaturases, cyclooxygenases, lipooxygenases) delayed differentiation, as determined by Oct4 and Nanog mRNA levels. In a separate study, unsaturated fatty acids such as arachidonic, linoleic, docosapentaenoic, and adrenic acid were present at elevated levels in ESCs compared to iPSCs, demonstrating that metabolic differences exist between pluripotent cell types (Panopoulos et al., 2012).

Various lipids and fatty acids can modulate the proliferation and differentiation of pluripotent stem cells and adult progenitors (Fehér and Gidáli, 1974; Kim et al., 2009b; Yun et al., 2009a), and albumin-associated lipids can promote self-renewal of hESCs (Garcia-Gonzalo and Belmonte, 2008). Cholesterol biosynthesis can also influence progenitor cell differentiation, as statins (inhibitors of cholesterol biosynthesis) were found to enhance differentiation of mouse C2C12 myoblasts (Bracha et al., 2010). Finally, prostaglandin E2 mediates effects in several cell types, including the regulation of EGF signaling in mESCs (Yun et al., 2009b), Wnt signaling and proliferation of hematopoietic stem cells (HSCs) (Fehér and Gidáli, 1974; Goessling et al., 2009; Hoggatt et al., 2009), and crypt stem cell survival following radiation (Cohn et al., 1997). Given the complexity of lipid metabolism in mammals, we have much to learn about the mechanisms through which these factors affect different cell types. However, these findings provide strong evidence that lipid metabolism influences stem cell fate (Das, 2011).

Molecular Regulators of Metabolism and the Stem Cell Phenotype

Although many of the mechanistic details regarding metabolic regulation have not been investigated directly in stem cells, several key factors involved in stem cell maintenance and reprogramming are known to control metabolism. For example, the MYC oncogene has been used as a pluripotency factor in combination with Oct4, Klf4, and Sox2 to induce somatic cells into the pluripotent state, acting in part as a driver of the stem cell phenotype (Takahashi et al., 2007). This gene encodes the c-Myc transcription factor which regulates cell cycle progression, growth, and metabolic pathways. c-Myc drives expression of a large set of genes involved in biosynthetic processes, replication processes, and non-coding RNAs (Laurenti et al., 2009; Smith

et al., 2011). Direct targets include enzymes in glycolysis, the PPP, nucleotide synthesis, and amino acid metabolism. Furthermore, c-Myc controls heterogeneous nuclear ribonucleoproteins hnRNPA1 and hnRNPA2, which regulate splicing of *PKM2* mRNA to the M2 isoform (David et al., 2010). Intriguingly, PKM2 itself has recently been shown to interact with HIF-1α and directly phosphorylate Stat3 (often activated in stem cells) in the nucleus (Gao et al., 2012).

Both directly and due to the low oxygen tensions present in the stem cell niche (Mohyeldin et al., 2010), the HIFα transcription factors have been implicated in regulating the stem cell phenotype and are well known to control metabolic processes. Constitutively expressed HIFα proteins are hydroxylated on proline residues when oxygen and other nutrients are replete, resulting in proteasomal degradation of these proteins (Ivan et al., 2001; Jaakkola et al., 2001). In response to metabolic stress this prolyl hydroxylation reaction is inhibited, allowing HIFα subunits to interact with transcriptional co-activators in the nucleus. The network induced by HIF stabilization has been well studied and includes many direct targets in glycolysis, including *GLUT1/3*, *HKs*, *ALDO*, *PGK*, *ENO*, and *LDHA* (Semenza, 2009; Gordan et al., 2007b). These changes lead to significant transformation of metabolic pathway activity measured using gene expression, metabolite levels, and flux-based approaches (Metallo et al., 2012; Wise et al., 2011; Papandreou et al., 2006; Kim et al., 2006). Complicating the interpretation of HIF biology is the presence of three HIFα proteins (HIF-1α, HIF-2α, and HIF-3α), which exhibit tissue-specific expression patterns and varied functions. For example, HIF-1α and HIF-2α exhibit differential effects on c-Myc-mediated transcription, with HIF-2α enhancing activity and HIF-1α antagonizing c-Myc function (Gordan et al., 2007a). However, there are many common metabolic targets between HIF-1α and HIF-2α, and both are associated with a glycolytic phenotype in cancer cells and stem cells.

HIF signaling also correlates with cell "stemness", as HIFα proteins can regulate factors involved in maintaining pluripotency. HIF-2α has been shown to regulate Oct-4 expression (Covello et al., 2006), and general application of low oxygen or expression of stable HIFα mutants induces a hESC-like transcriptional program in cancer cell lines (Mathieu et al., 2011). Hypoxia is also known to increase the efficiency of cellular reprogramming to the pluripotent state (Yoshida et al., 2009), and chemical activators of HIF signaling can increase the yield of iPSC colonies

during reprogramming (Zhu et al., 2010). Furthermore, hypoxia-mediated regulation of HIF-1α is required for maintenance of HSCs and the tumorigenicity of glioma stem cells (Li et al., 2009; Simsek et al., 2010; Takubo et al., 2010). These findings collectively highlight the influence of HIF signaling on metabolism and stem cell function.

The LKB1 protein has been shown to influence the maintenance and metabolic behavior of HSCs. Conditional knockout of this protein in hematopoietic progenitors induces metabolic activation of HSCs and ultimately causes depletion of the HSC compartment (Gan et al., 2010; Gurumurthy et al., 2010; Nakada et al., 2010). Results suggest that LKB1 enables HSCs to remain quiescent in the bone marrow, and loss of this gene affects several metabolic pathways in HSCs. LKB1 lies upstream of AMP-activated protein kinase and the mammalian target of rapamycin (mTOR), pathways involved in energy sensing and the coordination of anabolic/catabolic metabolism (Shackelford and Shaw, 2009). In the context of pluripotent cell cultures, mTOR activity directly correlates with the metabolic state and differentiation status of mESCs, as phosphorylated S6 kinase levels were elevated in mESCs with high $\Delta\psi_m$ (Schieke et al., 2008). Furthermore, inhibition of mTOR activity with rapamycin decreased metabolic activity and induced mesodermal differentiation of mESCs. Similar effects of mTOR inhibition on differentiation have been observed in hESCs (Zhou et al., 2009).

Regulatory proteins have also been linked to ROS levels in stem cells. The protein product of the ataxia telangiectasia mutated (*Atm*) gene ensures genomic stability by activating a cell cycle check point in response to DNA damage or oxidative stress (Ito et al., 2004; Liu et al., 2011). Intracellular concentrations of H_2O_2 were higher in hematopoietic progenitors cells isolated from *ATM*$^{-/-}$ mice than those isolated from the wild type (WT) animals, and *in vitro* colony formation was far less efficient in *ATM*$^{-/-}$ cells. These phenotypes were mostly rescued by administration of N-acetyl-L-cysteine (NAC). *ATM*-deficient mice administered NAC showed reduced signs of long-term bone marrow failure compared to untreated *ATM*$^{-/-}$ mice, and NAC treatment also restored the ability of isolated *ATM*$^{-/-}$ HSCs to reconstitute the bone marrow of irradiated mice to the level exhibited by WT cells. Downstream of *ATM* loss, activation of the tumor suppressor p16INK4a and the subsequent failure to inactivate Rb family members in response to ROS were implicated in the HSC phenotypes described above (Ito et al., 2004).

ROS levels were also elevated in neural stem cells in mice lacking functional transcripts of *Prdm16*, a gene preferentially expressed in hematopoietic and neural progenitors, and genes known to regulate ROS levels, such as hepatocyte growth factor (*Hgf*) and metallothienin2 (*Mt2*) (Ozaki et al., 2003; West et al., 2008), were expressed at lower levels in these cells (Chuikov et al., 2010). Therefore, the *Prdm16* transcription factor seems to play an important role in regulating ROS in neural progenitors (Chuikov et al., 2010). Finally, the FoxO subfamily of transcription factors regulates a diverse array of physiological processes, including induction of cell cycle arrest, apoptosis, and stress resistance. Their role in ROS management was investigated in HSCs using an Mx-conditional knockout of the *FoxO1*, *FoxO3*, and *FoxO4* genes (Tothova et al., 2007). Increased levels of ROS were observed in HSCs lacking FoxO expression, suggesting that FoxO regulation of ROS plays an important role in maintaining immature bone marrow cell populations. The fraction of HSCs in S, G2, and/or M phase, along with the ratio of cells in G1 to G0 increased in the absence of these genes, indicating an increased departure from the quiescent state. These phenotypes were all reversed in mice administered subcutaneous injections of NAC (Tothova et al., 2007), suggesting that FoxOs play a role in mitigating ROS levels in hematopoietic progenitors.

Conclusions

Stem cell biologists have focused largely on dissecting the molecular genetics which drive the phenotype of progenitor cells. However, great strides have been made in our understanding of how stem cell populations are metabolically different than more differentiated cell types. These changes are due, in part, to the need for biosynthetic precursors to fuel cell growth, as evidenced by increased flux through glycolysis in stem cell populations. Additional pathways may help maintain the "privileged" redox state of these cells, but the mechanisms driving this phenotype must be elucidated in greater detail moving forward. Also, the question of how metabolism functions in cells that proliferate slowly (*e.g.*, quiescent stem cells) requires significant attention; as such changes presumably affect all upstream metabolic pathways.

Knowledge of the specific enzymes and metabolites which protect stem cells and cancer

stem cells may greatly enhance treatments that target such cells. To make these discoveries, researchers will need to combine more advanced methods of metabolic characterization in order to identify the most activated pathways in stem cell phenotypes. Technological improvements in mass spectrometry and NMR are greatly improving the sensitivity, expansiveness, and interpretation of metabolomics measurements in mammalian systems (Dietmair et al., 2010). While non-targeted metabolomics techniques applied to stem cells can facilitate the discovery of functional biochemical variations in these systems (Yanes et al., 2010), systems-based approaches such as metabolic flux analysis are required to generate more mechanistic information. The use of stable isotope tracers allows scientists to make detailed calculations of intracellular fluxes which cannot be ascertained using stoichiometric models alone (Quek et al., 2010). On the other hand, genome-scale methods like flux balance analysis (FBA) enable the *in silico* exploration of extraordinarily large networks and can direct researchers to new potential targets that might not be considered otherwise (Folger et al., 2011; Mo and Palsson, 2009). Effective application of these methods is already occurring in model systems of cancer (Frezza et al., 2011). However, these approaches have not been extensively applied to investigations of pluripotent cells and adult progenitors, and significant obstacles must be overcome to effectively apply these techniques to stem cell biology. These challenges include expanding analytical coverage across the metabolome, obtaining measurements within intracellular compartments, studying cell behavior in the most relevant environments, and applying techniques to *in vivo* model systems. An additional challenge facing researchers as these approaches are applied to stem cell systems is cellular homogeneity. Stem cells can rapidly differentiate and modulate their state. The time scale of metabolic reactions complicates the use of traditional sorting methods to separate differentiated and undifferentiated cell populations from heterogeneous mixtures. Once researchers address these challenges, clinicians may be offered a vast new toolset to control and engineer stem cell behavior, as metabolic pathways lie at the core of cell and tissue function.

Acknowledgements

This chapter, in full, is a reprint of the material as it appears in "Exploring metabolic pathways that contribute to the stem cell phenotype", Biochimica et Biophysica Acta, vol. 1830, 2013. Nathaniel M. Vacanti is the primary author of this publication.

Chapter 2

Inner Mitochondrial Membrane Transport Regulates Cellular Function

Introduction

Metabolic enzymes and the reactions they catalyze allow cells to harvest energy stored in the chemical bonds of available nutrients and to rearrange those bonds to form the building blocks and precursors of biosynthetic molecules. Cells utilize energy by hydrolyzing the high energy phosphate bonds of adenosine triphosphate (ATP). For example, the conformational change in myosin heavy chain bound to an actin filament results in elevated tension across the sarcomere, thus is seemingly unfavorable. However this necessary process for muscle contraction occurs regularly because it is coupled to the very exergonic hydrolysis of ATP. Additionally synthesis of high energy structural molecules like fatty acids and cholesterol from lower energy building blocks also requires energy supplied in the form of ATP phosphate bond hydrolysis. Thus cells require a continuous supply of ATP to maintain homeostasis and perform their specialized and most basic functions.

The breakdown of glucose to two molecules of pyruvate, via glycolysis in the cytosol, releases energy that is coupled to the regeneration of ATP from adenosine diphosphate (ADP). However most of the energy contained within the chemical bonds of the original glucose molecule is still present in the two molecules of pyruvate. Complete catabolism of pyruvate, in the presence of oxygen, to carbon dioxide and water releases this energy and is coupled to the formation of ATP. Considering this accounts for the vast majority of energy released from glucose, it also

accounts for the vast majority of ATP synthesized.

The universally accepted chemiosmotic hypothesis proposed by Mitchell (1961) states exergonic oxidation of pyruvate in mitochondria is coupled to the establishment of an electrochemical proton gradient across the inner mitochondrial membrane, the dissipation of which drives the regeneration of ATP. Thus compartmentalization of energy metabolism within the cytosol and mitochondria is key to generating a continuous supply of ATP. Furthermore cytosolic products are required for mitochondrial functions and vise versa (Figure 2.1). To achieve this functional compartmentalization, selective transport of substrates, intermediates, and products across the inner mitochondrial membrane is essential. Herein the proteins that facilitate this transport and their regulatory roles in cellular function/dysfunction are reviewed. Inner membrane mitochondrial carriers facilitate the transport of substrates between the intermembrane space and the matrix. However substrates in the intermembrane space are frequently referred to as cytosolic, as is the case throughout this review, because small molecules are freely permeable across the outer mitochondrial membrane.

Annotated SLC25 Mitochondrial Carriers

Background

The human SLC25 family of mitochondrial carriers has 53 members (including one localized to peroxisomes) that share common structural motifs including including three repeated regions, each about 100 amino acids long and each containing two transmembrane α-helices. They are nuclear encoded and guided by a mitochondrial targeting sequence where they are imported by the translocase of the outer membrane complex and inserted by the translocase of the inner membrane complex (Gutiérrez-Aguilar and Baines, 2013; Palmieri, 2013). The mitochondrial members of this family whose substrates are identified are reviewed in this section, with emphases on the identifications of their substrates, their roles in the metabolic network, and their influences on cellular function/dysfunction.

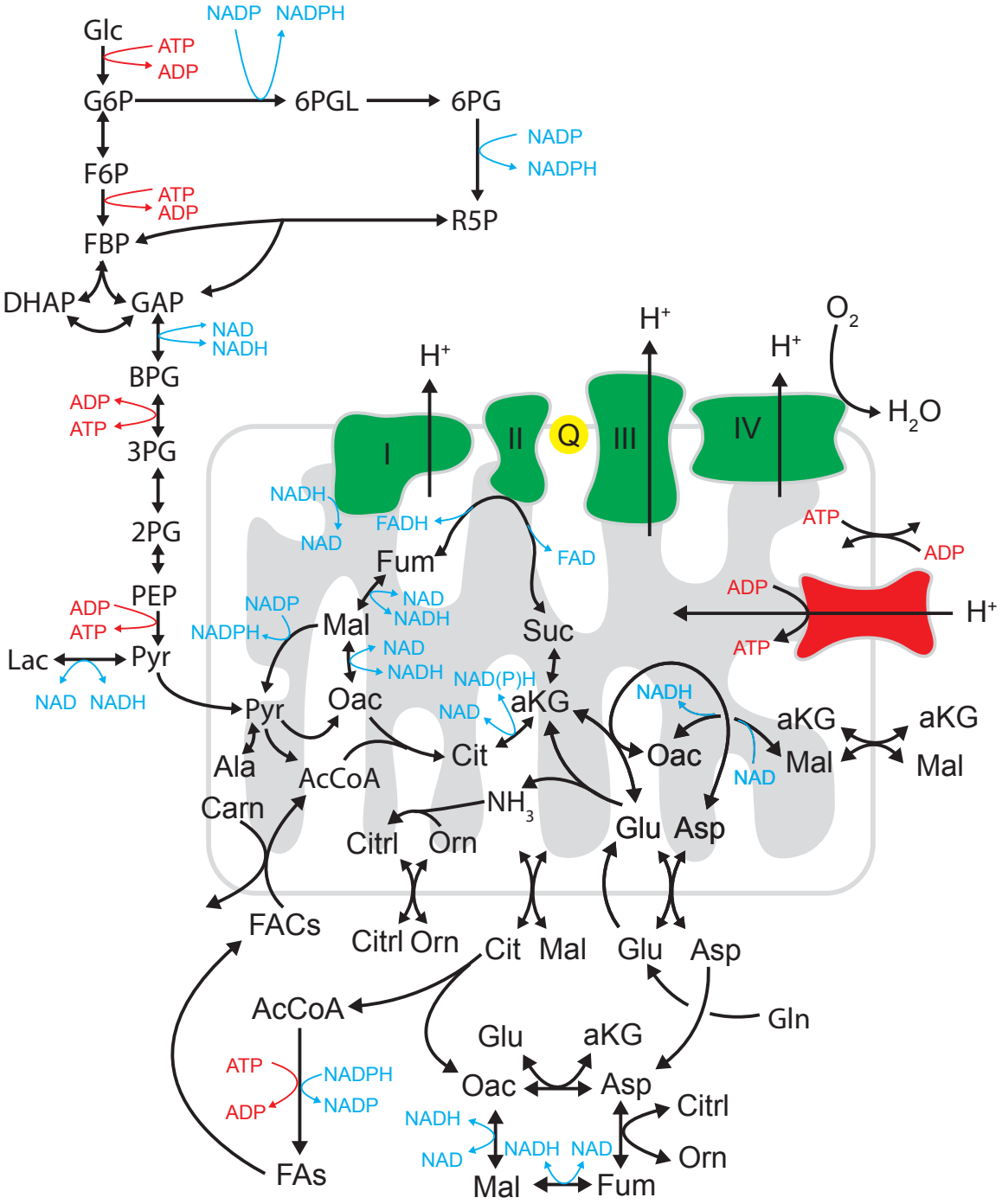

Figure 2.1: Schematic of Select Metabolic Pathways and Mitochondrial Carriers. Mitochondrial metabolism and thus the metabolic network is tightly controlled by mitochondrial access to substrates and intermediates and cytosolic access to products and precursors.

ATP/ADP

The adenine nucleotide translocator (ANT) exchanges matrix ATP for cytosolic ADP. Its four isoforms include ANT1 (SLC25A4), ANT2 (SLC25A5), ANT3 (SLC25A6), and ANT4 (SLC25A31). ANT was the first inner membrane protein whose activity was detected in isolated mitochondria (Pfaff et al., 1965), the first to be reconstituted into liposomes (Krämer and Klingenberg, 1979), the first to be sequenced (Aquila et al., 1982), and the first to be crystallized with a specific inhibitor (Pebay-Peyroula et al., 2003). The push to characterize and understand this transporter is driven by its critical role supplying ATP for cytosolic utilization and returning ADP to mitochondria for phosphorylation by ATP synthase. ANT1 is primarily expressed in heart and skeletal muscle, ANT2 in proliferating and undifferentiated cells, ANT3 ubiquitously, and ANT4 in the liver, testis, and brain (Stepien et al., 1992; Chevrollier et al., 2011; Dolce et al., 2005). Mutations in *ANT1* are responsible for 4% of incidents of autosomal dominant progressive external ophthalmoplegia (adPEO), a disease characterized by deletions in mtDNA with clinical manifestations including ophthalmoplegia, ptosis, and proximal myopathy (Lamantea et al., 2002). Reduced protein expression of ANT1 is also associated with Sengers syndrome, an autosomal recessive disease with clinical manifestations including congenital cataracts, hypertrophic cardiomyopathy, mitochondrial myopathy, and lactic acidosis. This disease is not linked to mutations in *ANT1*, thus the mechanism is thought to be transcriptional, translational, or post-translational (Jordens et al., 2002). However mutant *ANT1* is linked to cardiomyopathy, as ten homozygous null $ANT1^{-/-}$ patients monitored over six years presented progressive myocardial thickening, abnormal contractile mechanics and repolarization, cardiomyocyte degeneration, and structurally abnormal mitochondria; the severity of which correlated with mtDNA haplogroup (Strauss et al., 2013).

Cytosolic ATP levels and mitochondrial P_i levels are also influenced by the isoforms of the ATP-Mg^{2-}/$H_2PO_4^{2-}$ electroneutral antiporter which include APC2 (SLC25A23), APC1 (SLC25A24), and APC3 (SLC25A25). Its activity was observed in isolated mitochondria in the 1980s (Pollak and Sutton, 1980; Austin and Aprille, 1984) and three isoforms of the exchanger were identified by overexpression in *Escherichia coli* and liposomal reconstitution in 2004. APC1

is expressed primarily in the testis, and APC2/3 in many tissues (Fiermonte et al., 2004). APC1 is also believed to be protective against mitochondrial permeability transition induced cell death in cancer cells (Traba et al., 2012).

Inorganic Phosphate

SLC25A3 encodes the mitochondrial inorganic phosphate carrier (PiC) which transports $H_2PO_4^-$ into the matrix for oxidative phosphorylation via electroneutral $H_2PO_4^-/OH^-$ antiport and proposed, though disputed $H_2PO_4^-/H^+$ symport. In addition, the transporter also futilely exchanges $H_2PO_4^-$ for $H_2PO_4^-$ (Stappen and Krämer, 1994). Its activity was recognized in isolated mitochondria not long after the chemiosmotic hypothesis was proposed (Papa et al., 1969) and in 1998 the gene was overexpressed in *Escherichia coli* and the protein reconstituted into liposomes (Fiermonte et al., 1998a). Alternative splicing produces two variants, PiC_a expressed in heart and skeletal muscle and PiC_b expressed ubiquitously (Dolce et al., 1996). Homozygous inactivation of the heart and skeletal muscle splice variant (PiC_a) is lethal; two siblings each born with homozygous mutations in an exon specific to this variant passed away within one year of birth. However heterozygous inactivation is non-lethal, as both parents are carriers of this mutation (Mayr et al., 2007).

Nucleotides

The mitochondrial deoxynucleotide carrier, DNC (tentatively SLC25A19), supplies deoxynucleotide diphosphates to mitochondria as precursors to the triphosphate forms used for mtDNA replication. Dolce et al. (2001) examined the seven genes in *Caenorhabditis elegans* related to the mammalian adenine nucleotide transporters (ANTs). Four of these genes were not ANT isoforms in *Caenorhabditis elegans* and had a related expressed sequence tag in the human genome. This human expressed sequence tag was extended and overexpressed in *Escherichia coli* and the protein product purified and reconstituted into liposomes. It was found to selectively transport deoxynucleotide diphosphates and to a lesser extent exchange deoxynucleotide triphosphates for ADP or ATP. However Kang and Samuels (2008) argue that SLC25A19 is not the DNC, rather the thiamine pyrophosphate (ThPP) carrier. Among other evidence, they

cite a study of *SLC25A19*$^{-/-}$ mice where ThPP levels in embryonic fibroblast mitochondria are undetectable, but elevated in the post-mitochondrial supernatant relative to control mice, while quantities of mtDNA are unchanged (Lindhurst et al., 2006).

Amish microcephaly (MCPHA) is a rare metabolic disorder characterized by homozygous mutations in *SLC25A19* and results in death at infancy (Kelley et al., 2002; Rosenberg et al., 2002). As the function of SLC25A19 is disputed, the MCPHA disease mechanism is as well. The DNC is also believed to facilitate deleterious mtDNA damage by anti-viral treatment with nucleoside analogues (Sales et al., 2001), thus a definitive identification of the DNC may lead to strategies to combat this off-target effect.

Pyrimidine nucleotides also have dedicated carriers for their transport into the mitochondria. This activity was first observed when a purified mitochondrial fraction from acute lymphocytic leukemia cells was reconstituted into liposomes and shown to selectively transport dCTP (Bridges et al., 1999). The *Saccharomyces cerevisiae* ortholog, *Rim2p*, was subsequently overexpressed in *Escherichia coli*, the protein product purified and reconstituted into liposomes, and found to transport pyridine nucleotide and deoxynucleotide di- and tri- phosphates with a counter exchange mechanism. The authors hypothesize deoxynucleotide monophosphates are the exchanged substrates (Marobbio et al., 2006). A year later, sequence similarities led to the discovery of the mouse pyridine nucleotide carrier (Pnc1 or Slc25a33) which transports UTP and to a lesser extent CTP and TTP when reconstituted into liposomes (Floyd et al., 2007). Recently, sequence similarities led to confirmation that SLC25A36 is also a pyrimidine nucleotide and deoxy nucleotide di- and tri-, along with mono-, phosphate carrier spanning the inner mitochondrial membrane (Di Noia et al., 2014). Physiologically, insulin-like growth factor signaling induces PNC1 and promotes cell growth in transformed cells (Floyd et al., 2007; Favre et al., 2010).

S-Adenosylmethionine

S-adenosylmethionine (SAM) is synthesized from methionine and ATP outside of the mitochondria and is required for mitochondrial DNA and protein methylation. Horne et al. (1997) first observed the activity of a mitochondrial SAM carrier in isolated rat liver mitochondria.

Subsequently the yeast and human SAM carriers were overexpressed in *Escherichia coli* and the protein products reconstituted into liposomes. Yeast lacking the identified transporter, Sam5p, were biotin auxotrophs, as biotin synthesis requires SAM and occurs in yeast exclusively in the mitochondria. Both the Sam5p and the human protein, SAMC (SLC25A26), transport SAM when reconstituted into liposomes; the yeast carrier acting as a uniporter and the human carrier as an exchanger for S-adenosyl homocysteine (Marobbio et al., 2003; Agrimi et al., 2004). Defective SLC25A26 may be characteristic of Down syndrome as mitochondrial SAM levels are diminished even though mRNA levels are elevated (Infantino et al., 2011).

Folate

The activity of the mitochondrial folate transporter (MFT) was first observed by Horne et al. (1992) in isolated rat liver mitochondria. Subsequently *MFT* (*SLC25A32*) was cloned and shown to rescue glycine auxotrophy in Chinese hamster ovary cells deficient in mitochondrial folate uptake (Titus and Moran, 2000). Glycine is necessary for translation of mitochondrial encoded proteins and folate is required for its synthesis in mitochondria by serine hydroxymethyltransferase 2. Furthermore folate is necessary for formylmethionine synthesis, an amino acid required for mitochondrial translation initiation. Human MFT also rescues mitochondrial flavoprotein deficiencies in *Saccharomyces cerevisiae* resulting from a mutation in the yeast mitochondrial FAD transporter gene *Flx1*, thus the MFT may also transport FAD (Spaan et al., 2005).

Several pathological phenotypes are associated with defects in mitochondrial folate metabolism. Mitochondria isolated from the liver of rats fed chronic quantities of alcohol and human liver HepG2 cells chronically exposed to alcohol display significantly diminished *MFT* expression (Biswas et al., 2012), Chinese hampster ovary cells with a mutated mitochondrial folate carrier are less equiped to handle oxidative stress (Ye et al., 2010), and rats fed low folate diets display elevated liver mitochondrial DNA damage and intracellular superoxide levels (Chang et al., 2007).

Glycine

SLC25A38 is proposed to be the mitochondrial glycine carrier, however this is yet to be verified. Mutations in *SLC25A38* cause nonsyndromic autosomal recessive congenital sideroblastic anemia, characterized by erythroid precursors containing iron deposits within mitochondria. The only other gene whose mutation leads to this anemia is 5'-aminolevulinate synthase 2, which catalyzes the first reaction in mitochondrial heme synthesis from glycine. Furthermore zebrafish with its suspected orthologs knocked down and *Saccharomyces cerevisiae* lakcing its putative ortholog are deficient in hemoglobin and heme biosynthesis respectively (Guernsey et al., 2009).

Oxoadipate

Oxoadipate is an intermediate in the breakdown of lysine and tryptophan, and its passage to mitochondria allows further breakdown to acetyl coenzyme A and complete oxidation to carbon dioxide and water. Two isoforms of the yeast mitochondrial oxoadipate carrier were first identified by Palmieri et al. (2001a) and found to exchange α-ketoglutarate for 2-oxoadipate when reconstituted into liposomes. Soon after the same group identified a single isoform of the human ortholog, ODC (Fiermonte et al., 2001) or SLC25A21, with the same counter-exchange properties as the yeast isoforms. Counter exchange replenishes cytosolic α-ketoglutarate, a substrate in the first step of lysine catabolism. Defective ODC is a proposed disease mechanism of 2-oxoadipate acedemia, a disorder characterized by mental disabilities, hypotonia, and/or seizures (Fiermonte et al., 2001).

Glutamine

Glutamine enters the mitochondria through a mitochondrial glutamine carrier (MQC), then through the action of glutaminase followed by glutamine dehydrogenase or glutamate oxaloacetate/pyruvate transaminase, enters the TCA cycle as α-ketoglutarate. Mitochondrial glutamine is a major source of energy and biosynthetic intermediates for proliferating cells in culture, and this glutamine addiction is exacerbated when pyruvate oxidation is defective (Vacanti et al., 2014; Yang et al., 2014). Furthermore mitochondrial glutamine is believed to be a major

substrate for NADPH production used in reductive biosynthetic reactions and replenishment of reduced glutathione pools (Wise and Thompson, 2010).

The existence of SLC25A44 was determined using a hidden Markov model seeded with the known sequences of the SLC25 family members to search available data sets (Haitina et al., 2006). Its function as the human mitochondrial glutamine carrier, MQC, was discovered by perfoming ^{13}C tracing on *MQC* knockdown transformed cell lines and deducing the transporter's substrate from differential labeling patterns. TCA cycle intermediates acquired less carbon from ^{13}C labeled glutamine when *MQC* was knocked down in human carcinoma cells while permeabilized cells actually acquired more carbon from ^{13}C labeled glutamate. Furthermore, increases in glucose anaplerosis upon *MQC* knockdown are hypothesized to be an adaptation to inhibited glutamine anaplerosis (Vacanti et al., unpublished).

Glutamate

The mitochondrial glutamate carriers, GC1 (SLC25A22) and GC2 (SLC25A18) cotransport cytosolic glutamate into or out of the mitochondria along with H^+. Azzi et al. (1967) first observed the activity of the glutamate transporters in isolated mitochondria and Fiermonte et al. (2002) identified the proteins, overexpressed the genes in *Escherichia coli*, reconstituted the purified proteins into liposomes, and verified their cotransport properties described above. *GC1* is strongly expressed in the brain, liver, pancreas, and testis while *GC2* in the brain and testis (Fiermonte et al., 2002). Glutamate entering mitochondria can be converted to α-ketoglutarate for oxidation in the TCA cycle, and glutamate synthesized in mitochondria can be exported by the GC1/2.

Glutamate exported by the mitochodria is a known messanger for glucose stimulated induction of insulin secrection in pacreatic β-cells (Maechler and Wollheim, 1999) and can be regulated by GC1 (Casimir et al., 2009). GC1 is also critical for motor function, as a missense mutation has been identified in a form of autosomal recessive neonatal myoclonic epilepsy. Furthermore, expression analysis reveals *GC1* is specifically expressed in areas of the brain thought to contribute to the onset of myoclonic seizures (Molinari et al., 2005). Additionally, dysfunctional GC1 may be responsible for a form of neonatal encephalopathy (Molinari et al., 2009).

Glutamate also enters/exits mitochondria through the Ca^{2+} dependent aspartate/glutamate carriers AGC1 (SLC25A12) and AGC2 (SLC25A13). AGC1 was the first Ca^{2+} dependent mitochondrial transporter described and cloned, though at the time its substrate was unknown (del Arco and Satrústegui, 1998). A year later the gene that is mutated in adult onset type II citrullinaemia was determined to encode the mitochondrial transporter SLC25A13, thus its substrate was hypothesized to play a role in urea cycle function (Kobayashi et al., 1999). Subsequently Palmieri et al. (2001b) overexpressed both genes in *Escherichia coli*, reconstituted the purified proteins in liposomes, and determined both proteins facilitate the electrogenic exchange of cytosolic glutamate and H^+ for mitochondrial aspartate. Activation by Ca^+ allows for transmission of Ca^+ signals to mitochondria resulting in elevated mitochondrial NADH levels via malate/aspartate shuttle activity. AGC1 is also essential for synthesis of N-acetylaspartate which is required for myelin synthesis in the brain (Satrústegui et al., 2007).

Oxoglutarate

The oxoglutarate carrier, OGC (SLC25A11) fascilitates the exchange of a matrix α-ketoglutarate for a cytosolic dicarboxylate, primarily malate (Palmieri et al., 1972). It is an integral part of the malate/aspartate shuttle which, in effect, transports ctyosolic NADH into the mitochondria. Malate dependent oxoglutarate transport across the inner membrane was first observed in the 1960s (Meijer and Tager, 1966; Chappell, 1968) and the sequence of the protein responsible for its facilitated transport determined in 1990 (Runswick et al., 1990). Functionally, the OGC plays an important role in nutrient stimulated insulin release from pancreatic islets (Odegaard et al., 2010). Furthermore Chen et al. (2000) found the OGC to tranport glutathione when reconstituted into lipsomes, however this function of OGC has recently been disputed (Booty et al., 2015). Finally, physical interactions along with the observed effects of inhibitors suggest OGC also fascilitates the transport of porphyrin, a precursor to heme (Kabe et al., 2006).

Dicarboxylate

The dicarboxylate carrier, DIC (SLC25A10), exchanges matrix malate or succinate for cytosolic $H_2PO_4^-$. Its physical interaction with malate dehydrogenase in the matrix allows for effecicient substrate shuttling to gluconeogenesis. Malate dehydrogenase reduces oxaloacetate to malate in the matrix which is then effeciently passed to localized DIC for transport to the cytosol where it is oxidized back to oxaloacetate and is thus a substrate for gluconeogenesis. DIC also plays an important role in fatty acid synthesis, as it provides a source of cytosolic malate necessary for exchange with mitochondrial citrate through the citrate carrier, CIC. Cytosolic citrate then supplies AcCoA building blocks for *de novo* fatty acid synthesis. This role is illustrated by the failure of 3T3L-1 adipocytes to accumulate lipids during differentiation when DIC or CIC is inhibited (Kajimoto et al., 2005).

The kinetics of the dicarboxylate carrier were first characterized by Palmieri et al. (1971). Decades later the yeast DIC was identified by sequence similarities with the bovine oxoglutarate carrier (Palmieri et al., 1996), leading to the subsequent identification of the rat DIC (Fiermonte et al., 1998b). Both of these findings were confirmed by reconstituting the respective protein into liposomes and observing the aforementioned DIC transport characteristics (Palmieri et al., 1996; Fiermonte et al., 1998b). Researchers suggest the DIC also transports glutathione (Kamga et al., 2010; Wilkins et al., 2013), however this is disputed (Booty et al., 2015).

Coenzyme A

SLC25A42 was discovered by using the known SLC25 member sequences as the seeding set to construct a hidden Markov model. Available data sets were searched against the model and after filtration and manual curation, 14 new members of the SLC25 family, including SLC25A42, were identified (Haitina et al., 2006). Subsequently Fiermonte et al. (2009) reconstituted the transporter into liposomes and determined it exchanges matrix (deoxy)adenine nucleotides or adenosine 3',5'-diphosphate for cytosolic coenzyme A (CoA). CoA is not synthesized in the mitochondria and is an important cofactor for mitochondrial reactions including pyruvate dehydrogenase/citrate synthase and α-ketoglutarate deyhydrogenase/succinyl CoA hydrolase.

Graves' disease is an autoimmune disorder characterized by circulating thyroid-stimulating autoantibodies resulting in symptoms of hyperthyroidism (Kohn et al., 1986). The Graves' disease carrier (SLC25A16) was identified by screening the protein products of an expression library derived from a follicular thyroid carcinoma for interactions with immunoglobulin G from the serum of a patient with Graves' disease (Zarrilli et al., 1989). It is hypothesized to transport CoA into mitochondria as deletion of the gene encoding the highly homologous *Saccharomyces cerevisiae* protein Leu5p caused a 15-fold decline in mitochondrial CoA that is rescued by expression of the Graves' disease carrier (Prohl et al., 2001).

Citrate

Activity of the citrate carrier (CIC) or tricarboxylate carrier was first observed and its substrates determined in the 1960s; see LaNoue and Schoolwerth (1979) for a review. Stipani et al. (1980) later reconstituted the carrier into liposomes and verified it exchanges citrate for malate or phosphoenolpyruvate. The rat carrier was later cloned and determined to be a member of the mitochondrial carrier family (Slc25a1) (Kaplan et al., 1993). Furthermore CIC interacts with citrate synthase in yeast, thus facilitating efficient export from mitochondria (Grigorenko et al., 1990; Sandor et al., 1994) for cytosolic requirements such as fatty acid synthesis.

CIC inhibition induces autophagy (Catalina-Rodriguez et al., 2012) and its expression is reduced during starvation (Zara and Gnoni, 1995), hypothyroidism (Giudetti et al., 2006), and type I, though not type II diabetes (Kaplan et al., 1991a,b). Furthermore the sterol regulatory element in the *CIC* promotor allows for up-regulation by insulin (Infantino et al., 2007) and CIC activity regulates glucose-stimulated insulin secretion (Joseph et al., 2006).

Carnitine/Acylcarnitine

The carnitine/acylcarnitine carrier, CAC (SLC25A20), is part of the carnitine shuttle which transports fatty acyl-carnitines with 14 or more carbons into mitochondria in exchange for matrix carnitine. To obtain energy from fat, free fatty acids taken up from the blood are first converted to fatty acyl-CoA molecules by the acyl-CoA synthetases prior to conversion to fatty acyl-carnitines by carnitine acyltransferase I. Cytosolic fatty acyl-carnitine is then exchanged

for matrix carnitine by the CAC. Fatty acyl-carnitine is then reconverted to fatty acyl-CoA by carnitine acyl transferase II in the matrix prior to being catabolized in the β-oxidation pathway.

The exchange mechanism of fatty acyl-carnitine for carnitine by CAC reconstituted into liposomes was determined by Indiveri et al. (1994). Subequently the rat amino acid sequence was deduced from overlapping cDNA clones generated from polymerase chain reactions with primers designed based on sequences of internal peptides of the purified protein (Indiveri et al., 1997a). The rat sequence soon led to the cloning of the human gene by the same group (Huizing et al., 1997). In the years following, a second carnitine/acylcarnitine carrier, CACL (SLC25A29), was discovered by researchers interested in genes upregulated during liver regeneration (Sekoguchi et al., 2003). However, recently the group responsible for much of the pioneering work on CAC has claimed the human SLC25A29 does not transport carnitine or acylcarnitine, rather arginine, lysine, and to a lesser extent ornithine and histidine (Porcelli et al., 2014). CAC is highly expressed in the heart, skeletal muscle, and liver and to a much lower extent in the brain, pancreas, lung, and kidneys (Huizing et al., 1997) while CACL is highly expressed in the heart but also present in the liver, kidneys, and brain (Sekoguchi et al., 2003).

CAC and CACL expression increases in skeletal muscle with physical activity (Lammers et al., 2012; McGivney et al., 2010), and in cultured renal cell lines upon administration of statins or fibrates (Iacobazzi et al., 2009). CACL is also induced by fasting (Sekoguchi et al., 2003). Finally, CAC deficiency is a recessively inherited, life-threatening disorder. Clinical manifestations include hypoketotic hypoglycemia, cardiomyopathy, liver failure, and muscle weakness (Iacobazzi et al., 2004).

Uncoupling Proteins

The existence of a mechanism to uncouple the respiratory chain from ATP synthesis has long been suspected (Nicholls, 1976), and the major protein responsible, now known as UCP1, was discovered nearly four decades ago (Heaton et al., 1978). Currently five uncoupling proteins have been identified: UCP1/SLC25A7 , UCP2/SLC25A8 (Fleury et al., 1997), UCP3/SLC25A9 (Boss et al., 1997), UCP4/SLC25A27 (Mao et al., 1999), and UCP5/SLC25A14 (Yu et al., 2000). However the function of UCP2 as an uncoupling protein

is disputed as expression of the human paralog in yeast at physiological levels does not alter mitochondrial proton conductance (Stuart et al., 2001). Additionally Vozza et al. (2014) found UCP2 to exchange malate, oxaloacetate, and aspartate for phosphate and a proton. UCP1 is expressed primarily in brown adipose tissue (Bouillaud et al., 1985), UCP2 ubiquitously (Fleury et al., 1997), UCP3 in skeletal muscle (Boss et al., 1997), and UCP4/5 in the brain (Yu et al., 2000).

UCP1 is activated by fatty acids and inhibited by purine nucleotide di- and tri- phosphates (Locke et al., 1982). Though the mechanism of fatty acid activation is unknown, three models have been proposed. In the first, fatty acids act as cofactors embedding their carboxyl groups into UCP1 to provide a proton-buffering site. In the second model, fatty acids are protonated on the cytosolic side, "flip-flop" to the matrix side via UCP1, and are deprotonated in the more alkaline environment. Finally in the third model, fatty acids allosterically prevent nucleotides from inhibiting proton flux through UCP1 (Divakaruni and Brand, 2011).

Uncoupling respiration from ATP synthesis via proton leak through UCP1 provides a mechanism for non-shivering thermogenesis. The inefficiencies in maintaining proton separation across the inner mitochondrial membrane of brown fat cells require the respiratory chain to work harder and thus produce more heat. This is apparent in *UCP1*$^{-/-}$ mice, as they are more sensitive to cold than control animals (Enerbäck et al., 1997). UCP2 and UCP3 are activated by reactive oxygen species and covalently inactivated by reduced glutathione. Thus UCP2/3 serve as ROS sensors and regulators, with their increased activity lowering ROS production by altering the membrane potential (Mailloux and Harper, 2011). Furthermore UCP2 deficient mice display elevated glucose stimulated insulin secretion, UCP2 is markedly upregulated in obesity induced diabetes mouse models, and UCP2 deficiency restores first-phase insulin secretion, increases serum insulin and lowers serum glucose levels (Zhang et al., 2001).

Iron

Iron is an essential substrate for heme and iron-sulfur cluster synthesis which occur in mitochondria. Iron-sulfur clusters are integral parts of mitochondrial enzymes such as aconitase, complexes I-III, and ferrochelatase, and additionally for many essential enzymes outside

of mitochondria including those involved in nucleotide metabolism and DNA repair (Horowitz and Greenamyre, 2010). Iron enters mitochondria through the carriers MFRN1 (SLC25A37) and MFRN2 (SLC25A28). Li et al. (2001) discovered the human gene, now known as *MFRN2*, homolgous to yeast *mrs3/4* which Foury and Roganti (2002) identified as mitochondrial iron transporters. Subsequently a second mitochondrial iron transporter, Mfrn1, was identified and shown to be required for murine erythroid cell heme biosynthesis (Shaw et al., 2006). Both *MFRN2* and *Mfrn1* are ubiquitously expressed with higher levels of *MFRN2* transcript in the liver, heart, and skeletal muscle (Li et al., 2001; Shaw et al., 2006). Furthermore Mfrn1 physically interacts with ferrochelatase, facilitating efficient heme biosynthesis (Chen et al., 2010).

Ornithine

One turn of the urea cycle nets a loss of nitrogen from ammonia and glutamate to urea, which is excreted. Thus the urea cycle provides a means for cells to dispose of nitrogenous waste. Nitrogen from ammonia enters the urea cycle as carbamoyl phosphate and condenses with ornithine in mitochondria, producing citrulline. However urea production regenerates ornithine in the cytosol, therefore it must enter mitochondria through ORNT1 (SLC25A15) or ORNT2 (SLC25A2) to complete the cycle. Furthermore ornithine can only be synthesized in mitochondria and must be exported through the ORNT proteins for arginine synthesis in the cytosol.

Indiveri et al. (1992) first purified the ornithine carrier in rat liver mitochondria and Palmieri et al. (1997) cloned the yeast ortholog, *arg-11*. Soon after a detailed study of the carrier reconstituted into liposomes revealed it exchanges ornithine for citrulline and H^+ (Indiveri et al., 1997b). The yeast gene sequence allowed for identification of expressed sequence tag candidates and revealed the human gene, *ORNT1* (Camacho et al., 1999). Finally, a second ornithine transporter, ORNT2, was identified and characterized by two independent groups (Camacho et al., 2003; Fiermonte et al., 2003). *ORNT1* is expressed in many tissues, though most heavily in the liver, pancreas, testis, and lung. *ORNT2* is most heavily expressed in the liver, testis, and lung (Fiermonte et al., 2003).

Hyperornithinaemia-hyperammonaemia-homocitrullinuria (HHH) syndrome is an auto-

somal recessive disorder with clinical manifestations including arrested growth, seizures, and homocitrulline in the urine. The metabolic manifestations namesake to the syndrome led researchers to believe it is caused by defective mitochondrial ornithine transport (Fell et al., 1974); which was confirmed upon identifying the human transporter, ORNT1 (Camacho et al., 1999). Interestingly, ORNT2 displays functional redundancy as its expression in HHH syndrome patient fibroblasts partially rescues the disease metabolic phenotype (Camacho et al., 2003) and HHH syndrome patients with an activating mutation in ORNT2 display less severe symptoms (Camacho et al., 2006).

The Mitochondrial Pyruvate Carrier

Background

Pyruvate transport into mitochondria lies at the crossroads of the two major ATP and biosynthetic precursor producing metabolic pathways, glycolysis and the TCA cycle; thus influencing carbohydrate, amino acid, lipid, heme, ROS, urea, nucleotide, glucosamine, and folate metabolism. Dysregulation of the aforementioned pathways contributes to the pathogenesis of diabetes, obesity, cancer, neurological disorders, cardiovascular disease, myopathies, anemias, and nutrient deficiencies or toxic accumulations. As such the identity, characteristics, and regulatory effects of the mitochondrial pyruvate carrier are of great scientific and clinical interest. The existence of a dedicated carrier to facilitate the transport of pyruvate into the mitochondrial matrix was first proposed nearly half a century ago. In the decades following, specific inhibitors were identified and the carrier kinetics characterized (Halestrap and Denton, 1974; Papa et al., 1971). Finally in 2012 two independent groups identified the genes that encode the proteins composing the mitochondrial pyruvate carrier (Herzig et al., 2012; Bricker et al., 2012). In the years following a number of studies have examined the pathological effects and potential clinical applications of regulating pyruvate transport. These studies are reviewed herein.

Identification

As part of their effort to characterize mitochondrial proteins conserved through evolution, Bricker et al. (2012) examined what is now known as the mitochondrial pyruvate carrier (MPC) family of proteins. The growth defect of *mpc1Δ* yeast strains in glucose medium lacking leucine was rescued by human MPC1 but not MPC2, indicating MPC1 function is evolutionarily conserved. Mpc2 coprecipitates with itself and with Mpc1, but Mpc1 does not coprecipitate with itself, therefore Mpc1 and Mpc2 likely form a multimeric complex with Mpc2 being the major structural unit. Additionally a mutant form of Mpc1 was identified that is resistant to the known mitochondrial pyruvate transport inhibitor UK5099, suggesting Mpc1 is a component of the carrier studied for decades with this inhibitor. Finally, members of two families with defects in pyruvate oxidation have mutations that map to conserved residues of *MPC1*, and ectopic expression of *MPC1* partially or completely rescues this defect in patient fibroblasts.

In their simultaneously published study, Herzig et al. (2012) determined Mpc1 and either Mpc2 or Mpc3 are necessary for normal growth of *Sacharromyces cerevisiae* on amino acid free medium; however this requirement is mitigated by leucine. This is attributed to leucine providing a means to generate lipoic acid, a requisite cofactor for pyruvate dehydrogenase and ketoglutarate dehydrogenase, in the absence of mitochondrial pyruvate transport. Herzig et al. (2012) also found Mpc1 and Mpc2 interact by coimmunoprecipitating the yeast proteins, that ectopic expression of the mouse genes rescues defects in *mpc* deletion strains of *Sacharromyces cerevisiae*, and ectopic expression of murine Mpc1 and Mpc2 causes a fourfold increase in pyruvate uptake by *Lactococcus lactis*.

Regulatory Role

The identification of the proteins composing the mitochondrial pyruvate carrier has opened the door to a host of studies examining its role as a metabolic node impacting insulin sensitivity and secretion, substrate selection, growth, synthetic lethal targets, and adaptive responses. The breadth of the MPC's influence over metabolic processes is becoming clear as studies continue to probe its regulatory effect.

Given pyruvate is the end product of cytosolic glucose catabolism, many of the initial studies on the newly identified MPC constituent proteins have focused on its influence over the insulin response. Divakaruni et al. (2013) found thiazolidinediones (TZDs), a widely used class of insulin sensitizing drugs, actually inhibit the MPC at clinically relevant concentrations. TZDs are believed to exert their insulin sensitizing influence via activation of the peroxisome proliferator-activated receptor γ (PPARγ) which exhibits control over transcription of genes related to lipid uptake/synthesis, inflammation, and cell differentiation. Granted this is likely a major mechanism of TZD influence, as TZDs are known PPARγ agonists (Lehmann et al., 1995), the time-scale of transcriptional regulation does not explain the near immediate impacts of TZDs on pyruvate oxidation. Within minutes, pyruvate driven respiration is inhibited by administration of various TZDs to permeabilized proliferating mouse myoblasts, and this effect is overcome by supplementation with membrane permeable methyl pyruvate. Furthermore administration MSDC-0160, a TZD with reduced affinity for PPARγ, to permeabilized human skeletal muscle myotubes, neonatal rat ventricular myocytes, and rat cortical neurons causes a similar reduction in pyruvate driven respiration (Divakaruni et al., 2013). Finally, photo-catalyzable affinity probes show TZDs physically interact with the MPC (Colca et al., 2013; Rohatgi et al., 2013).

Though insulin sensitizing TZDs appear to inhibit MPC, deficiencies in MPC may not necessitate an improved insulin response. Vigueira et al. (2014) found mice homozygous for an N-terminal 16 amino acid truncation in Mpc2, imparting a partial pyruvate oxidation defect, displayed a normal response to insulin, but a glucose tolerance test yielded elevated plasma glucose and lactate along with reduced insulin levels compared to control animals. In accord with these findings, mice and 832/13 β cells administered UK5099, a potent MPC inhibitor, displayed reduced glucose clearance in intraperitoneal glucose tolerance tests and decreased glucose stimulated insulin secretion respectively (Patterson et al., 2014).

Two recent, simultaneously published, studies highlight the metabolic plasticity of cells faced with the challenge of impaired pyruvate oxidation. Genetic or pharmacological impairment of the MPC does not invoke a growth or respiratory defect in myoblasts and human carcinoma cells, rather proliferating cells adapt their substrate selection by switching to glutamine and fatty acids as oxidative fuels. Furthermore, the glutaminolysis pathway is upregulated as a means to

generate biosynthetic intermediates and, in a human a blastoma cell line, is exposed as a potential synthetic lethal target (Vacanti et al., 2014; Yang et al., 2014). Vacanti et al. (2014) also found branched chain amino acids, an early serum marker of insulin resistance, are more heavily oxidized by human skeletal muscle myotubes when the MPC is pharmacologically inhibited. Finally, these studies are consistent with earlier findings that Zaprinast, a phosphodiesterase inhibitor and lead compound for sildenafil (Viagra), inhibits Mpc resulting in an accumulation of aspartate and increased glutamate oxidation in mouse retina (Du et al., 2013).

A third study, also published simultaneously, highlights the MPC as a regulatory node for cell growth. Re-expression of *MPC1* and *MPC2* in human colon cancer cell lines impaired colony formation in soft agar and growth in xenograft tumor models. Additionally, *MPC1* is within the most frequently deleted regions among the nearly five-thousand cancer samples surveyed. Thus obliteration of a necessary component of the MPC contributes to a more "Warburg-like" metabolic state and tumorogenesis (Schell et al., 2014).

The MPC is also differentially regulated across varying muscle physiologies. The fastest twitch muscle fiber in mice, type 2B, contained drastically lower abundances of the MPC complex relative to fibers with a slower shortening velocity (Murgia et al., 2015) and rats improved muscle mass retention with age on calorie restricted diets, corresponding with increased muscle fiber MPC content (Chen et al., 2015).

Finally, yeast vary their subunit expression of Mpc in response to their environment. Depending on whether the conditions are oxidative or fermentive, yeast express the Mpc1/Mpc3 or Mpc1/Mpc2 complexes respectively (Timón-Gómez et al., 2013; Bender et al., 2015). Accordingly Mpc1/Mpc3 complex has a higher transport activity, thus promoting mitochondrial oxidative phosphorylation when oxygen is abundant (Bender et al., 2015).

Electrolyte Carriers

Background

The universally accepted chemiosmotic hypothesis states ATP synthesis is coupled to the dissipation of the proton gradient across the inner mitochondrial matrix. In turn this pro-

ton gradient is restored by coupling the pumping of protons across the inner mitochondrial matrix to the passage of electrons down the electron transport chain ultimately to molecular oxygen (Mitchell, 1961). Thus the energy required by ATP synthase is provided in the form of an electrochemical gradient across the inner mitochondrial matrix, such that a higher concentration of protons and positive charge accumulates in the intermembrane space (between the inner and outer mitochondrial membranes). Considering the separation of charge achieved by vectorial movement of protons by the ETC provides the driving force for ATP synthesis, ion channels capable of dissipating this separation have a powerful regulatory effect linking mitochondrial bioenergetics to cytosolic ion homeostasis (O'Rourke, 2007).

Calcium

Ca^{2+} is unique in that its flux into the matrix temporarily depolarizes the membrane though its presence can actually increase the protonmotive force and ATP synthesis. The mitochondrial enzymes pyruvate dehydrogenase, iso-citrate dehydrogenase, α-ketoglutarate dehydrogenase (McCormack et al., 1990), and ATP synthase (Territo et al., 2001) are all activated by Ca^{+2}, thus Ca^{2+} entry facilitates increased production of reduced pyridine nucleotide cofactor substrates for the ETC, H^{+} flux out of the matrix, and ATP production. While early studies in isolated mitochondria implicate ADP, ATP, and P_i concentrations as regulating ATP synthesis (Chance, 1972), experiments performed under physiological conditions show the rate of oxidative phosphorylation can change dramatically when ADP and P_i levels are relatively constant (Katz et al., 1989), leading investigators to believe mitochondrial Ca^{2+} may be a major regulator of oxidative phosphorylation (Gunter et al., 2004).

Transport of Ca^{2+} into mitochondria also serves as a buffering mechanism for cytoplasmic Ca^{2+} signaling (Rizzuto et al., 2012). Mitochondria sequester Ca^{2+} following neuronal depolarization in a manner dependent on proximity to the plasma membrane (Pivovarova et al., 1999), and mitochondrial uptake of Ca^{2+} near synaptic clefts serves to regulate Ca^{2+} induced neurotransmitter release (Billups and Forsythe, 2002; Medler and Gleason, 2002). Furthermore mitochondria influence endoplasmic reticulum (ER) Ca^{2+} stores as positive feedback activation of the inositol 1,4,5-triphosphate (IP3) receptor, and subsequent release of ER Ca^{2+}, is

suppressed by local mitochondrial Ca^{2+} uptake (Hajnóczky et al., 1999). Thus mitochondrial localization plays a key role in regulating Ca^{2+} signaling and defects in trafficking of these organelles is thought to contribute to neurological disorders (Chang and Reynolds, 2006). Finally the control exhibited by mitochondria on cytoplasmic Ca^{2+} acts quickly enough to influence cardiac myocyte calcium transients on a beat-to-beat basis (Maack et al., 2006), highlighting the sensitivity of this Ca^{2+} signaling control mechanism.

In addition to regulating oxidative phosphorylation and cytosolic calcium transients, Ca^{2+} flux into mitochondria also controls cell death by necrosis or apoptosis (Lemasters et al., 2009). In 1976 Ca^{2+} was first observed to cause a dramatic change in mitochondrial inner membrane permeability (Hunter et al., 1976) leading to depolarization and uncoupling of the membrane, a phenomena now known as the mitochondrial permeability transition (MPT). Once MPT has occurred, large conducting pores open allowing free diffusion of all solutes 1500 Da or less across the inner mitochondrial membrane (Lemasters et al., 2009). Theories on the identities of the proteins responsible for forming these pores have evolved over the last decade. One suggests cyclophilin D from the matrix, the adenine nucleotide translocator from the inner membrane, and the voltage dependent anion channel from the outer membrane form a large channel complex (Halestrap and Brenner, 2003). However the MPT has been observed in the absence of several of these hypothesized constituent proteins (Kokoszka et al., 2004; Krauskopf et al., 2006). Another theory suggests the pores are formed by mis-folded membrane proteins damaged by ROS, though the supporting evidence does not amount to definitive proof (He and Lemasters, 2002). Finally, recent findings indicate the MPT pores are formed by dimers of the ATP synthase complex (Giorgio et al., 2013). Though much about the mechanism of pore formation must be investigated, Ca^{2+} influx into mitochondria does contribute to MPT which can trigger cell death by necrosis from lack of ATP or apoptosis by release of cytochrome c (Qian et al., 1999).

Finally, transport of Ca^{2+} across the inner mitochondrial membrane exhibits control over the cellular autophagic response. IP3 receptor activated Ca^{2+} release and subsequent mitochondrial Ca^{2+} uptake is required to prevent the cellular autophagic response in nutrient rich environments. Chicken DT40 B lymphocytes with the IP3 receptors knocked out display

increased AMPK activation, inactivation of pyruvate dehydrogenase by phosphorylation, and increased autophagy. These effects are attributed to mitochondrial Ca^{2+} transport, as an inhibitor to the mitochondrial Ca^{2+} uniporter has similar effects on WT cells and no effect on the IP3 receptor knock out cells (Cárdenas et al., 2010).

Though the properties of Ca^{2+} transport, including kinetics, inhibitors, and stoichiometry, had all been observed, the identities of the transporters remained a mystery until a string of recent discoveries. If Ca^{2+} were allowed to reach electrical and chemical equilibrium across the inner mitochondrial matrix, the Nernst equation provides that the Ca^{2+} concentration in the matrix would be one-million fold higher than in the intermembrane space (Drago et al., 2011). As this is physiologically inconceivable, the presence of a rectifying outward Ca^{2+} flux was sought and observed in 1976 (Puskin et al., 1976). In 2009 Letm1 was putatively identified as the mitochondrial Ca^{2+}/H^{+} (Jiang et al., 2009) exchanger, and the following year NCLX was identified as the mitochondrial Ca^{2+}/Na^{+} exchanger (Palty et al., 2010). However the role of LETM1 in regulating mitochondrial Ca^{+} levels has recently been disputed (De Marchi et al., 2014). Early observations of charge movement across the inner mitochondrial membrane with Ca^{2+} uptake also suggest the existence of a Ca^{2+} uniporter (Rottenberg and Scarpa, 1974; Bernardi, 1999), and in 2011 the channel forming protein (MCU) was simultaneously identified by two independent groups (Baughman et al., 2011; De Stefani et al., 2011). Finally, recent findings suggest the mitochondrial calcium uniporter is a complex of the channel forming protein, MCU, and regulatory proteins MICU1 (Perocchi et al., 2010), MICU2 (Plovanich et al., 2013), and EMRE (Sancak et al., 2013).

Potassium

Transport of K^{+} across the inner mitochondrial membrane primarily serves to maintain mitochondrial volume homeostasis. This is accomplished through regulation of the mitochondrial K^{+} cycle. The electrical potential across the inner membrane generated by expulsion of protons by the ETC drives K^{+} flux into the matrix via K^{+} "leak" and through the mitochondrial ATP-sensitive K^{+} channel (mitoK_{ATP}). This apparent exchange of H^{+} for K^{+} drives up the alkalinity of the matrix providing a pH gradient to drive $H_2PO_4^{-}$ into mitochondria through the

electroneutral phosphate carrier. The uncoupling is not large enough to significantly affect the efficiency of the ETC and the net gain of ions by mitochondria causes the matrices to swell due to additional water uptake. Once a sufficient increase of volume is achieved, K^+ can be ejected through the K^+/H^+ antiporter leading to matrix contraction (Garlid and Paucek, 2003). Thus K^+ and subsequent water transport across the inner mitochondrial membrane provides a mechanism to control matrix volume.

The inner membrane is slightly permeable to water, and whether free diffusion of water across the membrane is solely responsible for matrix volume changes or if aquaporins aid in the process is debated (Kaasik et al., 2007). $AgNO_3$, a potent aquaporin inhibitor, inhibits mitochondrial swelling (Lee et al., 2005) and AQP8 (Calamita et al., 2005) and AQP9 (Amiry-Moghaddam et al., 2005), members of the aquaporin family, are present on the inner mitochondrial membrane in rat liver and brain respectively. However comparative measurements suggests their presence may not contribute to a functional increase in membrane water permeability (Yang et al., 2006).

Mitochondrial volume control plays an important role in regulating cellular function (Kaasik et al., 2007). Higher rates of respiration correlate with increased mitochondrial volume (Lim et al., 2002), enlargement of mitochondria due to K^+ channel openers induces the release of apoptosis signaling proteins cytochrome c and adenylate kinase 2 (Köhler et al., 1999), and increased volume reduces mitochondrial motility in neurons (Safiulina et al., 2006).

Opening of the mitoK_{ATP} channels also provides protection against ischemic injury in cardiac (Garlid et al., 2003) and neuronal tissues (Liu et al., 2002). The cardiac protective effects are often credited to ROS signaling, however conflicting reports state active mitoK_{ATP} increases (Carroll et al., 2001; Forbes et al., 2001) and decreases (Dzeja et al., 2003; Ferranti et al., 2003) ROS levels or their effects. Liu et al. (2002) attribute their observations of neural protection from ischemic injury to a mechanism involving mitoK_{ATP} induced mitochondrial depolarization. However others contest physiological K^+ influx does not significantly depolarize the inner mitochondrial membrane (Garlid, 2000). While mitochondrial K^+ transport is clearly involved in protecting against ischemic insult, many details of the mechanism require further investigation.

Though a definitive identification of the K^+/H^+ antiporter has not been made, observations of mutant yeast strains and subsequent rescue experiments suggest the human proteins LETM1 and LETMD1 may be involved in the antiport activity (Zotova et al., 2010). The gene(s) encoding the mitochondrial K_{ATP} channel is(are) also unidentified, though the channel activity has been observed in patch clamp experiments on rat liver mitoplasts (Inoue et al., 1991).

Concluding Remarks

As the powerhouses of the cell, mitochondria exhibit enormous regulatory control over cellular function. This control is established in the form of altering gradients across the inner membrane, releasing/taking up signaling molecules, synthesizing precursors and products for use outside of the matrix, and responding to changes in nutrient availability. Selective transport of nutrients, intermediates, and electrolytes into/out of the mitochondrial matrix is upstream of all of these forms of regulatory control, thus regulating mitochondrial carriers is central to maintaining cellular homeostasis and responding to stress or stimuli, and provides a bounty of pharmacological targets to correct cellular dysfunction.

Acknowledgements

The material in this chapter is currently being prepared for submission for publication. Nathaniel M. Vacanti is the primary author and Christian M. Metallo is a co-author of this material.

Chapter 3

Regulation of Substrate Utilization by the Mitochondrial Pyruvate Carrier

Summary

Pyruvate lies at a central biochemical node connecting carbohydrate, amino acid, and fatty acid metabolism, and the regulation of pyruvate flux into mitochondria represents a critical step in intermediary metabolism impacting numerous diseases. To characterize changes in mitochondrial substrate utilization in the context of compromised mitochondrial pyruvate transport, we applied ^{13}C metabolic flux analysis (MFA) to cells after transcriptional or pharmacological inhibition of the mitochondrial pyruvate carrier (MPC). Despite profound suppression of both glucose and pyruvate oxidation, cell growth, oxygen consumption, and tricarboxylic acid (TCA) metabolism were surprisingly maintained. Oxidative TCA flux was achieved through enhanced reliance on glutaminolysis through malic enzyme and pyruvate dehydrogenase (PDH) as well as fatty acid and branched-chain amino acid oxidation. Thus, in contrast to inhibition of complex I or PDH, suppression of pyruvate transport induces a form of metabolic flexibility associated with the use of lipids and amino acids as catabolic and anabolic fuels.

Introduction

Mitochondria execute core metabolic functions in eukaryotes ranging from catabolic energy conversion to anabolism of biosynthetic intermediates. Cells must negotiate their nutritional environment to control which substrates are metabolized in mitochondria while continuing to

meet their bioenergetic and/or biosynthetic needs. Pyruvate lies at the intersection of glycolysis, gluconeogenesis, and the tricarboxylic acid (TCA) cycle; as such, its transport into the mitochondrial matrix influences carbohydrate, fatty acid, and amino acid metabolism. Dysregulation of these processes contributes to the pathogenesis of numerous diseases, including diabetes and obesity (DeFronzo and Tripathy, 2009; Sugden et al., 2009), mitochondrial disorders (Kerr, 2013), cardiac failure (Fillmore and Lopaschuk, 2013), neurodegenerative disorders (Cunnane et al., 2010; Yao et al., 2011), and cancer (Currie et al., 2013; Tennant et al., 2010). Therefore, strategies that modulate the extent of pyruvate flux into mitochondrial pathways may have therapeutic potential by directly or indirectly affecting glucose, lipid, and/or amino acid homeostasis in the body.

Existence of a protein carrier to facilitate pyruvate transport into mitochondria has been recognized for decades (Halestrap and Denton, 1974; Papa et al., 1971). Although activity of this transporter and sensitivity to inhibitors have been characterized (Clark and Land, 1974; Halestrap and Denton, 1974; Papa and Paradies, 1974), the genes encoding this complex remained a mystery for many years. Two recent studies revealed strong evidence that the genes, renamed *MPC1* and *MPC2*, encode the multimeric mitochondrial pyruvate carrier (MPC) complex embedded in the inner mitochondrial membrane (Bricker et al., 2012; Herzig et al., 2012). Indeed, Herzig et al. (2012) observed that coexpression of *Mpc1* and *Mpc2* in *Lactococcus lactis* induced a 4-fold increase in pyruvate uptake. Consistent with these results, Bricker et al. (2012) described the functional redundancy of MPC across several species (yeast, *Drosophila*, human) and identified a mutation in *MPC1* that confers resistance to inhibition by the α-cyanocinnamate analog UK5099 (Halestrap, 1975). These discoveries provide an exciting potential drug target through which mitochondrial substrate utilization may be controlled in the context of metabolic disorders. In fact, the MPC has emerged as an unanticipated target of thiazolidinediones (Colca et al., 2013; Divakaruni et al., 2013), a class of insulin sensitizing drugs, and as a regulator of insulin secretion (Patterson et al., 2014; Vigueira et al., 2014), suggesting that this transporter plays a central role in substrate selection and metabolic signaling. Moreover, recent work shows that the phosphodiesterase inhibitor Zaprinast can alter aspartate and glutamate metabolism via the MPC (Du et al., 2013) and glutaminase (Elhammali et al., 2014).

The high biosynthetic and energetic demands of skeletal muscle myoblasts render them an ideal system to characterize the influence of mitochondrial pyruvate carrier function on metabolic flux and substrate selection. This study examines metabolic flux regulation by MPC in the context of the metabolic network in intact cells. *Mpc1* or *Mpc2* was chronically suppressed using lentiviral-mediated delivery of shRNAs and/or pharmacologically inhibited with UK5099 in both proliferating and differentiated mouse C2C12 muscle cells, several human transformed cell lines, and primary human skeletal myotubes (hSKMs). Surprisingly, proliferating myoblasts maintained growth and ATP-linked respiration despite profound inhibition of MPC activity; however, reliance on substrates for energy and biosynthetic metabolism shifted from glucose to amino acid and fatty acid oxidation. TCA flux and fatty acid synthesis were maintained through increased glutamine anaplerosis and oxidation, malic enzyme flux, and fatty acid oxidation. Finally, pharmacological inhibition of MPC activity in hSKMs increased the extent that branched-chain amino acids (BCAAs) were oxidized in the TCA cycle.

Results

Proliferation and Oxidative Metabolism Are Maintained upon *Mpc* Depletion

To investigate how metabolism is reprogrammed in response to MPC inhibition, we depleted Mpc levels in C2C12 myoblasts using targeting *Mpc1* (Mpc1KD), *Mpc2* (Mpc2KD), or control sequences (control). Stable knockdown was confirmed at the transcriptional and protein levels (Figures 3.1A and 3.1B). Despite the importance of glucose and pyruvate metabolism for biosynthesis and ATP generation, cell proliferation rates and ATP-linked respiration were unaffected by the absence of Mpc1 and Mpc2 (Figures 3.1C and 3.1D). In fact, *Mpc* knockdown only influenced oxygen consumption in the uncoupled state when all substrates were present, while pyruvate-dependent respiration in permeabilized cells was significantly compromised (Figure 3.1D). Surprisingly, *Mpc* knockdown had little effect on glucose and glutamine uptake, as well as lactate and glutamate secretion, though pyruvate secretion was significantly increased (Figure 3.1E).

We next performed a targeted metabolomic analysis to gain more insight into the intra-

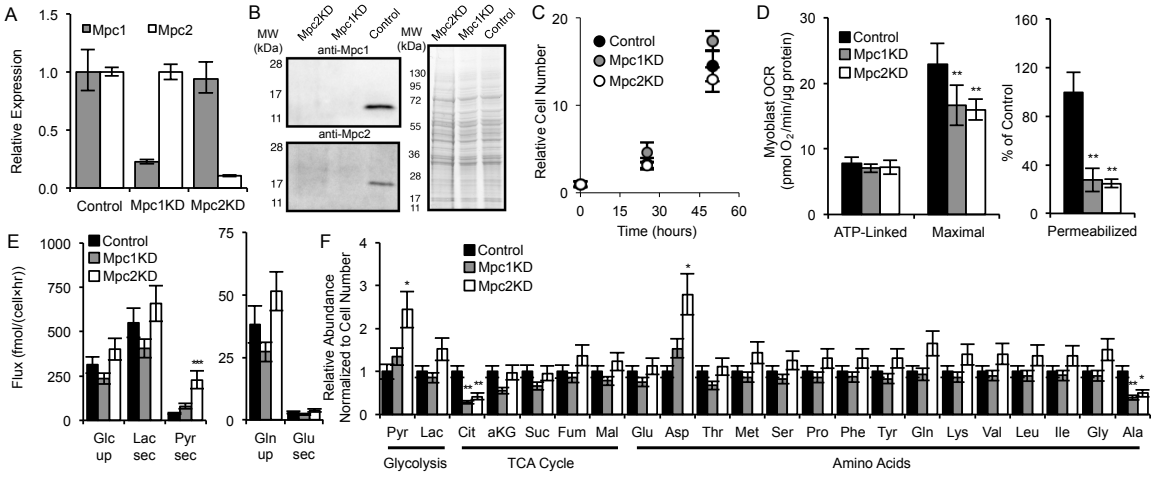

Figure 3.1: MPC Knockdown Does Not Affect the Overall Metabolic State of Cells. (A and B) Relative expression of *Mpc1* and *Mpc2* as determined by qPCR (A) and western blot (B). (C-E) Proliferation (C), oxygen consumption rates (OCRs; D), and extracellular substrate fluxes (E) of control, Mpc1KD, and Mpc2KD cells. (D) ATP-linked and maximal respiration of intact cells and pyruvate-dependent respiration in permeabilized cells (measured as outlined in Experimental Procedures). (F) Relative abundance of intracellular metabolites. Error bars represent minimum and maximum relative expression as calculated by qPCR data analysis software (A), standard deviation (SD) (C and E), or standard error of the mean (SEM) (D and F). *$p < 0.05$, **$p < 0.01$, and ***$p < 0.001$ by ANOVA with Dunnett's post hoc test.

cellular metabolic changes occurring upon Mpc depletion (Figure 3.1F). Intracellular pyruvate was elevated upon *Mpc* knockdown, whereas the abundances of most TCA cycle intermediates were unaffected. Citrate levels, however, were markedly decreased in Mpc1KD or Mpc2KD (Mpc1/2KD) cells, as this metabolite is generated predominantly from pyruvate-derived AcCoA under normal growth conditions (Metallo et al., 2012). Aspartate and alanine abundances were significantly increased and decreased, respectively, suggesting that amino acid metabolism was altered to maintain metabolic homeostasis.

Oxidative Glutaminolysis Supports the TCA Cycle in Cells Lacking Mpc

To gain more detailed insights into mitochondrial substrate utilization, we cultured cells in the presence of [U-$^{13}C_6$]glucose for 24 hr and observed steady-state isotopic labeling (Figure S3.1A). Consistent with the expected decrease in glucose-derived pyruvate oxidation, labeling of citrate and all TCA intermediates was significantly decreased in Mpc1/2KD cells relative to

controls (Figures 3.2A and 3.2B). While the relative abundances of fully labeled (M3) lactate and pyruvate were unchanged in Mpc1/2KD cells, the extent of alanine labeling from [U-$^{13}C_6$]glucose was significantly decreased (Figure 3.2C). Additionally, we observed an increase in de novo serine synthesis from glucose in the cytosol (Figure 3.2D), highlighting potential compartment-specific shifts in amino acid metabolism (Figure S3.1B).

Next, we cultured C2C12 myoblasts in the presence of [U-$^{13}C_5$]glutamine to detect changes in glutamine utilization in the context of decreased Mpc function. The abundance of fully labeled succinate, fumarate, α-ketoglutarate, and malate increased significantly in Mpc1/2KD cells (Figure 3.2E), suggesting that cells increase their reliance on glutamine anaplerosis when mitochondrial pyruvate transport is limited. Isotopic enrichment in citrate provides additional insight into the reprogramming of TCA metabolism. Increased M5 citrate abundance from [U-$^{13}C_5$]glutamine can arise via reductive carboxylation by isocitrate dehydrogenase (IDH) enzymes, and M6 citrate arises through the combined activity of glutaminolysis and pyruvate dehydrogenase (Figure 3.2F) (Le et al., 2012; Metallo and Vander Heiden, 2013). In the glutaminolysis pathway, glutamine is oxidized in the mitochondria and converted to pyruvate via malic enzymes (MEs). AcCoA is then generated by the PDH complex and condenses with oxaloacetate to form citrate (Figure 3.2F). The relative abundances of both M5 and M6 mass isotopomers were significantly increased in Mpc1/2KD cells (Figure 3.2G). Furthermore, the abundance of glutamine-derived alanine was significantly elevated (Figure 3.2H), consistent with higher flux through mitochondrial MEs as opposed to reductive carboxylation.

To further highlight the increased role of glutaminolysis in cells with *Mpc* knockdown, we measured uncoupled respiration in the absence or presence of the glutaminase inhibitor, bis-2-(5-phenylacetamido-1,3,4-thiazol-2-yl)ethyl sulfide (BPTES). Uncoupler-stimulated respiration in Mpc1/2KD cells was more sensitive to BPTES treatment, signifying an increased reliance on glutamine oxidation in these cells (Figure 3.2I). Collectively, these results provide evidence that cells with depleted Mpc1 or Mpc2 increase oxidative glutamine metabolism to maintain flux through the TCA cycle.

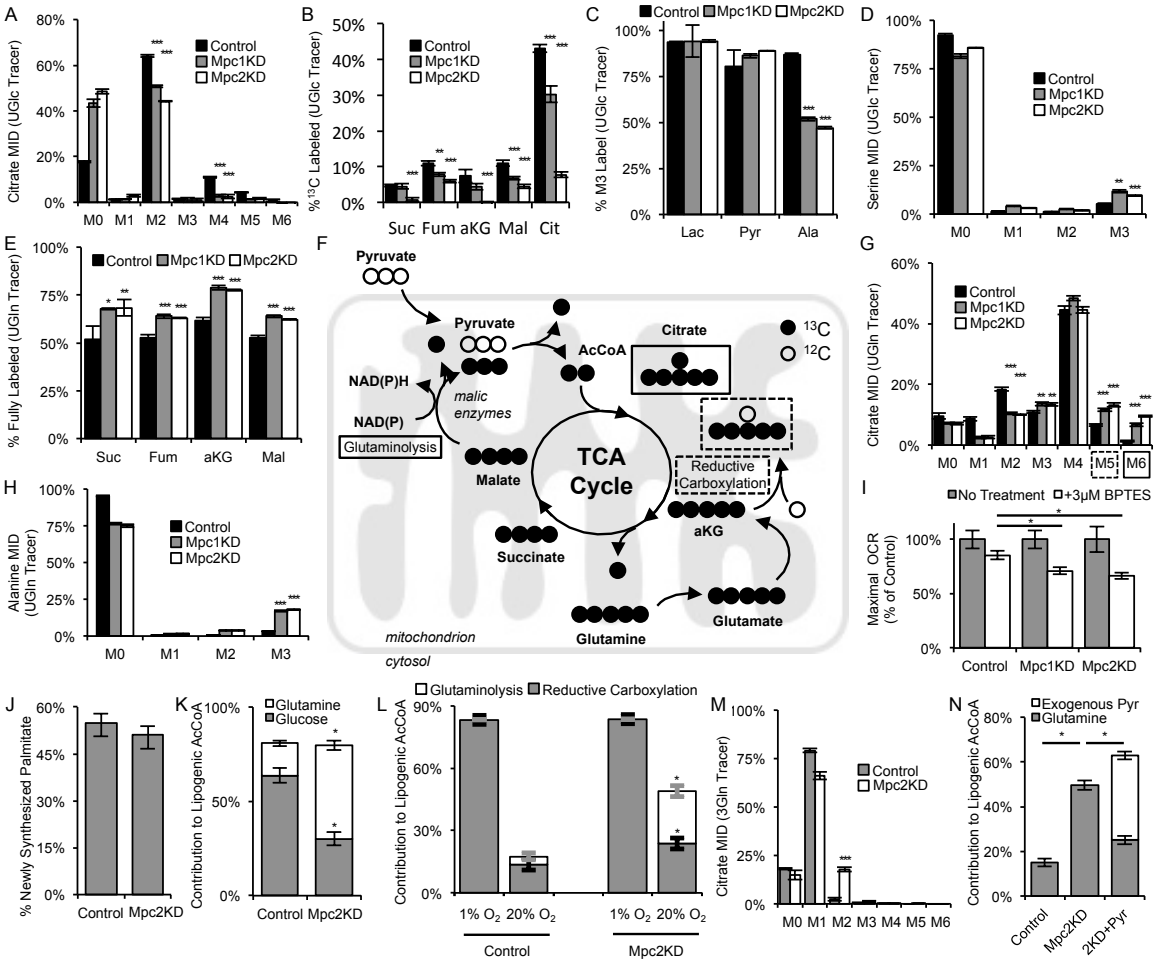

Figure 3.2: MPC Regulates Mitochondrial Substrate Utilization. (A) Citrate mass isotopomer distribution (MID) resulting from culture with [U-$^{13}C_6$]glucose (UGlc). (B) Percentage of ^{13}C-labeled metabolites from UGlc. (C) Percentage of fully labeled lactate, pyruvate, and alanine from UGlc. (D) Serine MID resulting from culture with UGlc. (E) Percentage of fully labeled metabolites derived from [U-$^{13}C_5$]glutamine (UGln). (F) Schematic of UGln labeling of carbon atoms in TCA cycle intermediates arising via glutaminolysis and reductive carboxylation. Mitochondrion schematic inspired by Lewis et al. (2014). (G and H) Citrate (G) and alanine (H) MIDs resulting from culture with UGln. (I) Maximal oxygen consumption rates with or without 3 μM BPTES in medium supplemented with 1 mM pyruvate. (J) Percentage of newly synthesized palmitate as determined by ISA. (K) Contribution of UGln and UGlc to lipogenic AcCoA as determined by ISA. (L) Contribution of glutamine to lipogenic AcCoA via glutaminolysis (ISA using [3-^{13}C]glutamine [3Gln]) and reductive carboxylation (ISA using [5-^{13}C]glutamine [5Gln]) under normoxia and hypoxia. (M) Citrate MID resulting from culture with 3Gln. (N) Contribution of UGln and exogenous [3-^{13}C]pyruvate (3Pyr) to lipogenic AcCoA. 2KD+Pyr refers to Mpc2KD cells cultured with 10 mM extracellular pyruvate. Error bars represent SD (A-E, G, H, and M), SEM (I), or 95% confidence intervals (J-L, and N). *$p < 0.05$, **$p < 0.01$, and ***$p < 0.001$ by ANOVA with Dunnett's post hoc test (A-E and G-I) or * indicates significance by nonoverlapping 95% confidence intervals (J-L and N).

Mpc Knockdown Induces Substrate Switching for De Novo Lipogenesis

We next quantified isotope enrichment in palmitate and performed isotopomer spectral analysis (ISA) to determine (1) the percent of newly synthesized palmitate after tracer addition and (2) the relative contribution of glucose and glutamine to lipogenic AcCoA (Kharroubi et al., 1992; Metallo et al., 2012). Although we observed no significant change in relative palmitate synthesis upon Mpc depletion (Figure 3.2J), the extent of glutamine conversion to the lipogenic AcCoA pool was significantly increased in Mpc2KD cells (Figure 3.2K). Glutamine can contribute carbon to fatty acid synthesis via reductive carboxylation or oxidative glutaminolysis. The former pathway is highly active in cells proliferating under hypoxia or those with a compromised respiratory chain (Metallo et al., 2012; Mullen et al., 2012; Scott et al., 2011; Wise et al., 2011), while the latter pathway has been observed in B cell lymphoma (Le et al., 2012). While the contribution of glutamine flux through reductive carboxylation to lipogenesis increased in control and Mpc2KD cells cultured under hypoxia (measured specifically using [5-^{13}C]glutamine (Yoo et al., 2008)), flux through this pathway did not account for the increased glutamine-derived AcCoA in Mpc2KD cells grown under normoxia. The increased glutamine-derived AcCoA was almost exclusively attributed to the glutaminolysis pathway, as evidenced by transfer of label from [3-^{13}C]glutamine to palmitate (Figures 3.2L and S3.1C). We also measured a significant increase in M2 labeling of citrate in Mpc2KD myoblasts cultured with [3-^{13}C]glutamine (Figure 3.2M), which arises from condensation of labeled oxaloacetate and AcCoA (Figure S3.1C). No change in labeling was observed in lactate (Figure S3.1D), providing evidence that this ME flux was catalyzed within the mitochondrial compartment. These results demonstrate that Mpc knockdown causes metabolic reprogramming that is distinct from hypoxia-associated PDH inhibition (Kim et al., 2006; Papandreou et al., 2006), with an increased proportion of mitochondrial AcCoA derived from mitochondrial ME and PDH activity rather than reductive carboxylation.

At high concentrations, pyruvate passively enters the matrix, bypassing the MPC (Bakker and van Dam, 1974; Halestrap, 1975). To further demonstrate that PDH activity is maintained in *Mpc* knockdown cells, we quantified how glutamine to AcCoA conversion was affected by exogenous pyruvate. In the presence of 10 mM extracellular pyruvate, Mpc2KD cells failed to

increase the contribution of glutamine carbon to palmitate synthesis. Indeed, this difference was entirely accounted for by the conversion of exogenous [3-^{13}C]pyruvate to lipogenic AcCoA through the PDH complex (Figure 3.2N).

Amino Acid and β-Oxidation Fuel Mitochondrial Metabolism upon *Mpc* Knockdown

To quantify changes in intracellular fluxes in a more unbiased and comprehensive manner, we conducted ^{13}C MFA on Mpc2KD and control cells. Steady-state mass isotopomer distributions (MIDs) measured in cells cultured with [U-$^{13}C_5$]glutamine and [1,2-$^{13}C_2$]glucose along with independently determined uptake/secretion fluxes were incorporated into a model of central carbon metabolism (Ahn and Antoniewicz, 2011; Murphy et al., 2012). The INCA software suite was used to estimate fluxes and associated confidence intervals using an elementary metabolite unit-based algorithm (Antoniewicz et al., 2006; Young, 2014). Results are illustrated in Figures 3.3A, S3.2A, and S3.2B and tabulated in Tables S3.1 and S3.2; a detailed description of the model, data, and assumptions are included in the Supplemental Experimental Procedures and in Table S3.3. Flux data indicated that mitochondrial pyruvate transport and PDH flux decreased significantly upon *Mpc2* knockdown. Oxidative TCA flux through IDH was also decreased with no absolute increase in reductive carboxylation flux, while pyruvate cycling and glutaminolytic flux were increased. Increased flux through mitochondrial MEs at least partially sustained AcCoA metabolism. Intriguingly, an acceptable fit for *Mpc2* knockdown cells could only be obtained when an exogenous source of AcCoA was included in the model. Flux from this AcCoA pool into the TCA cycle increased 5-fold in Mpc2KD cells compared to control cells, suggesting that oxidation of mitochondrial substrates other than glutamine were also induced upon Mpc depletion (Figure 3.3A and Tables S3.1 and S3.2). Given the lack of branched-chain amino acid (BCAA) oxidation to TCA intermediates observed in both control and Mpc2KD cells (Figure S3.2C), we hypothesized that this AcCoA was derived from β-oxidation. To more explicitly determine if *Mpc* knockdown drives an increase in fatty acid oxidation, we cultured Mpc2KD and control cells in the presence of [U-$^{13}C_{16}$]palmitate bound to BSA and observed ^{13}C enrichment in TCA intermediates. We observed a significant increase in the relative abundance

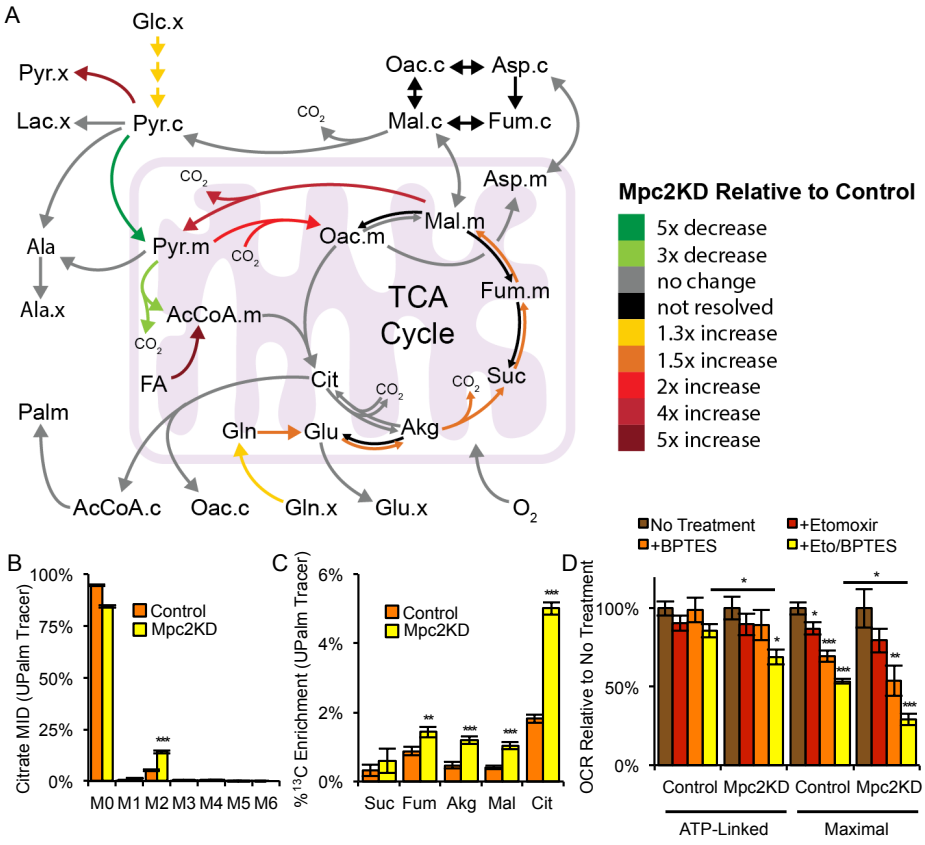

Figure 3.3: Mpc Knockdown Increases Fatty Acid Oxidation. (A) Schematic of changes in flux through metabolic pathways in Mpc2KD relative to control cells. (B) Citrate MID resulting from culture with [U-$^{13}C_{16}$]palmitate conjugated to BSA (UPalm). (C) Percentage of ^{13}C enrichment resulting from culture with UPalm. (D) ATP-linked and maximal oxygen consumption rate, with or without 20 µM etomoxir, with or without 3 µM BPTES. Culture medium supplemented with 0.5 mM carnitine. Error bars represent SD (B and C) or SEM (D). *$p < 0.05$, **$p < 0.01$, and ***$p < 0.001$ by two-tailed, equal variance, Student's t test (B-D), or by ANOVA with Dunnett's post hoc test (D).

of M2 citrate from this tracer in Mpc2KD compared to control cells (Figure 3.3B). Increased label incorporation into numerous TCA metabolites downstream of citrate was also detected (Figure 3.3C), indicating that knockdown of *Mpc2* induced a significant increase in fatty acid oxidation flux in C2C12 myoblasts.

To confirm the observed metabolic shifts in mitochondrial substrate utilization in an orthogonal manner, we quantified the ATP-linked and maximal respiration of each cell line in the presence of either or both BPTES and etomoxir. The former compound inhibits glutamine oxidation via glutaminase, whereas the latter inhibits fatty acid oxidation at carnitine palmitoyltransferase-1 (CPT1). ATP-linked respiration was only affected when all three pathways (i.e., pyruvate transport, glutamine, and fatty acid oxidation) were inhibited (Figures 3.1D, 3.3D, and S3.2D for raw values). On the other hand, maximal respiration was significantly decreased by each individual treatment, with the most pronounced effect being observed when BPTES and etomoxir were both added to the culture (Figures 3.1D, 3.3D, and S3.2E for raw values). The synergistic effect of inhibiting these three mitochondrial substrate oxidation pathways highlights the plasticity of mitochondrial metabolism in respiring cells and independently demonstrates that Mpc depletion potentiates cells to employ fatty acid and amino acid oxidation to meet their bioenergetic demands.

Small Molecule Inhibition of MPC Enhances Amino Acid and Fatty Acid Oxidation

Pharmacological inhibition of Mpc function rather than shRNAs may provide a more clinically relevant means of exploiting mitochondrial flexibility. To determine whether small molecules targeting the Mpc elicit effects similar to that of inhibition at the transcriptional level, we treated cells with UK5099, which covalently binds to Mpc and blocks pyruvate transport (Hildyard et al., 2004). Culture of proliferating C2C12 cells for 24 hr with 10 μM UK5099 in the presence of [U-$^{13}C_6$]glucose revealed a relative decrease in glucose flux to the TCA cycle, and results using [U-$^{13}C_5$]glutamine indicate that glutaminolytic flux through malic enzyme was significantly increased, as evidenced by the relative abundance of M6 citrate (Figures 3.4A and 3.4B). As observed in the comparison to hypoxia (Figure 3.2L), the metabolic response to

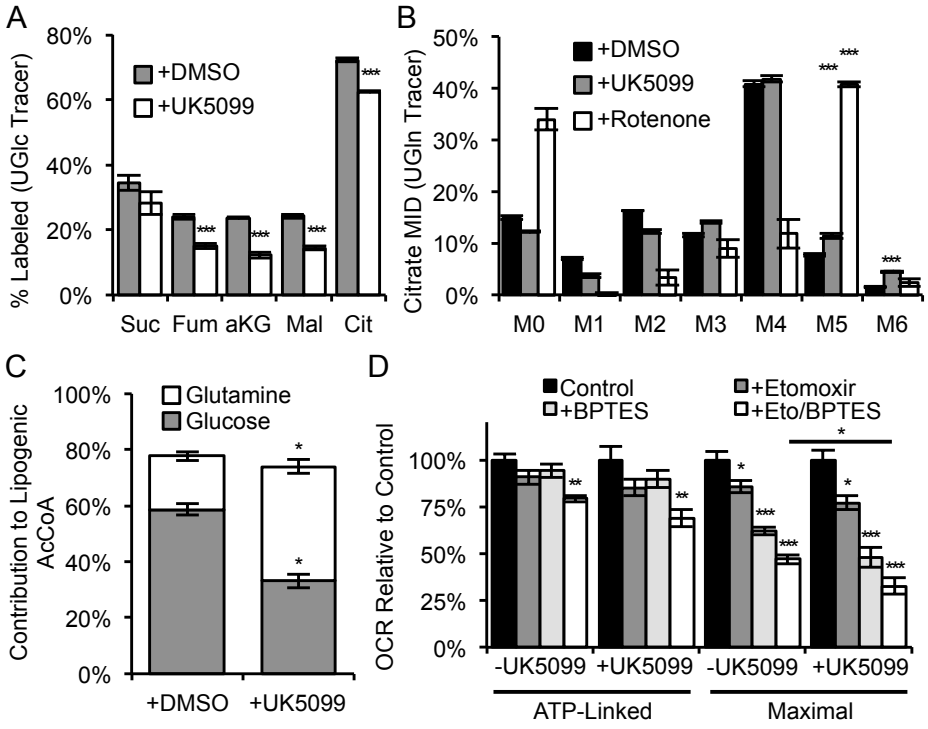

Figure 3.4: Metabolic Reprogramming Resulting from Pharmacological Mpc Inhibition Is Distinct from Hypoxia or Complex I Inhibition. (A) Percentage of ^{13}C-labeled metabolites from UGlc, with or without 10 μM UK5099. (B) Citrate MID resulting from culture with UGln, with or without 10 μM UK5099 or with or without 30 nM rotenone. (C) Relative contribution of UGlc and UGln to lipogenic AcCoA, with or without 10 μM UK5099. (D) ATP-linked and maximal oxygen consumption rate, with or without 10 μM UK5099, with or without 20 μM etomoxir, and with or without 3 μM BPTES. Culture medium supplemented with 0.5 mM carnitine. Cells were pretreated with 10 μM UK5099 (A and C). Error bars represent SD (A and B), 95% confidence intervals (C), or SEM (D). *$p < 0.05$, **$p < 0.01$, and ***$p < 0.001$ by two-tailed, equal variance, Student's t test (A and D), by ANOVA with Dunnett's post hoc test (B and D) or * indicates significance by nonoverlapping 95% confidence intervals (C).

UK5099 treatment is distinct from that occurring in response to complex I inhibition. Whereas oxidative TCA flux is maintained during UK5099 treatment, rotenone, a potent inhibitor of complex I, shuts down oxidative glutamine metabolism and increases reductive carboxylation activity, resulting in a dramatic increase in the relative abundance of M5 citrate from [U-$^{13}C_5$]glutamine (Figure 3.4B). C2C12 myoblasts also displayed a shift away from glucose to glutamine as a substrate for fatty acid synthesis in the presence of UK5099 (Figure 3.4C).

Additionally, ATP-linked and uncoupled oxygen consumption were measured when C2C12 cells were cultured for 24 hr with UK5099 to examine their dependency on different oxidative substrates. We observed no change in ATP-linked or maximal respiration with UK5099 treatment, presumably due to the metabolic plasticity of cells when other pathways (i.e., glutamine and fatty acid oxidation) were not inhibited (Figures 3.4D, S3.2F, and S3.2G for raw values). However, when cells were treated with combinations of UK5099, BPTES, and etomoxir, we detected a significant effect of UK5099 only with combinatorial treatments (Figures 3.4D, S3.2F, and S3.2G for raw values). These results further highlight the flexibility of oxidative mitochondrial metabolism that can be induced by Mpc inhibition such that C2C12 cells meet their energetic demands through glutamine and fatty acid oxidation.

Proliferating Human Transformed Cells Reprogram Metabolism upon MPC Inhibition

To validate these findings in human cells using independent shRNAs, MPC levels were also depleted in A549 carcinoma cells using shRNAs targeting *MPC1* (MPC1KD), *MPC2* (MPC2KD), or a control sequence. These cells were cultured with [U-$^{13}C_6$]glucose, [U-$^{13}C_5$]glutamine, and [U-$^{13}C_{16}$]palmitate-BSA to observe metabolic reprogramming in response to MPC depletion. Results supported findings in C2C12 myoblasts, as glucose conversion to citrate, TCA intermediates, and alanine were all significantly decreased in MPC1/2KD A549 cells (Figures S3.3A-S3.3C). On the other hand, glutamine anaplerosis and oxidation through malic enzymes were elevated upon *MPC* knockdown in these cells, as evidenced by labeling of TCA intermediates (citrate in particular) and alanine from [U-$^{13}C_5$]glutamine and [3-^{13}C]glutamine (Figures S3.3D-S3.3G). Finally, we observed that

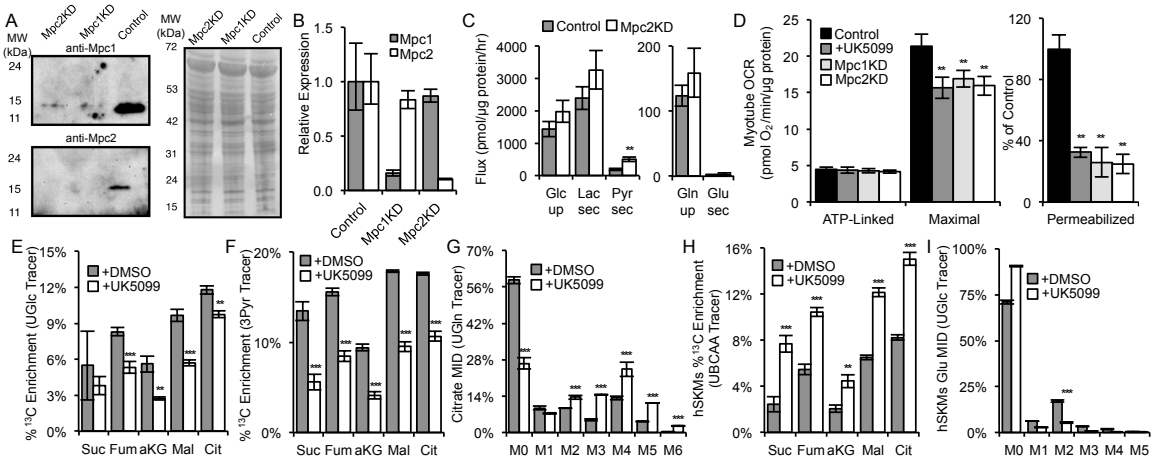

Figure 3.5: Mpc Controls Oxidative Substrate Utilization in Myotubes. (A and B) Protein (A) and mRNA (B) levels of Mpc1 and Mpc2. (C) Extracellular substrate fluxes in Control or Mpc2KD C2C12 myotubes. (D) ATP-linked and maximal OCR of intact C2C12 myotubes and pyruvate-dependent OCR of permeabilized C2C12 myotubes. (E and F) Percentage of ^{13}C enrichment resulting from culture of C2C12 myotubes with UGlc (E) and 3Pyr (F) for 2 hr, with or without 5 μM UK5099. (G) Citrate MID resulting from culture of C2C12 myotubes with UGln, with or without 10 μM UK5099. (H) Percentage of ^{13}C enrichment in patient 1 hSKMs cultured with [U-$^{13}C_5$]valine, [U-$^{13}C_6$]leucine, and [U-$^{13}C_6$]isoleucine (collectively UBCAA), with or without 10 μM UK5099. (I) hSKMs glutamate MID resulting from culture with [U-$^{13}C_6$]glucose, with or without 10 μM UK5099. Error bars represent minimum and maximum relative expression as calculated by qPCR data analysis software (B), SD (C and E-I), or SEM (D). *$p < 0.05$, **$p < 0.01$, and ***$p < 0.001$ by a two-tailed, equal variance, Student's t test (C and E-I), or by ANOVA with Dunnett's post hoc test (D).

MPC1KD A549 cells exhibited an increased reliance on fatty acid oxidation to fuel TCA cycle metabolism, as ^{13}C labeling of citrate and other TCA metabolites derived from [U-$^{13}C_{16}$]palmitate increased significantly (Figures S3.3H and S3.3I). A549 cells also responded to pharmacological inhibition of MPC by UK5099, as glucose contribution to the TCA cycle declined (Figure S3.3J) and glutamine oxidation increased (Figure S3.3K). Finally, both A549 cells and the Huh7 human hepatocarcinoma cell line increased their reliance on fatty acid oxidation to fuel TCA metabolism upon MPC inhibition (Figures S3.3L and S3.3M).

MPC Influences Mitochondrial Substrate Utilization in Differentiated Myotubes

To determine whether Mpc functions similarly in more differentiated cells, we formed myotubes using control, Mpc1KD, and Mpc2KD C2C12 cells via 4-day treatments with 2%

horse serum. Differentiation was confirmed by observing elongation and fusion of myoblasts to form multinucleated tubes using light microscopy and by immunofluorescent staining of desmin, a marker of differentiated muscle (Figure S3.4A). Maintenance of the knockdown upon differentiation was confirmed at the protein and mRNA levels (Figures 3.5A and 3.5B). Knockdown of *Mpc* did not affect glycolytic flux in C2C12 myotubes, as lactate secretion, glucose uptake, and the ratio of the two were surprisingly unchanged (Figure 3.5C). Furthermore, respiratory inhibition of intact cells presented with all substrates was evident only when oxidative phosphorylation was uncoupled, yet Mpc activity was clearly compromised as indicated by a decreased rate of pyruvate-driven respiration in permeabilized myotubes (Figure 3.5D).

Targeted metabolomic analysis revealed increases in intracellular abundances of pyruvate and aspartate in Mpc2KD myotubes (Figure S3.4B). In contrast to proliferating cells, myotubes rely primarily on glucose carbon for the generation of TCA intermediates (rather than glutamine) (Figure S3.4C). To better resolve changes in pyruvate metabolism upon *Mpc* knockdown or inhibition, we cultured myotubes in the presence of either [U-$^{13}C_6$]glucose or [3-^{13}C]pyruvate for 2 hr before quantifying isotopic labeling in TCA intermediates. Enrichment of glucose and pyruvate carbons in the TCA cycle was significantly decreased in response to UK5099 treatment (Figures 3.5E and 3.5F) or when comparing Mpc2KD to control myotubes (Figures S3.4D and S3.4E). Importantly, the pool sizes of all intermediates shown was less than or equal to those quantified in controls. As such, the decreased labeling observed under non-steady-state conditions is indicative of decreases in metabolic flux (rather than pool size changes). Additionally, we observed a significant increase in glutaminolysis in C2C12 myotubes treated with UK5099, as evidenced by steady-state labeling from [U-$^{13}C_5$]glutamine (Figure 3.5G). Similar trends were observed in myotubes generated using control or Mpc2KD cells (Figure S3.4F). Although the lower metabolic rate of nonproliferating myotubes (compared to proliferating cells) minimized the observed differences and limited our ability to quantify fatty acid oxidation in these cultures, results indicate that Mpc inhibition induces differentiated myotubes to increase glutamine oxidation.

Whereas glutamine is an important substrate for proliferating cells, BCAAs are critical bioenergetic substrates for muscle and other tissues, particularly in the fasted state (Rosenthal

et al., 1974). BCAAs have recently been demonstrated to accumulate in the context of obesity and insulin resistance (Adams, 2011; Newgard et al., 2009; Wang et al., 2011), though the mechanisms leading to this metabolic phenotype (i.e., higher intake, decreased catabolism) are not yet clear. We failed to detect significant flux through this pathway in any of the C2C12 myoblasts (Figure S3.2C), myotubes, or engineered lines generated here using [^{13}C]BCAA tracers. To determine whether MPC inhibition promoted BCAA catabolism in a more physiologically relevant system, we cultured hSKMs in medium containing [U-$^{13}C_5$]valine, [U-$^{13}C_6$]leucine, and [U-$^{13}C_6$]isoleucine in the presence or absence of UK5099. Notably, ^{13}C enrichment throughout the TCA cycle was significantly increased in hSKMs treated with 10 μM UK5099 compared to controls (Figures 3.5H and S3.4G). As expected, glucose oxidation was inhibited in hSKMs cultured with UK5099 (Figure 3.5I). Consistent increases in BCAA oxidation were observed in hSKMs obtained from two independent subjects (Figures 3.5H and S3.4G). These results suggest that mitochondrial substrate utilization can be controlled in terminally differentiated hSKMs by modulating Mpc activity to influence BCAA catabolism.

Discussion

Traditional approaches to modulate eukaryotic cell metabolism have focused on controlling enzyme activity and/or expression. Such treatments can cause bottlenecks and place constraints on cells that limit metabolism globally. Since metabolic processes in eukaryotes are segregated within the mitochondrial matrix, cytosol, and other subcellular compartments, an alternate approach may be to target compartment-specific transporters and exploit the inherent metabolic flexibility of cells to control substrate utilization. In this manner, cells and tissues that pathologically rely on particular nutrients (e.g., anabolic glucose metabolism in diabetes, obesity, and cancer) may be coaxed to shift toward a catabolic state of metabolism while maintaining enzyme activity throughout the cell. A critical step in this process is to functionally characterize how substrate utilization and intracellular metabolic activity (i.e., fluxes) are reprogrammed upon inhibition of specific transporters (Zamboni et al., 2008). Here we have outlined the metabolic phenotype of cell lines and hSKMs that emerge upon inhibition of the mitochon-

drial pyruvate transporter encoded by *MPC1* and *MPC2*. The observed changes in substrate utilization provide some insights through which MPC inhibition can elicit beneficial effects via reprogramming of mitochondrial metabolism.

Knockdown of either *Mpc1* or *Mpc2* abrogated expression of both proteins, as observed previously (Divakaruni et al., 2013). Comprehensive ^{13}C MFA integrating data from parallel tracer experiments using [^{13}C]glucose and [^{13}C]glutamine were applied to *Mpc* knockdown cells, as this modeling approach has been shown to increase flux resolution throughout central carbon metabolism (Ahn and Antoniewicz, 2012). Although ATP-linked respiration and cell growth remained unchanged, we identified specific changes in amino acid and fatty acid metabolism that were recapitulated using the MPC inhibitor UK5099. Glucose metabolism in the TCA cycle was significantly decreased, but not completely, presumably due to incomplete knockdown, passive diffusion, or the presence of an alternate or nonfacilitated transport mechanism. Rather than divert excess cytosolic pyruvate to lactate or alanine, this carbon was either secreted from cells as pyruvate or converted to serine. This latter activity may be driven by accumulation of glycolytic intermediates (Chaneton et al., 2012; Ye et al., 2012) or due to increased serine catabolism in mitochondria (Jain et al., 2012; Lewis et al., 2014). Notably, alanine levels were significantly decreased in *Mpc* knockdown cells, highlighting a role for mitochondrial pyruvate and mitochondrial alanine aminotransferase (ALT2) in mediating glutamine anaplerosis, which was previously described in cancer cells (Weinberg et al., 2010). The accumulation of aspartate in these cells provides evidence of the expected switch to rely on oxaloacetate and mitochondrial glutamic-oxaloacetic transaminase 2 (GOT2) to facilitate this process (Figure S3.1B). A similar response was observed in isolated retina treated with the MPC inhibitor Zaprinast (Du et al., 2013).

In addition to these metabolomic changes, we also observed increased amino acid and fatty acid oxidation upon inhibition of MPC. Elevated glutamine anaplerosis and oxidation are likely a consequence of decreased citrate synthase and oxidative IDH flux downstream of PDH while the ETC remained active (Fan et al., 2012; Le et al., 2012). We also observed a significant increase in BCAA oxidation upon MPC inhibition using hSKM cultures, which are of perhaps greater physiological relevance than C2C12 cells. Consistent with this change, Bricker et al.

(2012) and Herzig et al. (2012) both observed growth defects in medium lacking leucine or valine in their characterizations of yeast with *Mpc* deletions. Mpc inhibition may potentiate oxidation of BCAAs or other amino acids that accumulate in the context of insulin resistance (Adams, 2011; Newgard et al., 2009; Wang et al., 2011). Citrate mass isotopomer labeling and flux estimations also highlighted a significant increase in flux through malic enzyme upon *Mpc* knockdown, which could provide additional reducing equivalents (NAD[P]H) within the matrix. These results are consistent with the severe growth defect previously observed in yeast with deletions in both *mpc1* and mitochondrial malic enzyme growing on glucose (Bricker et al., 2012), highlighting the remarkably conserved nature of metabolism across species.

An initial lack of fit observed in our *Mpc* knockdown model led us to hypothesize that fatty acid oxidation was increased under these conditions. This response was validated by tracing with [^{13}C]palmitate-BSA in myoblasts and cancer cells and using either shRNAs or UK5099 to inhibit mitochondrial pyruvate transport. Here, β-oxidation was presumably stimulated, in part, due to decreases in citrate and the downstream lipogenic intermediate malonyl-CoA, which inhibits CPT1 (McGarry et al., 1983). In this manner, pharmacological inhibition of the MPC could stimulate catabolic metabolism in muscle or liver.

Our analyses also more explicitly delineate the roles of MPC1 and MPC2 as components of the mitochondrial pyruvate transporter. Although strong evidence supports this functionality (Bricker et al., 2012; Divakaruni et al., 2013; Herzig et al., 2012), MPC-mediated regulation of pyruvate dehydrogenase (PDH) complex activity has been suggested as an alternative function of the MPC proteins (Halestrap, 2012). While our MFA results indicated that overall flux through PDH was decreased in Mpc2 knockdown cells, supplementation of pyruvate at concentrations expected to enter mitochondria through passive diffusion abrogated the increase in glutamine to fatty acid conversion. Furthermore, conversion of [^{13}C]pyruvate carbons to lipogenic AcCoA confirmed that this pyruvate was metabolized by PDH, since carbon atoms in oxaloacetate do not enter the AcCoA pool without PDH activity.

These results also demonstrate that MPC inhibition elicits a distinct metabolic phenotype compared to hypoxia or ETC inhibition. Whereas elevated glycolytic rates and reductive carboxylation are predominant modes of metabolism under such conditions (Metallo et al.,

2012; Mullen et al., 2012; Scott et al., 2011; Wise et al., 2011), Mpc inhibition instead promoted oxidative glutaminolysis to fuel the mitochondrial AcCoA pool. Surprisingly, we observed no increase in reductive carboxylation flux. Fatty acid synthesis rates were also maintained upon *Mpc* knockdown, in contrast to that observed when comparing normoxic and hypoxic cell growth (Kamphorst et al., 2013; Metallo et al., 2012).

It is well established that oxidation of glucose and fatty acids are dynamically balanced in response to nutrient availability and hormonal control (Keung et al., 2013; Muoio et al., 2012), and disruptions of these processes are evident in metabolic and heart disease. Extensive studies support that inhibition of fatty acid oxidation, via genetic manipulation or pharmacologic intervention, can increase the rate of pyruvate oxidation (Fillmore and Lopaschuk, 2013). However, the converse principle has yet to be shown: that a reduction in pyruvate oxidation can stimulate β-oxidation. This may be partly due to the lack of a druggable therapeutic target. Our model, though, suggests that inhibition of mitochondrial pyruvate uptake can rewire cellular metabolism to boost fatty acid oxidation, which may provide an approach to further studies on the interplay between carbohydrate and fat metabolism. Given the importance of this metabolic control point, significant interest in identifying drugs that control MPC activity has emerged (Colca et al., 2013; Divakaruni et al., 2013; Du et al., 2013). The metabolic phenotype of MPC inhibition defined here using both shRNAs and UK5099 in cultured cell lines and hSKMs will provide a roadmap for molecular level validation of new compounds, facilitating the ability of researchers to identify drugs that target MPC versus other mitochondrial enzymes. Indeed, the phosphodiesterase inhibitor Zaprinast was recently demonstrated to inhibit mitochondrial pyruvate uptake. While Du et al. (2013) similarly observed an increase in aspartate levels, no evidence of glutaminolysis through malic enzyme was observed, potentially due to offtarget effects on mitochondrial glutaminase (Elhammali et al., 2014). These findings highlight the need for systems-level analyses of metabolism to functionally validate gene function and drug specificity. In turn, the identification of selective compounds that influence mitochondrial substrate transport and utilization may provide therapeutic avenues to exploit the exquisite flexibility of these organelles.

Experimental Procedures

Cell Culture and ^{13}C Tracing

C2C12, A549, and Huh7 cells were cultured in Dulbecco's modified Eagle's medium (DMEM) with 10% fetal bovine serum (FBS). Terminal differentiation of C2C12 cells was initiated by 4-day culture in DMEM with 2% horse serum. Human skeletal muscle satellite cells were proliferated in SkFM (Lonza) and then differentiated to myotubes in MEMα supplemented with 2% FBS as described previously (Henry et al., 1995). For tracer and MFA studies, custom, phenol red-free DMEM or amino acid-free DMEM/F12 (for hSKMs) was formulated by replacing the substrate of interest with ^{13}C-labeled glucose, glutamine, pyruvate, or BCAAs (all from Cambridge Isotopes) with other components unlabeled. Cultures were washed with PBS before adding tracer media for 15-30 hr unless otherwise specified. Fatty acid oxidation studies were conducted using [U-$^{13}C_{16}$]palmitate noncovalently bound to fatty acid-free BSA. [U-$^{13}C_{16}$]palmitate-BSA was added to culture medium at 5% of the final volume (50 μM final concentration) with 1 mM carnitine in medium formulated with FBS that was delipidated using fumed silica (Sigma) according to the manufacturer's instructions.

Metabolic Flux Analysis

MFA was performed using the elementary metabolite unit-based software package INCA. Inputs to the model include the chemical reactions and atom transitions of central carbon metabolism, measured substrate extracellular fluxes, the identity of the ^{13}C-labeled tracers, and mass isotopomer distributions of select intracellular metabolites. Assumptions are listed in the Supplemental Experimental Procedures.

Oxygen Consumption Measurements

Respiration was measured in adherent monolayers of C2C12 myocytes using a Seahorse XF96 Analyzer. Myoblasts were plated at 1×10^4 cells/well and grown for 2 days. Cells were assayed in unbuffered DMEM (Sigma #D5030) supplemented with 8 mM glucose and

3 mM glutamine. Unless stated in the figure legend, pyruvate was omitted from the assay medium. ATP-linked respiration was calculated as the oxygen consumption rate sensitive to 2 μg/ml oligomycin. Maximal respiration was calculated as the difference between protonophore-stimulated respiration (measured as the highest rate from sequential additions of FCCP; final concentrations between 400 and 800 nM) and nonmitochondrial respiration (measured after addition of 2 μM rotenone and 2 μM antimycin A). Where indicated, etomoxir (20 μM) or BPTES (3 μM) was added to the plate 20 min prior to basal respiration measurements. Respiration in permeabilized cells (1 nM XF PMP, Seahorse Bioscience) was measured in cells offered 5 mM pyruvate, 0.5 mM malate, 2 mM DCA, 2 μg/ml oligomycin, and 400 nM FCCP. All data are mean ± SEM of at least four biological replicates (with a minimum of five technical replicates per experiment). Statistical analysis was conducted using ANOVA of repeated measures with Dunnett's post hoc test. Where appropriate, the square root of normalized data was analyzed.

Metabolite Extraction and GC/MS Analysis

At the conclusion of a tracer experiment, the tracer media was removed from the culture wells, the cells were washed with a saline solution, and the bottom of the well was covered with cold methanol to lyse the cells and halt metabolism. Water containing norvaline at 5 μg/ml was charged to each well at a volume ratio of 1:2.5 relative to the methanol. The bottom of each well was scraped with a 1,000 μl pipette tip, and the cells were collected in 1.5 ml tubes. Cold chloroform containing 2 μg/ml of heptadodecnaoate was added to each sample at a 1:1 volume ratio relative to the methanol. The mixtures were vortexed, and the polar and nonpolar layers were separated and evaporated after centrifugation. Details of the derivatization process can be found in the Supplemental Experimental Procedures.

Derivatized metabolites were analyzed using a DB-35MS column (30 m × 0.25 mm internal diameter × 0.25 μm; Agilent J&W Scientific) in an Agilent 7890A gas chromatograph coupled to a 5975C mass spectrometer. Details of the chromatography method and mass spectrometry scanning parameters can be found in the Supplemental Experimental Procedures.

Human Subjects

All human skeletal muscle biopsies were obtained with approval from the University of California San Diego's Committee on Human Investigation. All donors provided informed written consent after listening to an explanation of the protocol.

Acknowledgements

We thank Sandra E. Wiley, Hui Zhang, Ryan LaCroix, Spencer Lee, and Mehmet G. Badur for technical assistance and members of the Metallo lab for discussions. This work was supported, in part, by NIH grants P30DK063491, R01CA188652, and T32HL105373 (to N.M.V.), DOD grant W81XWH-13-1-0105, a Hellman Faculty Fellowship, and a Searle Scholar Award (to C.M.M.), a grant from the Medical Research Service, Department of Veterans Affairs, VA San Diego Healthcare System (to R.R.H.), and NIH grant R01NS087611 and Seahorse Bioscience (to A.N.M.). A.N.M. and A.S.D. are consultants for Seahorse Bioscience.

This chapter, in full, is a reprint of the material as it appears in "Regulation of Substrate Utilization by the Mitochondrial Pyruvate Carrier", Molecular Cell, vol. 56, 2014. Nathaniel M. Vacanti is the primary author of this publication.

Chapter 4

Identification of a Mitochondrial Glutamine Carrier

Abstract

Herein we report the identification of a mitochondrial glutamine carrier, SLC25A44 (hereafter referred to as MQC). Systematic knockdown of un-annotated putative amino acid carrier SLC25 family members in human carcinoma cells reveals MQC as essential for growth. Stable isotope ^{13}C substrate tracing shows intact *MQC* knockdown (MQCKD) cells increase reliance on glucose anaplerosis, consistent with elevated *MPC1* transcript levels. Additionally ^{13}C tracing in permeabilized cells reveals MQCKD cells reduce relative glutamine and increase glutamate driven TCA cycle flux. Furthermore *MQC* expression is elevated in tissues where mitochondrial *GLS2* is highly expressed. Glutamine utilization as an oxidative substrate or biosynthetic precursor by mitochondria is believed to contribute to the pathogenesis of cancer, regulate the urea cycle and gluconeogenesis, and influence nutrient utilization in type II diabetes and obesity. Thus identification of MQC is central to understanding metabolic dysfunction in human disease.

Introduction

Mitochondria serve as the powerhouses of the cell, supplying energy in the form of ATP in addition to many precursors required for biosynthesis. Cellular homeostasis is intricately linked to mitochondrial function and central to this relationship is the exchange of fuel substrates,

signaling molecules, and biosynthetic intermediates across the inner mitochondrial membrane.

Over the past several decades a clearer picture of the proteins involved in regulating inner membrane transport has emerged. Though there are exceptions (*e.g.*, the pyruvate carrier and the calcium uniporter), most of these proteins belong to the SLC25 family. The SLC25 family includes 53 human members sharing a structure with three repeats, each about 100 amino acids long and containing two membrane spanning α-helices. Those members whose substrates are annotated play important roles in maintaining physiological and cellular homeostasis (Gutiérrez-Aguilar and Baines, 2013; Palmieri, 2013).

Herein we report the identification of a mitochondrial glutamine carrier, SLC25A44 (hereafter referred to as MQC). Systematic knockdown of un-annotated putative amino acid carrier SLC25 family members in human carcinoma cells reveals MQC as essential for growth. Stable isotope ^{13}C substrate tracing shows intact *MQC* knockdown (MQCKD) cells increase reliance on glucose anaplerosis, consistent with elevated *MPC1* transcript levels. Additionally ^{13}C tracing in permeabilized cells reveals MQCKD cells reduce relative glutamine and increase glutamate driven TCA cycle flux. Furthermore *MQC* expression is elevated in tissues where mitochondrial *GLS2* is highly expressed.

Glutamine is heavily oxidized by proliferating transformed cell mitochondria in culture and is believed to be the primary anaplerotic substrate. It is the obligate nitrogen donor for nucleotide and glucosamine biosynthesis, is a key substrate for gluconeogenesis in the liver and kidneys, and a regulator of systemic pH and the urea cycle in the liver. Glutamine flux through glutaminolysis is also believed to be a major source of biosynthetic NADPH (Wise and Thompson, 2010). Additionally stresses such as impaired pyruvate oxidation (Vacanti et al., 2014; Yang et al., 2014) or hypoxia (Metallo et al., 2012; Wise et al., 2011; Mullen et al., 2012) increase reliance on glutaminolysis and reductive carboxylation respectively. Finally, glutamine plays a major role in the balance of carbohydrates, amino acids, and fatty acids utilized for oxidative or biosynthetic reactions (Vacanti et al., 2014; Yang et al., 2014). Thus identifying MQC is fundamental to understanding the physiological dysfunctions of cancer, ammonia detoxification, and substrate impairment disorders such as type II diabetes and obesity.

Results

MQC Knockdown Alters Growth and Overall Metabolism in Proliferating Cells

As part of our efforts to identify the un-annotated SLC25 mitochondrial carriers, *MQC* was knocked down in A549 and Huh7 human carcinoma cell lines (producing A549 and Huh7 MQCKD cells respectively) using lentiviral-mediated delivery of a corresponding shRNA hairpin. Continuous expression of the hairpin was selected for by incubation with puromycin and the knockdown was verified at the mRNA level (Figure 4.1A). *MQC* knockdown produces a striking growth defect in both cell lines, indicating the importance of its function for proliferation (Figures 4.1B and S4.1A). Surprisingly this growth defect does not correspond to differences in glucose, lactate, glutamine, or glutamate uptake or secretion fluxes, though alanine secretion increases by an order of magnitude and pyruvate secretion is reduced (Figure 4.1C). This increase in alanine efflux is likely due to an increase in synthesis, as the steady-state abundance of alanine is significantly elevated (Figure 4.1D). The decrease in pyruvate efflux may be due to a higher ananplerotic flux as described below. Interestingly the elevated alanine and reduced aspartate abundances seen here contrast what is observed in proliferating cells when the mitochondrial pyruvate carrier (MPC) is knocked down (Vacanti et al., 2014), indicating MQC may transport an anaplerotic substrate supplementary to pyruvate. The Huh7 cell metabolome has a different response to *MQC* knockdown, indicating the two cell lines may adapt differently and steady-state metabolite abundances do not tell the whole story (Figure S4.1B).

Intact Cell ^{15}N- and ^{13}C- Labeled Substrate Tracing Elucidates MQC Function

Considering MQC is a putative amino acid carrier based on sequence similarities to other SLC25 family members (Palmieri, 2013), we first cultured A549 cells with [α-^{15}N]glutamine (αNQ). The α-nitrogen on glutamine remains after the action of glutaminase produces glutamate. Through the activity of aminotransferases, the labeled nitrogen ends up on a slew of amino acids (Figure 4.2A), of which we hypothesized *MQC* knockdown would produce differential labeling patterns. Consistent with increases in alanine excretion and steady-state abundance,

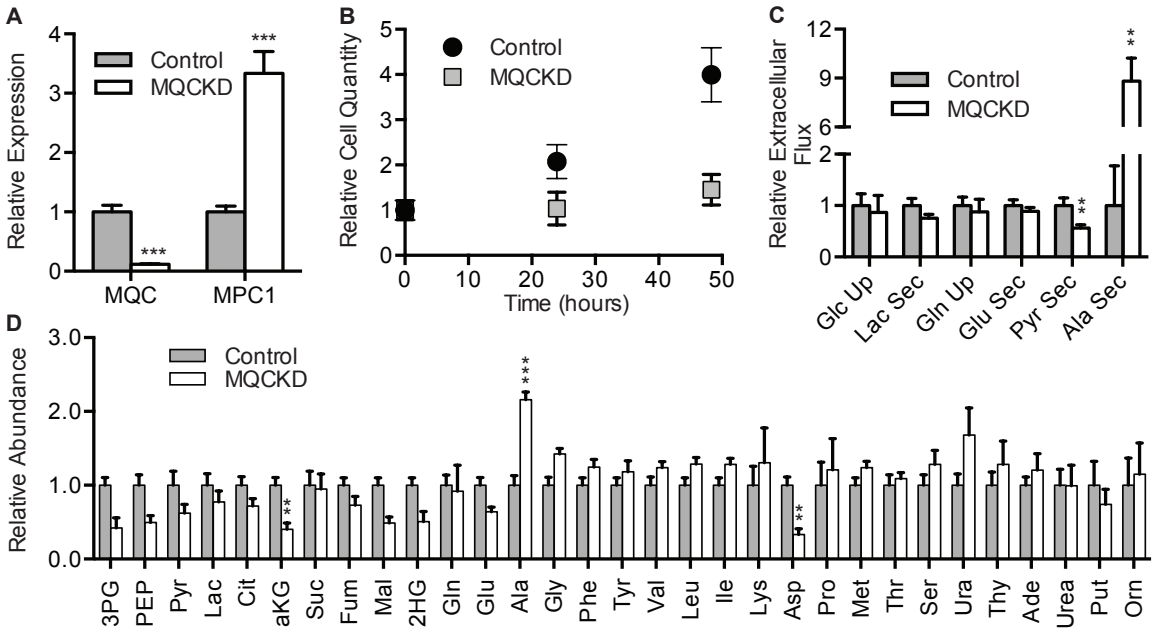

Figure 4.1: MQC Knockdown Effects on Growth, Substrate Flux, and Metabolite Pools. (A) Relative expression of *MQC* and *MPC1* as determined by qPCR. (B-D) Proliferation (B), extracellular fluxes (C), and metabolite abundances (D). All are A549 cells. Error bars indicate standard deviation (SD). *, **, and *** indicate $p < 0.05$, 0.01, and 0.001 by t-test. P-value indicators only provided if significant after correcting for multiple comparisons using the Holm-Sidak method.

αNQ preferentially labels alanine in MQCKD A549 cells (Figure 4.2B). Furthermore, culture with [U-$^{13}C_6$]glucose (UGlc; Figure S4.2A) reveals MQCKD A549 cells increase relative production of alanine without increasing the relative production of lactate or pyruvate derived from glucose (Figure 4.2C). Again, this is a striking contrast to proliferating cells with *MPC* knocked down. In *MPC* knockdown A549 cells, the abundance of fully labeled alanine derived from UGlc decreases without concordant reductions in fully labeled pyruvate or lactate (Vacanti et al., 2014) indicating glutamate pyruvate transaminase (catalyzes the pyruvate to alanine aminotransferase reaction) activity occurs primarily in mitochondria. Thus A549 cells are adapting to *MQC* knockdown by supplying mitochondria with more pyruvate. This is consistent with elevated *MPC1* expression (Figure 4.1A) and decreased pyruvate efflux (Figure 4.1C) upon *MQC* knockdown. Furthermore, MQCKD A549 cells utilize glucose more as an anaplerotic substrate as indicated by increased abundances of M3 malate and M5 citrate derived from UGlc (Figure 4.2D), which is consistent with a higher relative flux of pyruvate into mitochondria. Thus blocking MQC function likely prevents a key anaplerotic substrate from entering the TCA cycle.

To examine how *MQC* knockdown affects glutamine anaplerosis, Huh7 and A549 MQCKD cells were cultured with [U-$^{13}C_5$]glutamine (UGln; Figure S4.2B). Mass isotopomer abundances indicative of glutamine oxidation were all reduced in Huh7 MQCKD cells (Figure 4.2E) as well as A549 MQCKD cells (Figure S4.2C) with the exception of M5 α-ketoglutarate. Considering downstream TCA cycle metabolites show reduced glutamine carbon incorporation, separate pools of α-ketoglutarate unaffected by glutamine oxidation must be predominant in A549 cells.

Glutamine transport into mitochondria lies upstream of mitochondrial glutaminase, thus glutaminase inhibition is expected to have similar effects on glutamine oxidation as impaired MQC function. This is indeed the case as *MQC* knockdown along with administration of the glutaminase inhibitors BPTES and CB-839 additively decrease incorporation of UGln carbon into fumarate (Figure 4.2F). Taken together these data indicate MQC transports an anaplerotic substrate upstream or immediately downstream of glutaminase into mitochondria. In other words, MQC is likely a glutamine or glutamate carrier.

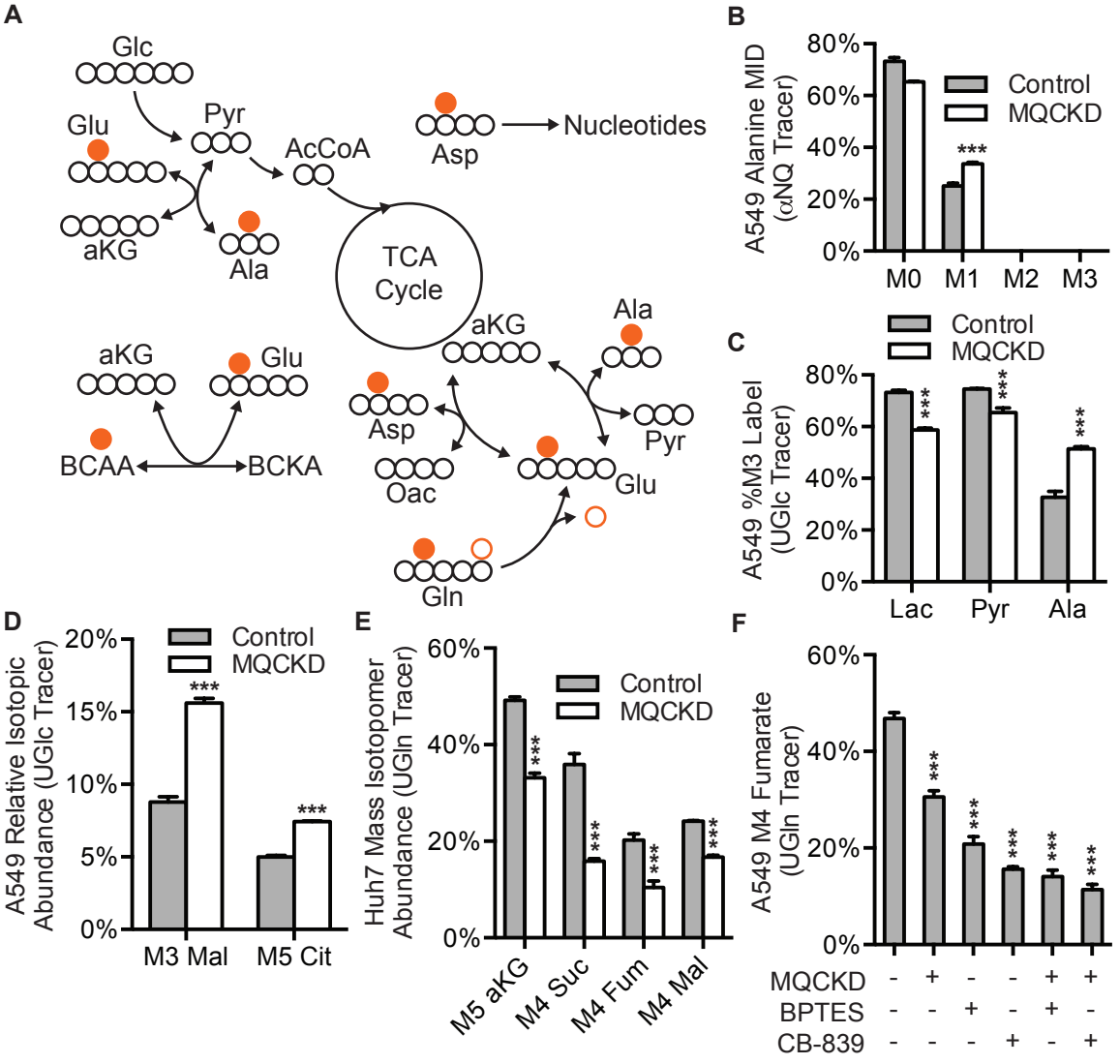

Figure 4.2: ^{15}N-Glutamine, ^{13}C-Glucose, and ^{13}C-Glutamine Tracing on MQCKD Cells. (A) Schematic of [α-^{15}N]glutamine (αNQ) labeling nitrogenous metabolites. (B) A549 alanine MID resulting from culture with αNQ. (C) A549 lactate, pyruvate, and alanine M3 relative mass isotopomer abundances resulting from culture with [U-$^{13}C_6$]glucose (UGlc). (D) A549 relative mass isotopomer abundances indicating glucose anaplerosis resulting from culture with UGlc. (E) Huh7 TCA cycle intermediate relative mass isotopomer abundances resulting from culture with [U-$^{13}C_5$]glutamine (UGln). (F) Control and MQCKD A549 M4 fumarate relative mass isotopomer abundances resulting from culture with UGln and where indicated, 10 μM BPTES and 1 μM CB-839. Error bars indicate SD. *, **, and *** indicate $p < 0.05$, 0.01, and 0.001 by t-test. P-value indicators only provided if significant after correcting for multiple comparisons using the Holm-Sidak method (C-F). Significance indicated without correction for multiple comparisons (B).

Permeabilized Cell ^{13}C-Glutamine/^{13}C-Glutamate Tracing Reveals MQC as a Glutamine Carrier

Glutamine carbon atoms also enter mitochondria independently of direct glutamine import. Cytosolic glutaminase converts glutamine to glutamate, and glutamate passes through one of the several mitochondrial glutamate carriers. To distinguish between these modes of entry, we employed ^{13}C-glutamine/^{13}C-glutamate tracing on permeabilized cells. Recombinant, mutant perfringolysin O (XF Plasma Membrane Permeabilizer; Seahorse Bioscience) forms large pores in cholesterol rich plasma membranes, leaving mitochondrial membranes intact. The non-membrane bound cytoplasmic enzymes along with all of the intracellular small molecules diffuse out of the cell leaving mitochondria exposed to the extracellular environment (Figure 4.3A). Mitochondrial metabolism in permeabilized cells is different in that it is driven by ADP supplied in the medium rather than a demand for ATP. Furthermore permeabilized cells can only oxidize what is supplied in the medium since the free cytosolic enzymes are not present to convert substrates.

This system is ideal for examining glutamine oxidation independent of cytosolic glutaminase activity. However this assay is not informative if ^{13}C-labeled glutamine is the only substrate available to mitochondria, as much of the power in stable isotope tracing lies in its ability to distinguish changes in relative fluxes. If glutamine is the only available substrate, then glutamine will account for all of the oxidative flux regardless if 90% of the mitochondrial glutamine carriers are knocked down. Therefore a competing substrate, in this case malate, must also be present. Culture of permeabilized MQCKD A549 cells with ADP, malate, and UGln reveals that mass isotopomer abundances of TCA cycle intermediates, indicative of glutamine oxidation, are reduced, and this is most pronounced for malate, the competing substrate (Figure 4.3B).

To further assess glutamine versus glutamate oxidation, permeabilized A549 cell TCA cycle intermediate labeling resulting from culture with [5-^{13}C]glutamine (5Gln) and malate is directly compared with the labeling resulting from culture with [5-^{13}C]glutamate (5Glu) and malate. The presence of the glutaminase inhibitor, BPTES, severely reduces the relative contribution of 5Gln as an oxidative substrate (the ratio of the M1 relative mass isotopomer abundance

with BPTES to that without BPTES is much less than 100% for fumarate and malate) while it has no effect on relative 5Glu oxidation (these same ratios are near 100%) (Figure 4.3C). This is as expected considering glutamine transport into mitochondria is upstream while glutamate oxidation is downstream of glutaminase in permeabilized cells. Similar results are obtained by knocking down *MQC*; a defect in relative 5Gln oxidation is observed, however relative 5Glu oxidation actually increases (the MQCKD M1 relative mass isotopomer abundances are greater than the control cell M1 relative mass isotopomer abundances for fumarate and malate) indicating mitochondria are better equipped to metabolize glutamate when MQC function is impaired (Figure 4.3D). Finally tissue specific expression of *MQC* resembles that of *GLS2* and *GLS* (Figure S4.3A). Taken together these data suggest impairment of MQC restricts glutamine oxidation independent of mitochondrial glutamate transport.

Discussion

Communication between mitochondria and the cytosol is essential for regulating metabolism and maintaining cellular homeostasis. Central to this communication is the exchange of nutrients, intermediates, and signaling molecules between the compartments; thus the proteins that facilitate this exchange are key regulators of the metabolic network. Numerous studies have highlighted the regulatory roles of mitochondrial inner membrane transporters on cellular homeostasis. The mitochondrial pyruvate carrier (MPC) is a node that directs carbohydrate, amino acid, and fatty acid oxidation (Vacanti et al., 2014; Yang et al., 2006). The dicarboxylate and tricarboxylate carriers influence adipocyte lipid accumulation (Kajimoto et al., 2005), and the mitochondrial iron carrier, Mfrn1, couples iron transport to heme synthesis (Chen et al., 2010). Additionally, mitochondrial carrier function influences organism phenotypes. The uncoupling protein, UCP1, allows for non-shivering thermogenesis and *UCP1*$^{-/-}$ mice are more sensitive to cold (Enerbäck et al., 1997). Impairment of the adenine nucleotide translocator 1 is associated with cardiomyopathies (Jordens et al., 2002; Strauss et al., 2013), *MPC* is frequently deleted in cancer (Schell et al., 2014), and the glutamate carrier, GC1, regulates glucose stimulated insulin release (Casimir et al., 2009).

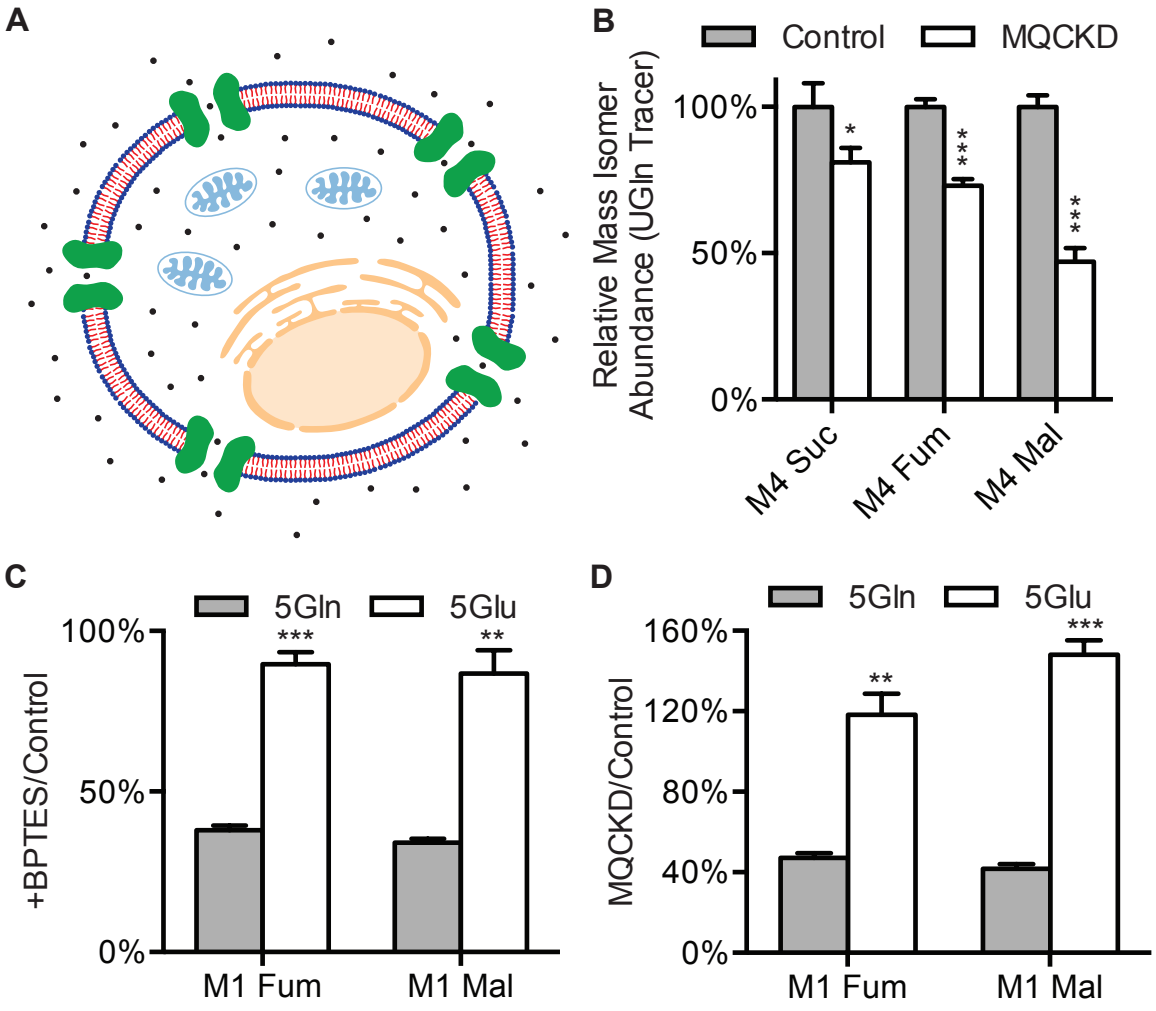

Figure 4.3: ^{13}C-Glutamine and ^{13}C-Glutamate Tracing in Permeabilized Cells. (A) Schematic of a permeabilized cell with cytosolic enzymes absent and mitochondria exposed to the extracellular environment. (B) Relative mass isotopomer abundances of TCA cycle intermediates resulting from culture with UGln and indicative of glutamine oxidation. (C) Ratios of M1 relative abundances resulting from culture with [5-^{13}C]glutamine (5Gln) and [5-^{13}C]glutamate (5Glu). Ratios are presented as the M1 relative mass isotopomer abundance with, over that without 10 μM BPTES in the medium. Therefore a value of 100% indicates BPTES has no effect on the oxidation of the labeled metabolite, values less than 100% indicate BPTES causes a defect in oxidation of the labeled metabolite, and values greater than 100% indicate BPTES causes the labeled metabolite to be preferentially oxidized. (D) Analogous to the experiment presented in (C), except with MQCKD instead of BPTES. All are permeabilized A549 cells. Error bars indicate standard error of the mean (SEM). *, **, and *** indicate $p < 0.05$, 0.01, and 0.001 by t-test. P-value indicators only provided if significant after correcting for multiple comparisons using the Holm-Sidak method.

Though considered a non-essential amino acid, rapid growth or conditions of stress can render glutamine conditionally essential (Lacey and Wilmore, 1990). Glutamine is the obligate nitrogen donor for nucleotide and glucosamine synthesis in the cytosol. In mitochondria, glutamine is an oxidizable anaplerotic substrate that replenishes TCA cycle intermediates, a source for biosynthetic NADPH, and supplies glutamate for non-essential amino acid synthesis. Thus glutamine is believed to be imperative for continued proliferation in many tumors (Wise and Thompson, 2010; Hensley et al., 2013). Furthermore, inhibiting aminotransferase activity with amino-oxyacetic acid impairs growth in xenograft tumor models (Thornburg et al., 2008) and glutaminase inhibition delays growth in lymphoma xenografts (Wang et al., 2010). Thus activities of glutaminase and aminotransferases, which occur downstream of MQC, are critical for tumor growth.

Mitochondrial glutamine metabolism is also a key regulator of systemic pH, ammonia detoxification, and gluconeogenesis in the liver and kidneys. Both renal and hepatic glutaminase are localized to mitochondria, thus the conversion of glutamine to glutamate requires transport of glutamine into the mitochondrial matrix, implicating MQC as a key regulatory point. Acidosis induces renal uptake of glutamine, its subsequent conversion to glutamate and ammonia, and secretion of ammonia in the urine (van de Poll et al., 2004). Furthermore elevated acidity decreases hepatic glutaminase activity and ammonia production, thus decreasing urea cycle flux, bicarbonate consumption, and counteracting rising acidity (Häussinger and Schliess, 2007). Finally glutamine is a major substrate for glucose production via gluconeogenesis in the liver and kidneys, with the first step being glutamine transport into mitochondria for conversion to glutamate (Stumvoll et al., 1999).

The importance of glutamine as an oxidizable substrate, biosynthetic precursor, and regulator of pH and glucose homeostasis suggests understanding its localization is key to uncovering the mechanisms contributing to the pathogenesis of metabolic diseases. Identification of a mitochondrial glutamine carrier is a fundamental discovery which allows further elucidation of the role glutamine plays in regulating the metabolic network.

Acknowledgements

The material in this chapter is currently being prepared for submission for publication. Nathaniel M. Vacanti is the primary author and Ajit S. Divakaruni, Anne N. Murphy, and Christian M. Metallo are co-authors of this material.

Chapter 5

Conclusions

A central theme to the works presented in this dissertation is that metabolism is a fundamental regulator of cellular phenotype. This is presented as a case study in the first chapter, "Exploring Metabolic Pathways that Contribute to the Stem Cell Phenotype", examining how components of the metabolic network support and regulate the stem cell phenotype. Substrate and pathway utilization are crucial determinants of differentiation status while the interplay between molecular signaling and metabolism drives stem cell fate. The field of stem cell metabolism as a whole is in its infancy, and much work remains on determining: how culture conditions affect metabolism, characteristic alterations in pathway utilization as stem cells differentiate down specific lineages, and the metabolic requirements for remaining in an undifferentiated state.

The second chapter, "Inner Mitochondrial Membrane Transport Regulates Cellular Function", takes a more focused look at a very under appreciated aspect of metabolic regulation; transport of substrates, signaling molecules, and intermediates across the inner mitochondrial membrane. Mitochondrial carrier activity exhibits elegant control over the metabolic network and thus cellular homeostasis. Cells adapt to impaired transport by up-regulating parallel or alternate pathways, modifying carrier utilization in response to stress or signaling molecules, and adjusting their phenotypes in response to carrier activity. Though many carriers have been studied extensively, much of this work has been done in isolation. Future work must elucidate how specific perturbations in transport activity effect the metabolic network as a whole, and how that translates into altered cellular phenotypes that can correct dysfunctional regulation.

The third chapter, "Regulation of Substrate Utilization by the Mitochondrial Pyruvate

Carrier", applies the principle of examining a specific metabolic node as it relates to the network as a whole. ^{13}C tracing and metabolic flux analysis (MFA) are employed to examine how perturbations in pyruvate transport into the mitochondrial matrix affect substrate utilization and flux through alternate pathways. Computational modeling through the application of MFA prove to be instrumental in guiding experimental design to elucidate metabolic network adaptations to impaired pyruvate oxidation. Proliferating cells increase glutamine and fatty acid oxidation while up-regulating utilization of glutamine as a lipogenic precursor via the glutaminolysis pathway. Furthermore, differentiated human skeletal myotubes rely more heavily on branched chain amino acids as an oxidative fuel source. Future work must focus on how these adaptations can be exploited to treat metabolic dysfunctions and elucidating the mechanisms behind others' findings including that re-expression of the mitochondrial pyruvate carrier (MPC) impairs growth in xenograft tumor models (Schell et al., 2014).

The fourth chapter, "Identification of a Mitochondrial Glutamine Carrier", solves the inverse problem of that posed in the third chapter. Rather than determine the regulatory control exhibited by a known transporter, for the first time ^{13}C tracing is used to elucidate an unknown transporter's substrate from its pre-determined regulatory influence. Critical to this methodology is the ability to examine alterations in fluxes throughout the metabolic network resulting from inhibition of the node of interest. Furthermore, examining transporter function *in situ* rather than as a recombinant protein reconstituted into liposomes circumvents the problem of promiscuity of carrier proteins under non-physiological conditions. Both the networks of intact cells and those permeabilized to expose mitochondria to the extracellular environment were studied using ^{13}C tracing. Regulatory responses to impaired SLC25A44 function include: elevated glucose anaplerosis and *MPC1* expression and decreased glutamine oxidation in intact cells along with increased glutamate oxidation and decreased glutamine oxidation in permeabilized cells. Additionally, SLC25A44 is co-expressed with mitochondrial glutaminase (*GLS2*). Taken together, these data indicate SLC25A44 is a mitochondrial glutamine carrier (MQC). Future work will likely focus on the role this carrier plays in glutamine addicted tumors, urea cycle and gluconeogenesis regulation, and substrate selection in metabolic disorders such as obesity and type II diabetes.

This dissertation begins with a general case study of metabolic regulation, becomes focused on mitochondrial transport as a brand of regulation, applies the principles of examining an intact metabolic network to elucidate the regulatory role of a known transporter, and concludes by elucidating the function of a previously un-annotated mitochondrial carrier. Highlighted in these works are the value of methodologies which examine metabolism in intact networks. Metabolic pathways operate in concert with molecular signaling, the extracellular environment, and other metabolic pathways. Therefore studying the effects of perturbations *in situ* is essential to understanding metabolic function and dysfunction.

Supplement to Chapter 1

Abbreviations

2HG, (R)2-hydroxyglutarate; 2PG, 2-phosphoglycerate; 3PG, 3-phosphoglycerate; 6PG, 6-phosphogluconate; 6PGL, 6-phosphgluconolactone; 8-OHdG, 8-hydroxy-2'-deoxyguanosine; AcCoA, acetyl coenzyme A; ACLY, ATP citrate lyase; ACO1, aconitase 1; ACO2, aconitase 2; ALDH, aldehyde dehydrogenase; ALDO, aldolase; ATP, adenosine triphosphate; BPG, 1,3-bisphosphoglycerate; CIT, citrate; CYS, cysteine; DHAP, dihydroxyacetone phosphate; ENO, enolase; ESCs, embryonic stem cells; F6P, fructose-6-phosphate; FAs, fatty acids; FBP, fructose-1,6-bisphosphate; FH, fumarate hydratase; FUM, fumarate; G6P, glucose-6-phosphate; G6PD, glucose-6-phosphate dehydrogenase; GAP, glyceraldehyde-3-phosphate; GAPDH, glyceraldehyde-3-phosphate dehydrogenase; GCLC, glutamate-cysteine ligase; GCLM, glutamate-cysteine ligase modifier subunit; GlcNAc, N-acetylglucosamine; GLN, glutamine; GLS, glutaminase; GLU, glutamate; Gluc, glucose; GLY, glycine; GSR, glutathione reductase; GSH, glutathione (reduced); GSS, glutathione synthetase; GSSG, glutathione (oxidized); HBP, hexosamine biosynthesis pathway; hESCs, human embryonic stem cells; HIFs, hypoxia inducible factors; HK, hexokinase; HSC, hematopoietic stem cell; ICT, isocitrate; IDH, isocitrate dehydrogenase; iPSCs, induced pluripotent stem cells; LAC, lactate; LDH, lactate dehydrogenase; MAL, malate; MalCoA, malonyl coenzyme A; MEETHF, methylenetetrahydrofolate; MEFs, mouse embryonic fibroblasts; mESCs, mouse embryonic stem cells; MSCs, mesenchymal stem cells; mTOR, mammalian target of rapamycin; NAC, N-acetyl-L-cysteine; NAD^+, nicotinamide adenine dinucleotide (oxidized); NADH, nicotinamide adenine dinucleotide (reduced); $NADP^+$, nicotinamide adenine dinucleotide

phosphate (oxidized); NADPH, nicotinamide adenine dinucleotide phosphate (reduced); OAC, oxaloacetate; OXPHOS, oxidative phosphorylation; PDH, pyruvate dehydrogenase; PDK, pyruvate dehydrogenase kinase; PEP, phosphoenolpyruvate; PFK, phosphofructokinase; PGAM, phosphoglycerate mutase; PGD, phosphogluconate dehydrogenase; PGK, phosphoglycerate kinase; PHI, phosphohexose isomerase; PKM1, pyruvate kinase M1; PKM2, pyruvate kinase M2; PPP, pentose phosphate pathway; PSCs, pluripotent stem cells; PYR, pyruvate; R5P, ribulose-5-phosphate; ROS, reactive oxygen species; SDH, succinate dehydrogenase; SER, serine; SHMTs, serine hydroxymethyltransferases; SUC, succinate; TALDO, transaldolase; TCA, tricarboxylic acid; THF, tetrahydrofolate; TKT, transketolase; UCP2, uncoupling protein 2; WT, wild type; αKG, α-ketoglutarate; γ-GLU-CYS, γ-glutamylcysteine; $\Delta\psi_m$, mitochondrial membrane potential

Supplement to Chapter 3

Supplemental Experimental Procedures

Metabolic Flux Analysis Assumptions

1. Metabolism and isotopic labeling were at steady state.

2. Cells were assumed to grow exponentially.

3. Labeled CO_2 formed did not reincorporate in carboxylation reactions.

4. Protein turnover occured at a negligible rate compared to glucose and glutamine consumption.

5. Pyruvate, acetyl-CoA, oxaloacetate, malate, fumarate, and aspartate existed in cytosolic and mitochondrial pools. Malate, and aspartate were allowed to exchange freely between the compartments.

6. The relative flux of glucose through the pentose phosphate pathway vs. glycolysis was assumed to be the M1/(M1+M2) ratio of lactate ^{13}C abundances resulting from culture of C2C12 cells with [1,2-$^{13}C_2$]glucose.

7. The per cell biomass requirements of proliferating C2C12 myoblasts were similar to those reported previously (Grassian et al., 2014).

Determination of Extracellular Fluxes

Initial and final quantities of glucose, lactate, glutamine, and glutamate present were determined using a Yellow Springs Instrument while pyruvate and alanine levels were measured using GC/MS. The extracellular fluxes, in units of fmol/cell/hour, were determined by solving the differential equations listed as Equations S3.1-S3.3:

$$\frac{dX}{dt} = \mu X \tag{S3.1}$$

$$\frac{dN_i}{dt} = q_i X \tag{S3.2}$$

$$\frac{dN_{Gln}}{dt} = q_i X - kN_{Gln} \tag{S3.3}$$

where X represents the number of cells present, μ the cellular growth rate (in hr^{-1}), N_i the moles of substrate i present, q_i the extracellular flux of substrate i (in moles/cell/hr), and k the degradation rate of glutamine (in hr^{-1}). Equations S3.1 and S3.2 were used to solve for glucose, lactate, glutamate, pyruvate, and alanine extracellular fluxes while Equations S3.1 and S3.3 (which considers glutamine degradation) were used to solve for the glutamine extracellular flux. k was set to 0.0045 hr^{-1} (Tritsch and Moore, 1962). Solving Equations S3.1-S3.3 yields Equations S3.4-S3.6 respectively.

$$X = X_0 e^{\mu t} \tag{S3.4}$$

$$q_i = \frac{\mu \left(N_{i,f} - N_{i,0}\right)}{X - X_0} \tag{S3.5}$$

$$q_{Gln} = \frac{N_{Gln,f} - N_{Gln,0} e^{-kt}}{\left(\frac{1}{\mu + k}\right)\left(X - X_0 e^{-kt}\right)} \tag{S3.6}$$

where the subscripts 0 and f indicate initial and final values respectively.

Separation and Chemical Derivatization of Polar Metabolites and Fatty Acids

Fatty acid methyl esters (FAMEs) were formed from the extracted fatty acids by adding 500 µL of 2% H_2SO_4 in methanol to the dried contents of the non-polar layer and heating at

50°C for at least two hours. FAMEs were extracted from the solution by washing with 100 µL of a saturated NaCl solution and 500 µL of hexane. The hexane layer was removed, evaporated and re-dissolved with 40 µL of hexane for injection.

Dried polar metabolites were dissolved in 15 µL of 2% (m/v) methoxyamine hydrochloride in pyridine and incubated for 60 minutes at 37°C. 20 µL of N-tert-butyldimethylsiyl-n-methyltrifluoroacetamide with 1% tert-butyldimethylchlorosilane was then added and the solution incubated at 37°C for an additional 30 minutes to form methoxyamine-tert-butyldimethylsiyl (MOX-tBDMS) derivatives.

Gas Chromatography and Mass Spectrometry

GC/MS analysis was performed using an Agilent 7890A GC connected to an Agilent 5975C MS. 1 µL of sample was injected at 270°C using helium as the carrier gas flowing at 1 mL/min. Split mode was used to avoid sample overloading. To separate the MOX-tBDMS derivatized polar metabolites the chromatography oven was held at 100°C for 2 minutes, increased to 255°C at 3.5°C/min, increased to 320°C at 15°C/min, and held at 320°C for 3 minutes. To separate FAMEs the oven temperature was held at 100°C for 3 minutes, increased to 205°C at 25°C/min, increased to 230°C at 5°C/min, increased to 300°C at 25°C/min, and held at 300°C for 2 minutes. The MS operated in electron impact mode with the source and quadrapole held at 150°C and 230°C respectively and scanned over the range of 100-650 m/z for methoxyamine-tBDMS dervitized polar metabolites and 100-350 m/z for FAMEs. Mass isotopomer distributions (MIDs) were determined by integrating ion fragments. When required, MIDs were corrected for natural abundances using an algorithm adapted from one described previously (Fernandez et al., 1996). Percent ^{13}C enrichment was calculated from MIDs corrected for natural isotopic abundances as shown in Equation S3.7.

$$E = \frac{100\%}{n} \sum_{i=1}^{n} iM_i \tag{S3.7}$$

where E is the percent ^{13}C enrichment, i iterates the number of possible ^{13}C labeled carbons on a metabolite fragment (one to the number of metabolite carbons), n is the number of

metabolite carbons, and M_i is the relative abundance of the mass isotopomer containing i ^{13}C carbon atoms. The quantity "percent ^{13}C labeled" is 100% minus the percent of a metabolite containing zero ^{13}C carbon atoms.

Proliferation Assay

C2C12 myoblasts were plated 3000 cells per well in 96 well plates, one plate for each time point. After cells attached (time=0) and each day after plates were fixed with 4% paraformaldehyde and stored at 4°C in PBS. Total biomass over time was quantified by measuring absorbance at 590 nm after staining using 0.9% crystal violet and re-dissolving with 4:1:1 (v:v:v) ethanol:methanol:water.

Preparation of BSA-[U-$^{13}C_{16}$]Palmitate Conjugates

BSA-palmitate conjugates were prepared by dissolving sodium palmitate or [U-$^{13}C_{16}$]sodium palmitate (Cambridge Isotopes) to a concentration of 2.5 mM in a 150 mM NaCl solution at 70°C. Using a glass pipette, 40 mL palmitate solution were added to 50 mL of a 0.34 mM Ultra Fatty Acid Free BSA (Roche) solution at 37°C. A 1 mM working BSA-Palmitate conjugate solution was prepared by adjusting the pH to 7.4 and diluting to a final volume of 100 mL with 150 mM NaCl.

Gene Expression Analysis

Isolation of mRNA from C2C12 myoblasts and myotubes was performed using a nucleic acid purification kit (NucleuSpin) per the manufacturer's instructions. The isolated mRNA was used to synthesize cDNA using a cDNA synthesis kit (Bio Rad) per the manufacturer's instructions. Quantitative polymerase chain reaction (qPCR) analysis was then performed using the Power SYBR Green PCR Master Mix (Applied Biosystems) per the manufacturer's instructions. Relative expression was quantified using the $2^{-\Delta\Delta C_T}$ method with β-actin as the endogenous control.

Western Blot Analysis

Crude mitochondrial fractions from virally transduced cells were isolated as in (Divakaruni et al., 2013). Mitochondrial protein was solubilized and separated by SDS-PAGE on a Laemmli gel. Proteins were transferred to a PVDF membrane by semi-dry transfer (Bio-Rad), immunoblotted for either MPC1 (Abcam ab74871; 1:1000) or MPC2 (Sigma SAB4501091; 1:1000), and visualized by chemiluminescence (FluorChem E, ProteinSimple). After immunoblotting, the PDVF membrane was stripped, Coomassie-stained, and densitometry was measured post hoc as a protein loading control.

Production of Stable Knockdown Myoblasts and Transformed Cells

Lentival shRNA plasmids targeting mouse Mpc1 (NM_018819.3-336s1c1: CCGGCAAACGAAGTAGCTCAGCTCACTCGAGTGAGCTGAGCTACTTCGTTTGTTTTTT), mouse Mpc2 (NM_027430.2-474s21c1: CCGGTTGGAGTTTGTTCGCTGTTAACTCGAGTTAACAGCGAACA AACTCCAATTTTTG), human MPC1 (AAATCTCGAGATTTAATACTTGTAAGGCAGCTTTTT), or a non-targeting/scrambled control construct were packaged in 293FT cells using FuGENE 6 as a transfection agent for the desired pLKO vector, VSV-G, gag/pol, and rev. The 293FT cell culture medium containing the lentiviral constructs was collected and filtered (0.45 μm) to remove any cells. Polybrene was added to a final concentration of 8 μg/mL. Cells in 6-well plates were cultured with 0.5 mL of the virus-containing medium for 4 hours before addition of 2 mL of virus free medium. Transduced cells were then selected with 2 μg/mL puromycin.

Supplemental Figures and Tables

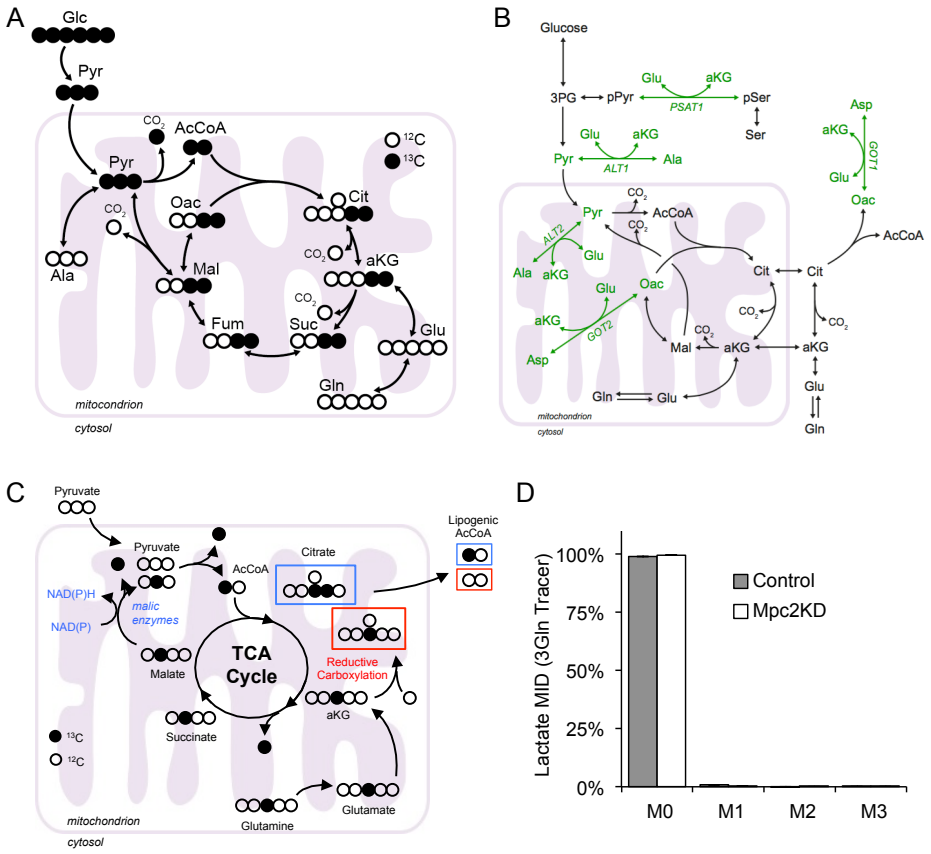

Figure S3.1: Probing Carbohydrate and Amino acid Metabolism. (A) Schematic of UGlc derived carbon atom transitions in the TCA cycle. (B) Schematic of key amino acid metabolism pathways. (C) Schematic of 3Gln derived carbon atom transitions in the TCA cycle. (D) C2C12 myoblast lactate MID resulting from culture with [3-^{13}C]glutamine (3Gln). Error bars indicate SD.

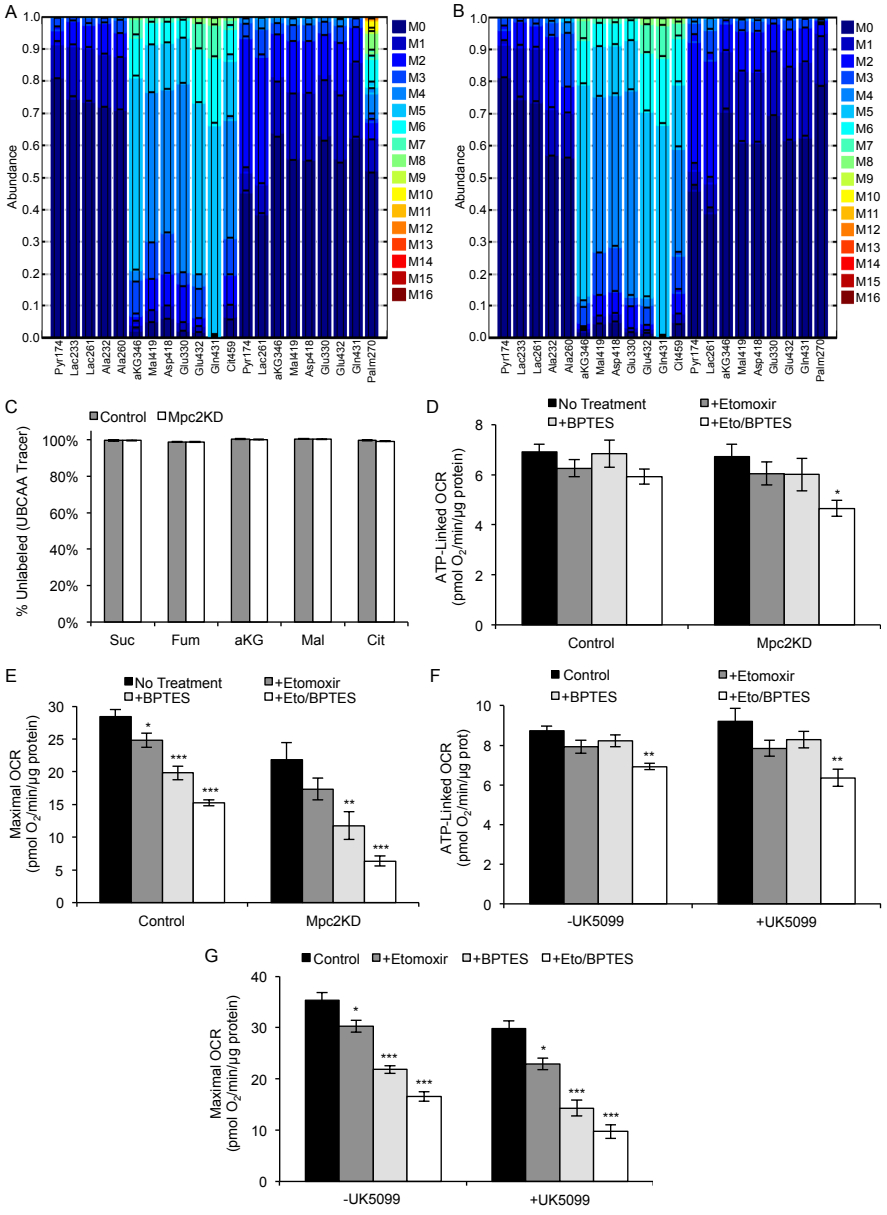

Figure S3.2: Simulation Results and C2C12 Myoblast Branched Chain Amino Acid Metabolism and Oxygen Consumption. (A, B) Simulated MIDs overlaid with measured input MIDs for Control (A) and Mpc2KD (B) cell MFA model. Columns 1-12 and 13-21 correspond to the MIDs resulting from incubation with [U-$^{13}C_5$]glutamine and [1,2-$^{13}C_2$]glucose respectively. (C) Relative abundance of M0 mass isotopomers resulting from culture with [U-$^{13}C_5$]valine, [U-$^{13}C_6$]leucine, and [U-$^{13}C_6$]isoleucine (collectively UBCAA). (D) ATP-linked oxygen consumption rate (OCR). (E) Maximal OCR. (F) ATP-linked OCR. (G) Maximal OCR. Culture medium supplemented with 0.5 mM carnitine (D-G). Concentrations used: 20 µM etomoxir, 3 µM BPTES (D-G), 10 µM UK5099 (F,G). Error bars indicate SD (C), SEM (D-G). *, **, and *** indidcate $p<0.05$, 0.01, and 0.001 respectively by ANOVA with Dunnett's post-hoc. All are C2C12 myoblasts.

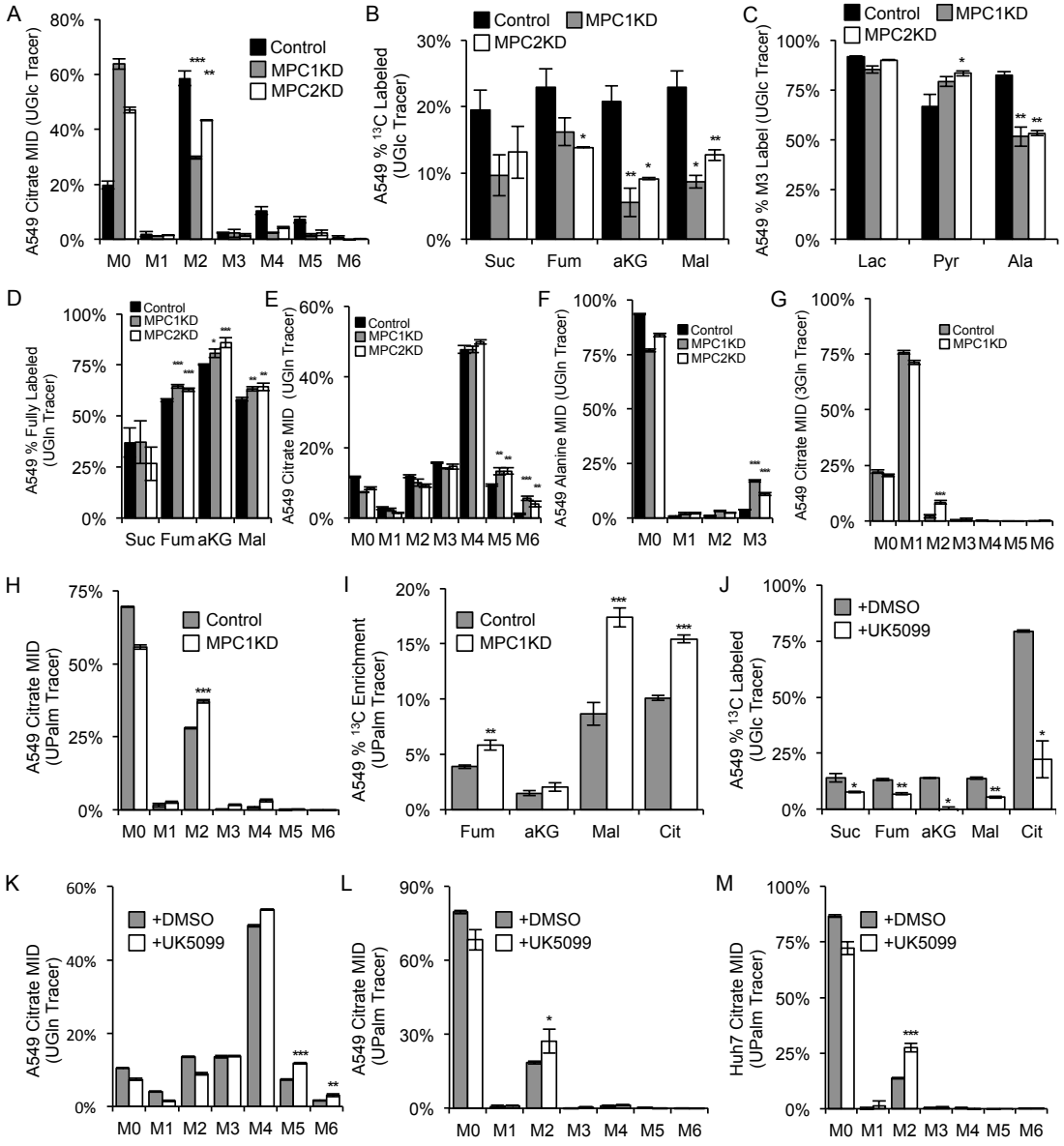

Figure S3.3: Human Transformed Cells Respond to MPC Inhibition. (A-C) Citrate MID (A), % ^{13}C labeled TCA cycle intermediates (B), and M3 labeled lactate, pyruvate, and alanine (C) resulting from culture with UGlc. (D-F) % fully labeled TCA cycle intermediates (D), Citrate MID (E), and alanine MID (F) resulting from culture with UGln. (G) Citrate MID resulting from culture with 3Gln. (H, I) Citrate MID (H) and % ^{13}C enrichment of TCA cycle intermediates (I) resulting from culture with UPalm. (J) % ^{13}C labeled TCA cycle intermediates resulting from culture with UGlc, $\pm$10 μM UK5099. (K) Citrate MID resulting from culture with UGln, $\pm$2 μM UK5099. (L-M) A549 (L) and Huh7 (M) cell citrate MID resulting from culture with UPalm, $\pm$10 μM UK5099. Error bars indicate a standard deviation. *, **, and *** indicate $p<0.05$, 0.01, and 0.001 respectively by ANOVA with Dunnett's post-hoc test (A-F) or by a two-tailed, equal variance, Student's t-test (G-M). All are A549 cells unless indicated otherwise.

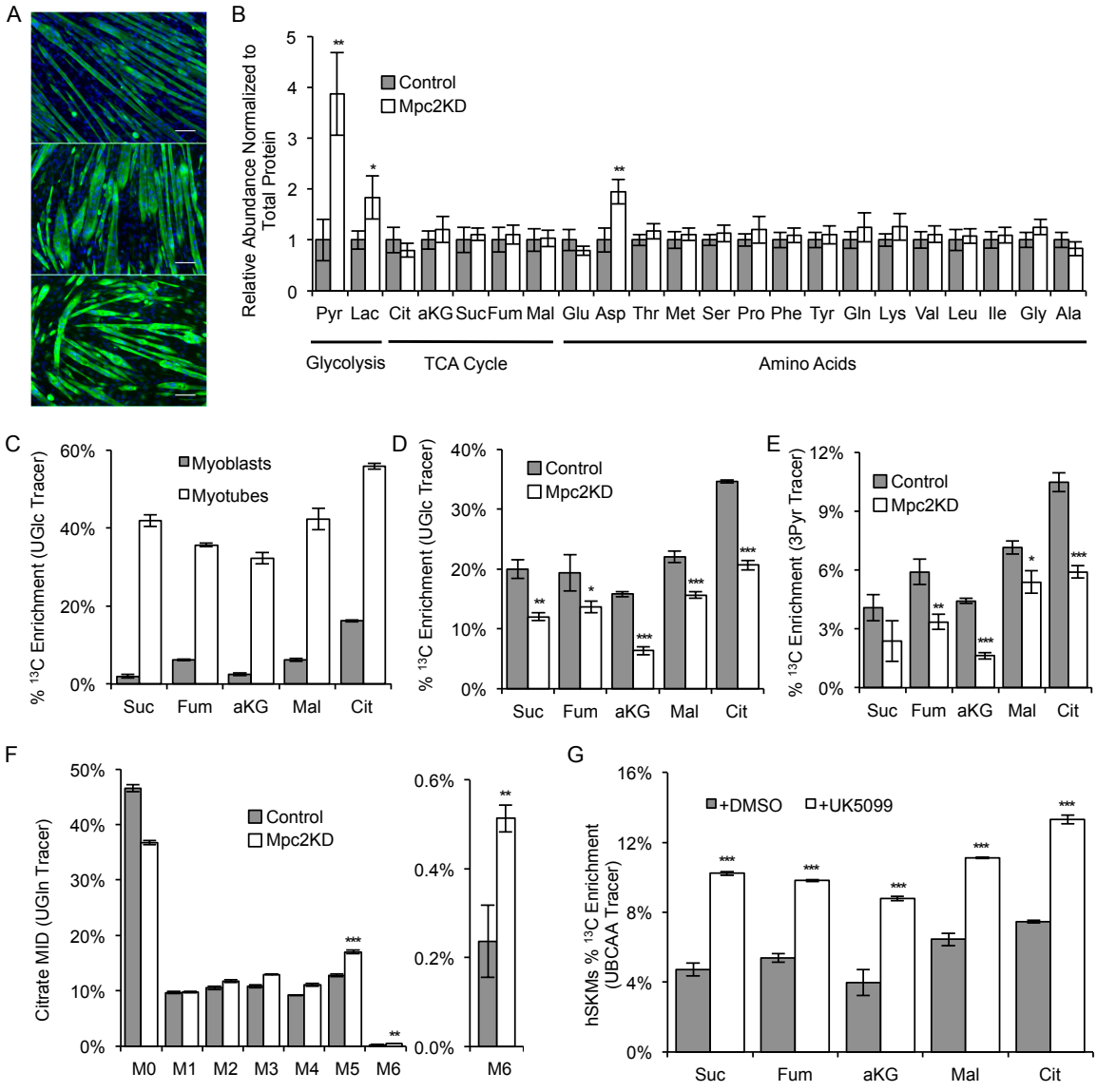

Figure S3.4: Myotubes Respond to Mpc Inhibition. (A) Immunofluorescent staining for desmin, a marker of differentiated myotubes, in Control (top), Mpc1KD (middle), and Mpc2KD (bottom) C2C12 cells differentiated to myotubes. Scale bar is 100 μm. (B) Relative abundance of intracellular metabolites in C2C12 myotubes. (C) % ^{13}C enrichment in C2C12 myotubes and myoblasts resulting from culture with UGlc. (D-E) C2C12 myotube % ^{13}C enrichment 2 hours after incubation with UGlc (D) and 3Pyr (E). (F) Citrate MID resulting from culture of C2C12 myotubes with UGln. (G) % ^{13}C enrichment in Patient 2 hSKMs cultured with with [U-$^{13}C_5$]valine, [U-$^{13}C_6$]leucine, and [U-$^{13}C_6$]isoleucine (collectively UBCAA). Error bars represent a SD. *, **, and *** indidcate $p<0.05$, 0.01, and 0.001 respectively by a two-tailed, equal variance Student's t-test.

Table S3.1: Metabolic Flux Analysis on Control C2C12 Myoblasts. A net flux is the reverse subtracted from the forward flux while an exchange flux is the minimum of the forward and reverse fluxes. If no type is specified, then the flux is a net flux where the reverse reaction was not included in the model.

Pathway/Reaction	Number and Type	Flux (fmol/cell/hr)	Lower bound (fmol/cell/hr)	Upper bound (fmol/cell/hr)
Glycolysis (net fluxes)				
Glc.x -> G6P	R1	320.6	292.3	349.1
G6P -> F6P	R2 net	316.2	287.8	344.4
F6P -> DHAP + GAP	R3	316	287.9	344.1
DHAP -> GAP	R4 net	316	287.9	344.1
GAP -> 3PG	R5 net	631.8	575.6	688.6
3PG -> PEP	R6	631.8	575.6	688.6
PEP -> Pyr.c	R7	644.4	575.1	701.7
Pyr.c -> Lac	R8 net	537.8	481.5	595.2
Lac -> Lac.x	R9	537.8	481.5	595.2
Pyr.c -> Ala	R10	12.77	4.349	18.4
Pyr.m -> Ala	R11	8.921	4.688	17.66
Pyr.c -> Pyr.x	R12	39.33	33.88	44.79
Ala -> Ala.x	R13	9.295	4.173	14.42
Pentose Phosphate Pathway (net fluxes)				
G6P -> P5P + CO2	R14	4.467	3.511	5.424
P5P + P5P -> S7P + GAP	R15 net	-0.1144	-0.4894	0.2597
S7P + GAP -> F6P + E4P	R16 net	-0.1144	-0.4894	0.2597
P5P + E4P -> F6P + GAP	R17 net	-0.1144	-0.4894	0.2597
Anaplerotic Reactions (net fluxes)				
Pyr.c -> Pyr.m	R18	54.5	47.35	64.18
Pyr.m + CO2 -> Oac.m	R19	2.531	1.946	3.208
Oac.c -> PEP + CO2	R20	12.63	0	17.66
Mal.m -> Pyr.m + CO2	R21	4.974	2.562	7.502
Mal.c -> Pyr.c + CO2	R22	1.00×10^{-7}	0	17.64
Pyr.m -> AcCoA.m + CO2	R23	48.02	41.94	54.41
FAO -> AcCoA.m	R24	7.747	5.092	10.58
Glu -> Akg	R25 net	21.04	17.63	24.53
Gln -> Glu	R26 net	31.8	28.23	35.45
Gln.x -> Gln	R27	38.45	34.51	42.44
Glu -> Glu.x	R28	3.001	2.586	3.416
TCA Cycle (net fluxes)				
AcCoA.m + Oac.m -> Cit	R29	55.77	49.31	62.38
Cit -> Akg + CO2	R30 net	5.042	2.806	6.283
Akg -> Suc + CO2	R31	26.08	22.23	30.16
Suc -> Fum.m	R32 net	26.08	22.23	30.16
Fum.m -> Mal.m	R33 net	26.08	22.23	30.16
Mal.m -> Oac.m	R34 net	24.51	-46.77	79.13
Oac.m -> Asp.m	R35 net	-28.73	-100.7	26.37
Mal.c -> Oac.c	R36 net	-3.4	-70.26	∞
Oac.c -> Asp.c	R37 net	34.7	-18.28	∞
Asp.c -> Fum.c	R38	1.00×10^{-7}	-1.02×10^{-10}	∞
Mal.c -> Fum.c	R39 net	-1.00×10^{-7}	-∞	0
Mal.c -> Mal.m	R40 net	3.4	-68.51	57.39
Asp.m -> Asp.c	R41 net	-28.73	-100.7	26.37

Table S3.1: Metabolic Flux Analysis on Control C2C12 Myoblasts, continued.

Pathway/Reaction	Number and Type	Flux (fmol/cell/hr)	Lower bound (fmol/cell/hr)	Upper bound (fmol/cell/hr)
Biomass				
Cit -> AcCoA.c + Oac.c	R42	50.72	44.62	56.98
0*AcCoA.c + 0*AcCoA.c + 0*AcCoA.c + 0*AcCoA.c + 0*AcCoA.c + 0*AcCoA.c + 0*AcCoA.c + 0*AcCoA.c -> Palm.s	R43	1.30×10^{-5}	0	∞
Palm.d -> Palm.s	R44	2.14×10^{-5}	0	∞
114*Asp.c + 152*Glu + 237*Ala + 127*Gln + 970*AcCoA.c + 92*P5P -> Biomass	R45	0.05229	0.046	0.05874
Dilution/Mixing				
0*Pyr.c -> Pyr.mnt	R46	0.5438	0.09823	0.7485
0*Pyr.m -> Pyr.mnt	R47	0.4562	0.2515	0.9018
0*Mal.c -> Mal.mnt	R48	1.00×10^{-7}	5.00×10^{-8}	1
0*Mal.m -> Mal.mnt	R49	1	0	1
0*Asp.c -> Asp.mnt	R50	0.004925	5.00×10^{-8}	1
0*Asp.m -> Asp.mnt	R51	0.9951	0	1
0*Fum.m -> Fum.mnt	R52	0.8233	5.00×10^{-8}	1
0*Fum.c -> Fum.mnt	R53	0.1767	0	1
Glu.d -> Glu	R54	0.1747	0	0.588
Pyr.mnt -> Pyr.fix	R55	1	1	1
Asp.mnt -> Asp.fix	R56	1	1	1
Mal.mnt -> Mal.fix	R57	1	1	1
Fum.mnt -> Fum.fix	R58	1	1	1
Glycolysis (exchange fluxes)				
G6P <- F6P	R2 exch	9.99×10^{-8}	0	∞
DHAP <- GAP	R4 exch	1.00×10^{7}	0	∞
GAP <- 3PG	R5 exch	5.77×10^{5}	0	∞
Pyr.c <- Lac	R8 exch	4.33×10^{5}	0	∞
Pentose Phosphate Pathway (exchange fluxes)				
P5P + P5P <- S7P + GAP	R15 exch	1.00×10^{7}	0.7823	∞
S7P + GAP <- F6P + E4P	R16 exch	3.184	0.801	∞
P5P + E4P <- F6P + GAP	R17 exch	7.56×10^{5}	0	∞
Anaplerotic Reactions (exchange fluxes)				
Glu <- Akg	R25 exch	1756	354.1	∞
Gln <- Glu	R26 exch	1.227	0	5.287
TCA Cycle (exchange fluxes)				
Cit <- Akg + CO2	R30 exch	5.65	4.556	7.607
Suc <- Fum.m	R32 exch	0.4795	0	∞
Fum.m <- Mal.m	R33 exch	1.00×10^{-7}	0	∞
Mal.m <- Oac.m	R34 exch	1.00×10^{-7}	0	49.8
Oac.m <- Asp.m	R35 exch	6.627	0	∞
Mal.c <- Oac.c	R36 exch	1.58×10^{6}	0	∞
Oac.c <- Asp.c	R37 exch	1.00×10^{-7}	0	∞
Mal.c <- Fum.c	R39 exch	5.63×10^{5}	0	∞
Mal.c <- Mal.m	R40 exch	118.1	13.26	∞
Asp.m <- Asp.c	R41 exch	1.00×10^{-7}	0	∞

SSE = 80.4
Expected SSE = [73.1 174.0] (99.9% conf., 117 DOF)

Table S3.2: Metabolic Flux Analysis on Mpc2KD C2C12 Myoblasts. Net and exchange fluxes defined as in the caption to Table S3.1.

Pathway/Reaction	Number and Type	Flux (fmol/cell/hr)	Lower bound (fmol/cell/hr)	Upper bound (fmol/cell/hr)
Glycolysis (net fluxes)				
Glc.x -> G6P	R1	424.2	387.9	460.6
G6P -> F6P	R2 net	420.4	384	456.9
F6P -> DHAP + GAP	R3	419.8	383.4	456.2
DHAP -> GAP	R4 net	419.8	383.4	456.2
GAP -> 3PG	R5 net	839.3	766.6	912
3PG -> PEP	R6	839.3	766.6	912
PEP -> Pyr.c	R7	855.3	766.6	928.4
Pyr.c -> Lac	R8 net	611.6	539.6	683.4
Lac -> Lac.x	R9	611.6	539.6	683.4
Pyr.c -> Ala	R10	9.877	8.258	11.24
Pyr.m -> Ala	R11	6.407	5.272	8.178
Pyr.c -> Pyr.x	R12	222.7	191.8	253.6
Ala -> Ala.x	R13	4.091	2.985	5.199
Pentose Phosphate Pathway (net fluxes)				
G6P -> P5P + CO2	R14	3.836	0.9028	6.762
P5P + P5P -> S7P + GAP	R15 net	-0.2981	-1.294	0.697
S7P + GAP -> F6P + E4P	R16 net	-0.2981	-1.294	0.697
P5P + E4P -> F6P + GAP	R17 net	-0.2981	-1.294	0.697
Anaplerotic Reactions (net fluxes)				
Pyr.c -> Pyr.m	R18	11.11	8.024	16.43
Pyr.m + CO2 -> Oac.m	R19	6.553	4.699	9.848
Oac.c -> PEP + CO2	R20	16.04	0	22.21
Mal.m -> Pyr.m + CO2	R21	19.53	15.97	23.5
Mal.c -> Pyr.c + CO2	R22	1.00×10^{-7}	0	22.24
Pyr.m -> AcCoA.m + CO2	R23	17.68	14.18	22.4
FAO -> AcCoA.m	R24	34.79	29.97	39.42
Glu -> Akg	R25 net	34.88	29.71	40.29
Gln -> Glu	R26 net	45.58	40.31	51.01
Gln.x -> Gln	R27	52.11	46.56	57.75
Glu -> Glu.x	R28	3.797	3.271	4.32
TCA Cycle (net fluxes)				
AcCoA.m + Oac.m -> Cit	R29	52.47	46.49	58.59
Cit -> Akg + CO2	R30 net	2.594	1.178	4.276
Akg -> Suc + CO2	R31	37.47	31.66	43.69
Suc -> Fum.m	R32 net	37.47	31.66	43.69
Fum.m -> Mal.m	R33 net	37.47	31.66	43.69
Mal.m -> Oac.m	R34 net	46.52	-99.13	129.7
Oac.m -> Asp.m	R35 net	0.602	-144.3	85.74
Mal.c -> Oac.c	R36 net	-28.58	-129.4	116.6
Oac.c -> Asp.c	R37 net	5.266	-79.92	433
Asp.c -> Fum.c	R38	1.00×10^{-7}	0	∞
Mal.c -> Fum.c	R39 net	-1.00×10^{-7}	$-\infty$	0
Mal.c -> Mal.m	R40 net	28.58	-116.6	112.3
Asp.m -> Asp.c	R41 net	0.602	-144.3	85.74

Table S3.2: Metabolic Flux Analysis on Mpc2KD C2C12 Myoblasts, continued.

Pathway/Reaction	Number and Type	Flux (fmol/cell/hr)	Lower bound (fmol/cell/hr)	Upper bound (fmol/cell/hr)
Biomass				
Cit -> AcCoA.c + Oac.c	R42	49.88	43.88	55.97
0*AcCoA.c + 0*AcCoA.c + 0*AcCoA.c + 0*AcCoA.c + 0*AcCoA.c + 0*AcCoA.c + 0*AcCoA.c + 0*AcCoA.c -> Palm.s	R43	0.09072	0	3.20×10^{6}
Palm.d -> Palm.s	R44	0.9542	3.13×10^{-7}	∞
114*Asp.c + 152*Glu + 237*Ala + 127*Gln + 970*AcCoA.c + 92*P5P -> Biomass	R45	0.05142	0.04523	0.0577
Dilution/Mixing				
0*Pyr.c -> Pyr.mnt	R46	0.9447	0.9159	0.9699
0*Pyr.m -> Pyr.mnt	R47	0.05533	0.03005	0.08414
0*Mal.c -> Mal.mnt	R48	0.613	5.00×10^{-8}	1
0*Mal.m -> Mal.mnt	R49	0.387	0	1
0*Asp.c -> Asp.mnt	R50	0.04039	5.00×10^{-8}	1
0*Asp.m -> Asp.mnt	R51	0.9596	0	1
0*Fum.m -> Fum.mnt	R52	0.5044	5.00×10^{-8}	1
0*Fum.c -> Fum.mnt	R53	0.4956	0	1
Glu.d -> Glu	R54	0.9037	0.4202	1.407
Pyr.mnt -> Pyr.fix	R55	1	1	1
Asp.mnt -> Asp.fix	R56	1	1	1
Mal.mnt -> Mal.fix	R57	1	1	1
Fum.mnt -> Fum.fix	R58	1	1	1
Glycolysis (exchange fluxes)				
G6P <- F6P	R2 exch	1.00×10^{-7}	0	∞
DHAP <- GAP	R4 exch	1.00×10^{-7}	0	∞
GAP <- 3PG	R5 exch	0.04608	0	∞
Pyr.c <- Lac	R8 exch	1.00×10^{-7}	0	∞
Pentose Phosphate Pathway (exchange fluxes)				
P5P + P5P <- S7P + GAP	R15 exch	1.00×10^{7}	7.084	∞
S7P + GAP <- F6P + E4P	R16 exch	10.62	7.084	33.17
P5P + E4P <- F6P + GAP	R17 exch	9.92×10^{5}	30.13	∞
Anaplerotic Reactions (exchange fluxes)				
Glu <- Akg	R25 exch	5677	271.4	∞
Gln <- Glu	R26 exch	3.357	0	15.52
TCA Cycle (exchange fluxes)				
Cit <- Akg + CO2	R30 exch	6.172	4.836	7.573
Suc <- Fum.m	R32 exch	0.05958	0	∞
Fum.m <- Mal.m	R33 exch	1.00×10^{-7}	0	∞
Mal.m <- Oac.m	R34 exch	1.00×10^{-7}	0	87.45
Oac.m <- Asp.m	R35 exch	1.00×10^{-7}	0	∞
Mal.c <- Oac.c	R36 exch	1.00×10^{7}	97	∞
Oac.c <- Asp.c	R37 exch	1.00×10^{-7}	0	∞
Mal.c <- Fum.c	R39 exch	1.00×10^{-7}	0	∞
Mal.c <- Mal.m	R40 exch	123.7	36.07	∞
Asp.m <- Asp.c	R41 exch	273.1	0	∞

SSE = 82.5
Expected SSE = [61.4 155.6] (99.9% conf., 102 DOF)

Table S3.3: Metabolite Fragments Considered in MFA. "Metabolite" refers to the MOX-tBDMS derivatized metabolite that was fragmented during GC/MS analysis. "Carbons" refers to the metabolite carbons that are part of the derivatized metabolite fragment. "Formula" is the chemical formula, and "m/z" is the mass to charge ratio of the derivatized metabolite fragment.

Metabolite	Carbons	Formula	m/z
Pyruvate	1,2,3	$C_6H_{12}O_3NSi$	174
Lactate	2,3	$C_{10}H_{25}O_2Si_2$	233
Lactate	1,2,3	$C_{11}H_{25}O_3Si_2$	261
Alanine	2,3	$C_{10}H_{26}ONSi_2$	232
Alanine	1,2,3	$C_{11}H_{26}O_2NSi_2$	260
aKG	1,2,3,4,5	$C_{14}H_{28}O_5NSi_2$	346
Malate	1,2,3,4	$C_{18}H_{39}O_5Si_3$	419
Aspartate	1,2,3,4	$C_{18}H_{40}O_4NSi_3$	418
Glutamate	2,3,4,5	$C_{16}H_{36}O_2NSi_2$	330
Glutamate	1,2,3,4,5	$C_{19}H_{42}O_4NSi_3$	432
Glutamine	1,2,3,4,5	$C_{19}H_{43}O_3N_2Si_3$	431
Citrate	1,2,3,4,5,6	$C_{20}H_{39}O_6Si_3$	459
Palmitate	1-16	$C_{17}H_{34}O_2$	270

Supplement to Chapter 4

Experimental Procedures

Cell Culture and Tracing in Intact Cells

A549 and Huh7 cells were cultured in Dulbecco's modified Eagle's medium (DMEM) supplemented with 10% fetal bovine serum, 100 units/ml penicillin, and 100 μg/ml streptomycin at 37°C and 5% CO_2. For tracer studies, custom, phenol red-free DMEM was formulated by replacing the substrate of interest with ^{13}C-labeled glucose, ^{13}C-labeled glutamine, or ^{15}N-labeled glutamine. All other components were unlabeled. Cultures were washed with phosphate buffered saline before adding tracer medium and allowing to incubate for 24 hours.

Tracing in Permeabilized Cells

Cells were plated to near confluent in 6-well plates. Basal medium containing 125 mM sucrose, 65 mM KCl, 5 mM KH_2PO_4, 20 mM HEPES, 1 mM MgCl, 0.5 mM EGTA, and 0.2% bovine serum albumin was prepared in cell culture water. Immediately prior to the experiment, unlabeled malate and the glutamine or glutamate tracer were each added to a final concentration of 1 mM, and ADP to a final concentration of 4 mM. 1 ml of tracer medium was charged to each well and the cells placed in a 37°C incubator without supplemented CO_2. The metabolites were extracted as described below after 20 minutes.

Metabolite Extraction and GC/MS Analysis

At the conclusion of a tracer experiment, the tracer medium was removed from the culture wells, intact cells were washed with a saline solution (9 g/L NaCl), permeabilized cells washed twice with 150 mM NaCl, and the bottom of each well was covered with 400 µl cold methanol to lyse the cells and halt metabolism. Water containing norvaline at 2.5 µg/ml was charged to each well at a volume ratio of 1:2.5 relative to the methanol. The bottom of each well was scraped with a 1,000 µl pipette tip, and the cells were collected in 1.5 ml tubes. Cold chloroform was added to each sample at a 1:1 volume ratio relative to the methanol. The mixtures were vortexed, and the polar and nonpolar layers separated and evaporated after centrifugation.

Determination of Extracellular Fluxes

Initial and final quantities of glucose, lactate, glutamine, and glutamate present were determined using a Yellow Springs Instrument while pyruvate and alanine levels were measured using GC/MS. The extracellular fluxes were determined by solving the differential equations listed as Equations S4.1-S4.3:

$$\frac{dX}{dt} = \mu X \tag{S4.1}$$

$$\frac{dN_i}{dt} = q_i X \tag{S4.2}$$

$$\frac{dN_{Gln}}{dt} = q_i X - kN_{Gln} \tag{S4.3}$$

where X represents the number of cells present (see normalization described below), μ the cellular growth rate (in hr^{-1}), N_i the moles of substrate i present, q_i the extracellular flux of substrate i (in moles/cell/hr), and k the degradation rate of glutamine (in hr^{-1}). Equations S4.1 and S4.2 were used to solve for glucose, lactate, glutamate, pyruvate, and alanine extracellular fluxes while Equations S4.1 and S4.3 (which considers glutamine degradation) were used to solve for the glutamine extracellular flux. k was set to 0.003 hr^{-1}. Solving Equations S4.1-S4.3

yields Equations S4.4-S4.6 respectively.

$$X = X_0 e^{\mu t} \tag{S4.4}$$

$$q_i = \frac{\mu \left(N_{i,f} - N_{i,0}\right)}{X - X_0} \tag{S4.5}$$

$$q_{Gln} = \frac{N_{Gln,f} - N_{Gln,0} e^{-kt}}{\left(\frac{1}{\mu + k}\right)\left(X - X_0 e^{-kt}\right)} \tag{S4.6}$$

where the subscripts 0 and f indicate initial and final values respectively.

Normalization

Extracellular fluxes and metabolite abundances are normalized to a representation of cell quantity. The quantity of control cells was set to 1 and the quantity of MQCKD cells was determined by calculating the average fractional abundance of each metabolite fragment (using gas chromatography/mass spectrometry) relative to the control cells. Extracellular fluxes and metabolite abundances are presented as relative values.

Separation and Chemical Derivatization of Polar Metabolites

Dried polar metabolites were dissolved in 20 µL of 2% (m/v) methoxyamine hydrochloride in pyridine and incubated for 60 minutes at 45°C. 20 µL of N-tert-butyldimethylsiyl-n-methyltrifluoroacetamide with 1% tert-butyldimethylchlorosilane was then added and the solution incubated at 45°C for an additional 30 minutes to form methoxyamine-tert-butyldimethylsiyl (MOX-tBDMS) derivatives.

Gas Chromatography and Mass Spectrometry

GC/MS analysis was performed using an Agilent 7890A GC connected to an Agilent 5975C MS. 1 µL of sample was injected at 270°C using helium as the carrier gas flowing at 1 ml/min. To separate the MOX-tBDMS derivatized polar metabolites the chromatography oven was held at 100°C for 2 minutes, increased to 255°C at 3.5°C/min, increased to 320°C at 15°C/min, and held at 320°C for 3 minutes. To separate FAMEs the oven temperature was

held at 100°C for 3 minutes, increased to 205°C at 25°C/min, increased to 230°C at 5°C/min, increased to 300°C at 25°C/min, and held at 300°C for 2 minutes. The MS operated in electron impact mode with the source and quadrapole held at 150°C and 230°C respectively and scanned over the range of 100-650 m/z for methoxyamine-tBDMS dervitized polar metabolites and 100-350 m/z for FAMEs. Mass isotopomer distributions (MIDs) were determined by integrating ion fragments. When required, MIDs were corrected for natural abundances using an algorithm adapted from one described previously (Fernandez et al., 1996).

Growth Assay

Cells were plated in 6-well plates at known densities. At the specified time points, cells were removed from the wells with trypsin and counted.

Gene Expression Analysis

Isolation of mRNA from cells was performed using a nucleic acid purification kit (Qiagen) per the manufacturer's instructions. The isolated mRNA was used to synthesize cDNA using a cDNA synthesis kit (Applied Biosystems) per the manufacturer's instructions. Quantitative polymerase chain reaction (qPCR) analysis was then performed using the Power SYBR Green PCR Master Mix (Bio-Rad) per the manufacturer's instructions. Relative expression was quantified using the $2^{-\Delta\Delta C_T}$ method with ribosomal protein L27 as the endogenous control gene.

Production of Stable Knockdown Transformed Cells

Lentival shRNA plasmids targeting human SLC25A44 (NM_014655.1-467s1c1: CCGGGCCAGAGTAACACAGTCAAATCTCGAGATTTGACTGTGTTACTCTGGCTTTTTTG) or a non-targeting control construct were packaged in 293FT cells using FuGENE 6 as a transfection agent for the desired pLKO vector, VSV-G, gag/pol, and rev. The 293FT cell culture medium containing the lentiviral constructs was collected and filtered (0.45 μm) to remove any cells. Polybrene was added to a final concentration of 8 μg/ml. Cells in 6-well plates were cultured with 0.5 ml of the virus-containing medium for 4 hours before addition of 2 ml of virus free medium. Transduced cells were then selected with 2 μg/ml puromycin.

Supplemental Figures

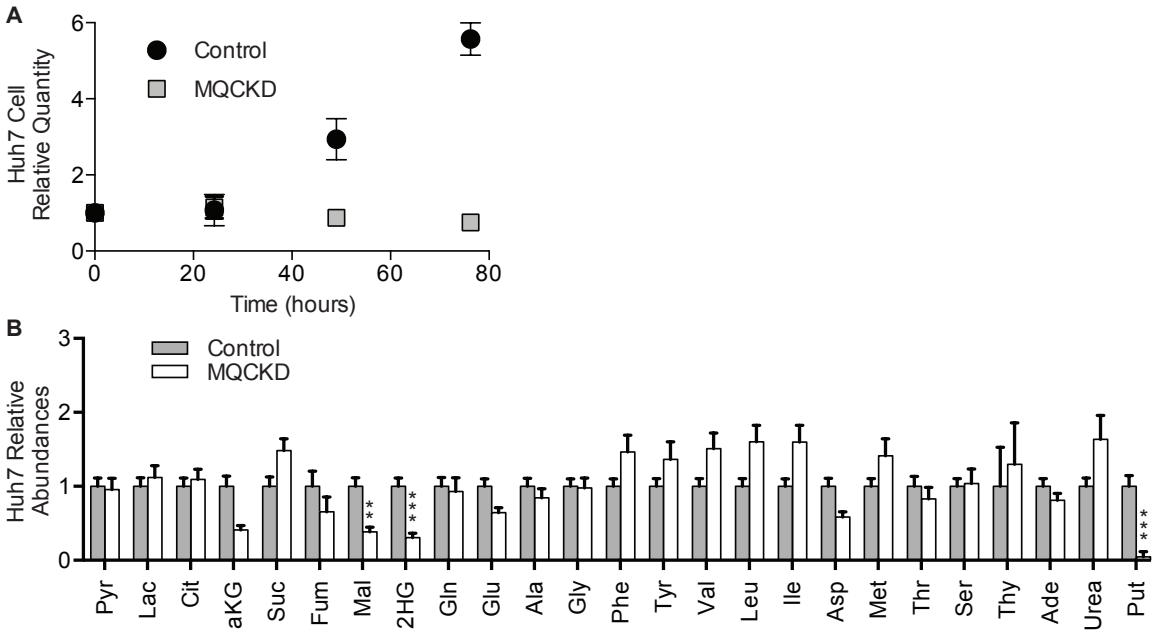

Figure S4.1: MQC Knockdown Effects on Growth and Metabolite Pools. (A-B) Proliferation (A) and metabolite abundances (B). All are Huh7 cells. Error bars indicate SD. *, **, and *** indicate $p < 0.05$, 0.01, and 0.001 by t-test. P-value indicators only provided if significant after correcting for multiple comparisons using the Holm-Sidak method.

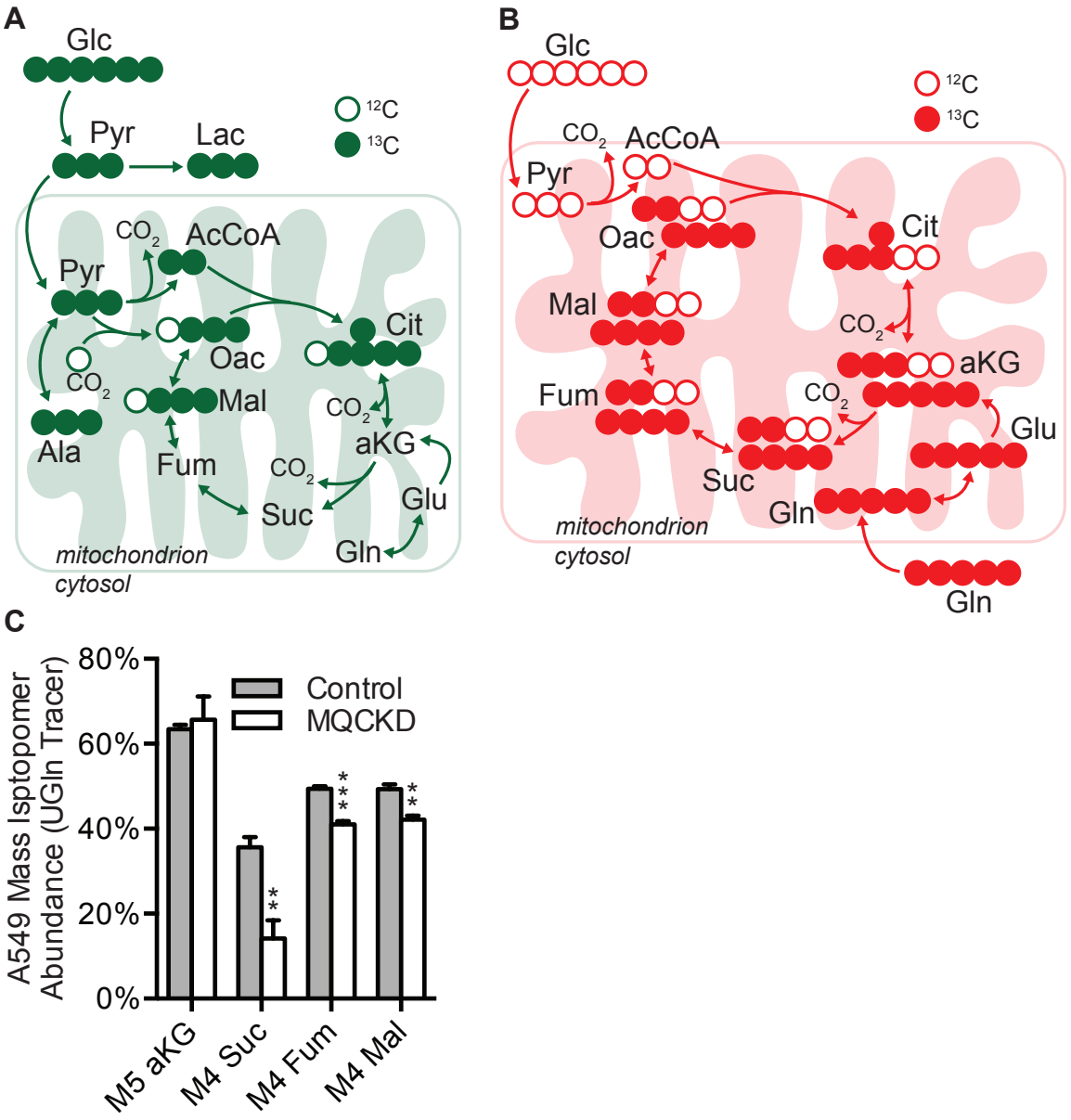

Figure S4.2: ^{13}C-Glucose and ^{13}C-Glutamine Labeling Schematics and A549 Cell Glutamine Oxidation. (A-B) Schematic of UGlc (A) and UGln (B) labeling. (C) A549 cell TCA cycle intermediate relative mass isotopomer abundances resulting from culture with UGln, and indicative of glutamine oxidation. Error bars indicate SD. *, **, and *** indicate $p < 0.05$, 0.01, and 0.001 by t-test. P-value indicators only provided if significant after correcting for multiple comparisons using the Holm-Sidak method.

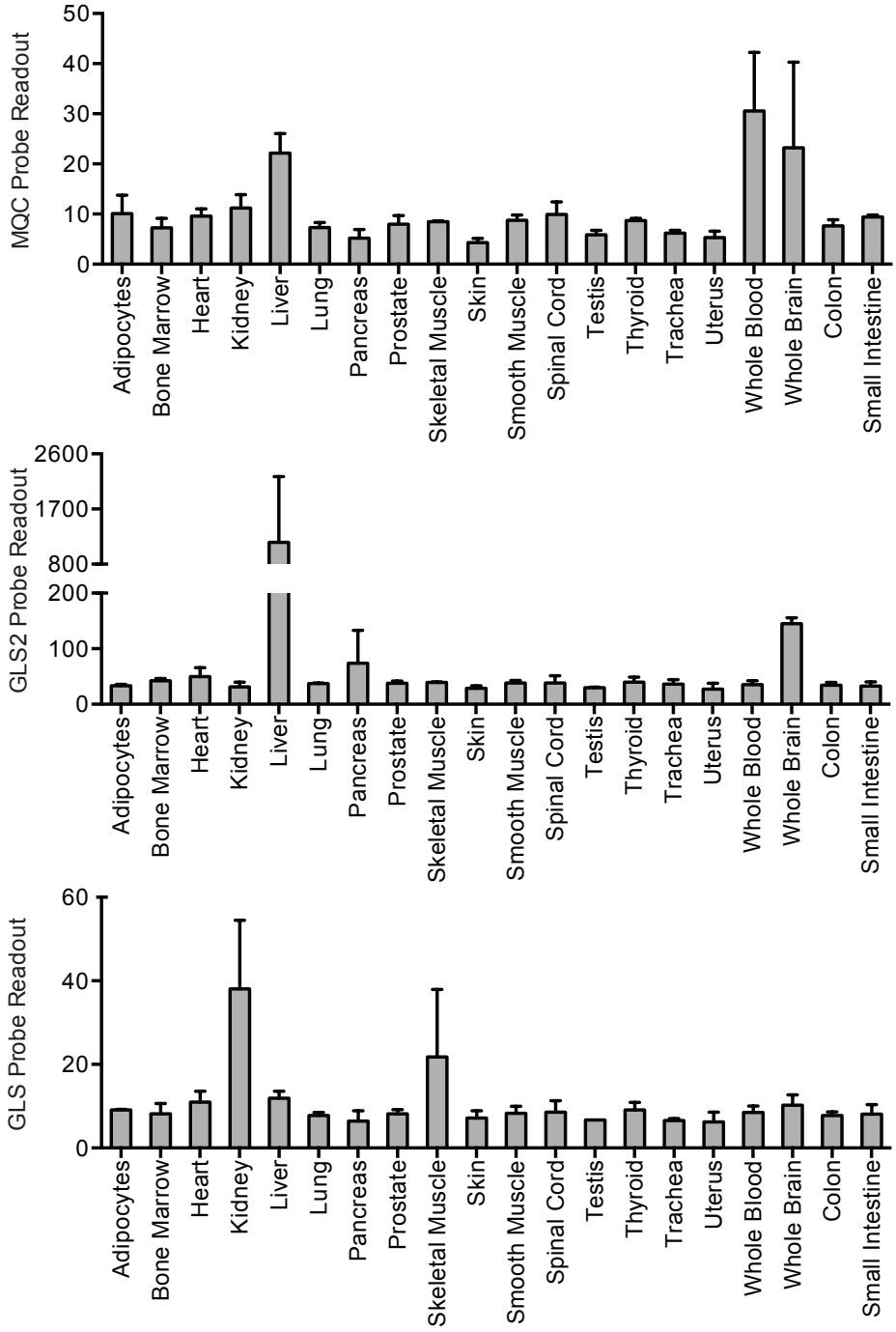

Figure S4.3: Tissue Specific Expression of *MQC*, *GLS2*, and *GLS*. Readouts for *MQC*, *GLS2*, and *GLS* are from microarray probes "212683_at", "205531_s_at", and "203158_s_at" respectively. Data collected by Su et al. (2004) and accessed from BioGPS (Wu et al., 2009).

References

Adams, S. H. (2011). Emerging perspectives on essential amino acid metabolism in obesity and the insulin-resistant state. *Advances in nutrition*, 2(6):445–456.

Agrimi, G., Di Noia, M. A., Marobbio, C. M. T., Fiermonte, G., Lasorsa, F. M., and Palmieri, F. (2004). Identification of the human mitochondrial S-adenosylmethionine transporter: bacterial expression, reconstitution, functional characterization and tissue distribution. *Biochem. J.*, 379(Pt 1):183–190.

Ahn, W. S. and Antoniewicz, M. R. (2011). Metabolic flux analysis of CHO cells at growth and non-growth phases using isotopic tracers and mass spectrometry. *Metabolic engineering*, 13(5):598–609.

Ahn, W. S. and Antoniewicz, M. R. (2012). Parallel labeling experiments with [1,2-(13)C]glucose and [U-(13)C]glutamine provide new insights into CHO cell metabolism. *Metabolic engineering*, 15:34–47.

Al-Hajj, M., Wicha, M. S., Benito-Hernandez, A., Morrison, S. J., and Clarke, M. F. (2003). Prospective identification of tumorigenic breast cancer cells. *Proc. Natl. Acad. Sci. U.S.A.*, 100(7):3983–3988.

Amiry-Moghaddam, M., Lindland, H., Zelenin, S., Roberg, B. A., Gundersen, B. B., Petersen, P., Rinvik, E., Torgner, I. A., and Ottersen, O. P. (2005). Brain mitochondria contain aquaporin water channels: evidence for the expression of a short AQP9 isoform in the inner mitochondrial membrane. *FASEB J.*, 19(11):1459–1467.

Anderson, D. G., Levenberg, S., and Langer, R. (2004). Nanoliter-scale synthesis of arrayed biomaterials and application to human embryonic stem cells. *Nature biotechnology*, 22(7):863–866.

Antoniewicz, M. R., Kelleher, J. K., and Stephanopoulos, G. (2006). Determination of confidence intervals of metabolic fluxes estimated from stable isotope measurements. *Metabolic engineering*, 8(4):324–337.

Aquila, H., Misra, D., Eulitz, M., and Klingenberg, M. (1982). Complete amino acid sequence of the ADP/ATP carrier from beef heart mitochondria. *Hoppe-Seyler's Z. Physiol. Chem.*, 363(3):345–349.

Austin, J. and Aprille, J. R. (1984). Carboxyatractyloside-insensitive influx and efflux of adenine nucleotides in rat liver mitochondria. *J. Biol. Chem.*, 259(1):154–160.

Azzi, A., Chappell, J. B., and Robinson, B. H. (1967). Penetration of the mitochondrial membrane by glutamate and aspartate. *Biochem. Biophys. Res. Commun.*, 29(1):148–152.

Bakker, E. P. and van Dam, K. (1974). The movement of monocarboxylic acids across phospholipid membranes: evidence for an exchange diffusion between pyruvate and other monocarboxylate ions. *Biochimica et biophysica acta*, 339(2):285–289.

Bao, S., Wu, Q., McLendon, R. E., Hao, Y., Shi, Q., Hjelmeland, A. B., Dewhirst, M. W., Bigner, D. D., and Rich, J. N. (2006). Glioma stem cells promote radioresistance by preferential activation of the DNA damage response. *Nature*, 444(7120):756–760.

Baughman, J. M., Perocchi, F., Girgis, H. S., Plovanich, M., Belcher-Timme, C. A., Sancak, Y., Bao, X. R., Strittmatter, L., Goldberger, O., Bogorad, R. L., Koteliansky, V., and Mootha, V. K. (2011). Integrative genomics identifies MCU as an essential component of the mitochondrial calcium uniporter. *Nature*, 476(7360):341–345.

Ben-Porath, I., Thomson, M. W., Carey, V. J., Ge, R., Bell, G. W., Regev, A., and Weinberg, R. A. (2008). An embryonic stem cell-like gene expression signature in poorly differentiated aggressive human tumors. *Nature genetics*, 40(5):499–507.

Bender, T., Pena, G., and Martinou, J. C. (2015). Regulation of mitochondrial pyruvate uptake by alternative pyruvate carrier complexes. *EMBO J.*, 34(7):911–924.

Bernardi, P. (1999). Mitochondrial transport of cations: channels, exchangers, and permeability transition. *Physiol. Rev.*, 79(4):1127–1155.

Bhatia, M., Wang, J. C., Kapp, U., Bonnet, D., and Dick, J. E. (1997). Purification of primitive human hematopoietic cells capable of repopulating immune-deficient mice. *Proc. Natl. Acad. Sci. U.S.A.*, 94(10):5320–5325.

Billups, B. and Forsythe, I. D. (2002). Presynaptic mitochondrial calcium sequestration influences transmission at mammalian central synapses. *J. Neurosci.*, 22(14):5840–5847.

Biswas, A., Senthilkumar, S. R., and Said, H. M. (2012). Effect of chronic alcohol exposure on folate uptake by liver mitochondria. *Am. J. Physiol., Cell Physiol.*, 302(1):C203–209.

Blair, I. A. (2001). Lipid hydroperoxide-mediated DNA damage. *Experimental gerontology*, 36(9):1473–1481.

Booty, L. M., King, M. S., Thangaratnarajah, C., Majd, H., James, A. M., Kunji, E. R., and Murphy, M. P. (2015). The mitochondrial dicarboxylate and 2-oxoglutarate carriers do not transport glutathione. *FEBS Lett.*, 589(5):621–628.

Boss, O., Samec, S., Paoloni-Giacobino, A., Rossier, C., Dulloo, A., Seydoux, J., Muzzin, P., and Giacobino, J. P. (1997). Uncoupling protein-3: a new member of the mitochondrial carrier family with tissue-specific expression. *FEBS Lett.*, 408(1):39–42.

Bouillaud, F., Ricquier, D., Thibault, J., and Weissenbach, J. (1985). Molecular approach to thermogenesis in brown adipose tissue: cDNA cloning of the mitochondrial uncoupling protein. *Proc. Natl. Acad. Sci. U.S.A.*, 82(2):445–448.

Bracha, A. L., Ramanathan, A., Huang, S., Ingber, D. E., and Schreiber, S. L. (2010). Carbon metabolism-mediated myogenic differentiation. *Nature chemical biology*, 6(3):202–204.

Brafman, D. A., Chang, C. W., Fernandez, A., Willert, K., Varghese, S., and Chien, S. (2010). Long-term human pluripotent stem cell self-renewal on synthetic polymer surfaces. *Biomaterials*, 31(34):9135–9144.

Bricker, D. K., Taylor, E. B., Schell, J. C., Orsak, T., Boutron, A., Chen, Y. C., Cox, J. E., Cardon, C. M., Van Vranken, J. G., Dephoure, N., Redin, C., Boudina, S., Gygi, S. P., Brivet, M., Thummel, C. S., and Rutter, J. (2012). A mitochondrial pyruvate carrier required for pyruvate uptake in yeast, drosophila, and humans. *Science*, 337(6090):96–9100.

Bridges, E. G., Jiang, Z., and Cheng, Y. C. (1999). Characterization of a dCTP transport activity reconstituted from human mitochondria. *J. Biol. Chem.*, 274(8):4620–4625.

Calamita, G., Ferri, D., Gena, P., Liquori, G. E., Cavalier, A., Thomas, D., and Svelto, M. (2005). The inner mitochondrial membrane has aquaporin-8 water channels and is highly permeable to water. *J. Biol. Chem.*, 280(17):17149–17153.

Camacho, J. A., Mardach, R., Rioseco-Camacho, N., Ruiz-Pesini, E., Derbeneva, O., Andrade, D., Zaldivar, F., Qu, Y., and Cederbaum, S. D. (2006). Clinical and functional characterization of a human ORNT1 mutation (T32R) in the hyperornithinemia-hyperammonemia-homocitrullinuria (HHH) syndrome. *Pediatr. Res.*, 60(4):423–429.

Camacho, J. A., Obie, C., Biery, B., Goodman, B. K., Hu, C. A., Almashanu, S., Steel, G., Casey, R., Lambert, M., Mitchell, G. A., and Valle, D. (1999). Hyperornithinaemia-hyperammonaemia-homocitrullinuria syndrome is caused by mutations in a gene encoding a mitochondrial ornithine transporter. *Nat. Genet.*, 22(2):151–158.

Camacho, J. A., Rioseco-Camacho, N., Andrade, D., Porter, J., and Kong, J. (2003). Cloning and characterization of human ORNT2: a second mitochondrial ornithine transporter that can rescue a defective ORNT1 in patients with the hyperornithinemia-hyperammonemia-homocitrullinuria syndrome, a urea cycle disorder. *Mol. Genet. Metab.*, 79(4):257–271.

Cárdenas, C., Miller, R. A., Smith, I., Bui, T., Molgó, J., Müller, M., Vais, H., Cheung, K. H., Yang, J., Parker, I., Thompson, C. B., Birnbaum, M. J., Hallows, K. R., and Foskett, J. K. (2010). Essential regulation of cell bioenergetics by constitutive InsP3 receptor Ca2+ transfer to mitochondria. *Cell*, 142(2):270–283.

Carroll, R., Gant, V. A., and Yellon, D. M. (2001). Mitochondrial K(ATP) channel opening protects a human atrial-derived cell line by a mechanism involving free radical generation. *Cardiovasc. Res.*, 51(4):691–700.

Casimir, M., Lasorsa, F. M., Rubi, B., Caille, D., Palmieri, F., Meda, P., and Maechler, P. (2009). Mitochondrial glutamate carrier GC1 as a newly identified player in the control of glucose-stimulated insulin secretion. *J. Biol. Chem.*, 284(37):25004–25014.

Catalina-Rodriguez, O., Kolukula, V. K., Tomita, Y., Preet, A., Palmieri, F., Wellstein, A., Byers, S., Giaccia, A. J., Glasgow, E., Albanese, C., and Avantaggiati, M. L. (2012). The

mitochondrial citrate transporter, CIC, is essential for mitochondrial homeostasis. *Oncotarget*, 3(10):1220–1235.

Chance, B. (1972). The nature of electron transfer and energy coupling reactions. *FEBS Lett.*, 23(1):3–20.

Chaneton, B., Hillmann, P., Zheng, L., Martin, A. C., Maddocks, O. D., Chokkathukalam, A., Coyle, J. E., Jankevics, A., Holding, F. P., Vousden, K. H., Frezza, C., O'Reilly, M., and Gottlieb, E. (2012). Serine is a natural ligand and allosteric activator of pyruvate kinase m2. *Nature*, 491(7424):458–462.

Chang, C. M., Yu, C. C., Lu, H. T., Chou, Y. F., and Huang, R. F. (2007). Folate deprivation promotes mitochondrial oxidative decay: DNA large deletions, cytochrome c oxidase dysfunction, membrane depolarization and superoxide overproduction in rat liver. *Br. J. Nutr.*, 97(5):855–863.

Chang, D. T. and Reynolds, I. J. (2006). Mitochondrial trafficking and morphology in healthy and injured neurons. *Prog. Neurobiol.*, 80(5):241–268.

Chappell, J. B. (1968). Systems Used for the Transport of Substrates into the Mitochondria. *Br. Med. Bull.*, 24:150–157.

Chen, C. N., Lin, S. Y., Liao, Y. H., Li, Z. J., and Wong, A. M. (2015). Late-onset caloric restriction alters skeletal muscle metabolism by modulating pyruvate metabolism. *Am. J. Physiol. Endocrinol. Metab.*, 308(11):E942–949.

Chen, Q., Vazquez, E. J., Moghaddas, S., Hoppel, C. L., and Lesnefsky, E. J. (2003). Production of reactive oxygen species by mitochondria: central role of complex III. *The Journal of biological chemistry*, 278(38):36027–36031.

Chen, W., Dailey, H. A., and Paw, B. H. (2010). Ferrochelatase forms an oligomeric complex with mitoferrin-1 and Abcb10 for erythroid heme biosynthesis. *Blood*, 116(4):628–630.

Chen, Z., Putt, D. A., and Lash, L. H. (2000). Enrichment and functional reconstitution of glutathione transport activity from rabbit kidney mitochondria: further evidence for the role of the dicarboxylate and 2-oxoglutarate carriers in mitochondrial glutathione transport. *Arch. Biochem. Biophys.*, 373(1):193–202.

Chevrollier, A., Loiseau, D., Reynier, P., and Stepien, G. (2011). Adenine nucleotide translocase 2 is a key mitochondrial protein in cancer metabolism. *Biochim. Biophys. Acta*, 1807(6):562–567.

Cho, Y. M., Kwon, S., Pak, Y. K., Seol, H. W., Choi, Y. M., Park, D. J., Park, K. S., and Lee, H. K. (2006). Dynamic changes in mitochondrial biogenesis and antioxidant enzymes during the spontaneous differentiation of human embryonic stem cells. *Biochemical and biophysical research communications*, 348(4):1472–1478.

Christofk, H. R., Vander Heiden, M. G., Harris, M. H., Ramanathan, A., Gerszten, R. E., Wei, R., Fleming, M. D., Schreiber, S. L., and Cantley, L. C. (2008). The m2 splice isoform of pyruvate kinase is important for cancer metabolism and tumour growth. *Nature*, 452(7184):230–233.

Chuikov, S., Levi, B. P., Smith, M. L., and Morrison, S. J. (2010). Prdm16 promotes stem cell maintenance in multiple tissues, partly by regulating oxidative stress. *Nature cell biology*, 12(10):999–991006.

Clark, J. B. and Land, J. M. (1974). Differential effects of 2-oxo acids on pyruvate utilization and fatty acid synthesis in rat brain. *The Biochemical journal*, 140(1):25–29.

Cohn, S. M., Schloemann, S., Tessner, T., Seibert, K., and Stenson, W. F. (1997). Crypt stem cell survival in the mouse intestinal epithelium is regulated by prostaglandins synthesized through cyclooxygenase-1. *The Journal of clinical investigation*, 99(6):1367–1379.

Colca, J. R., McDonald, W. G., Cavey, G. S., Cole, S. L., Holewa, D. D., Brightwell-Conrad, A. S., Wolfe, C. L., Wheeler, J. S., Coulter, K. R., Kilkuskie, P. M., Gracheva, E., Korshunova, Y., Trusgnich, M., Karr, R., Wiley, S. E., Divakaruni, A. S., Murphy, A. N., Vigueira, P. A., Finck, B. N., and Kletzien, R. F. (2013). Identification of a mitochondrial target of thiazolidinedione insulin sensitizers (mTOT)–relationship to newly identified mitochondrial pyruvate carrier proteins. *PLoS ONE*, 8(5):e61551.

Covello, K. L., Kehler, J., Yu, H., Gordan, J. D., Arsham, A. M., Hu, C. J., Labosky, P. A., Simon, M. C., and Keith, B. (2006). HIF-2alpha regulates oct-4: effects of hypoxia on stem cell function, embryonic development, and tumor growth. *Genes & development*, 20(5):557–570.

Cunnane, S., Nugent, S., Roy, M., Courchesne-Loyer, A., Croteau, E., Tremblay, S., Castellano, A., Pifferi, F., Bocti, C., Paquet, N., Begdouri, H., Bentourkia, M., Turcotte, E., Allard, M., Barberger-Gateau, P., Fulop, T., and Rapoport, S. I. (2010). Brain fuel metabolism, aging, and alzheimer's disease. *Nutrition*, 27(1):3–20.

Currie, E., Schulze, A., Zechner, R., Walther, T. C., and Farese, R. V. (2013). Cellular fatty acid metabolism and cancer. *Cell metabolism*, 18(2):153–161.

Dang, C. V., Kim, J. W., Gao, P., and Yustein, J. (2008). The interplay between MYC and HIF in cancer. *Nature reviews. Cancer*, 8(1):51–56.

Dang, L., White, D. W., Gross, S., Bennett, B. D., Bittinger, M. A., Driggers, E. M., Fantin, V. R., Jang, H. G., Jin, S., Keenan, M. C., Marks, K. M., Prins, R. M., Ward, P. S., Yen, K. E., Liau, L. M., Rabinowitz, J. D., Cantley, L. C., Thompson, C. B., Vander Heiden, M. G., and Su, S. M. (2009). Cancer-associated IDH1 mutations produce 2-hydroxyglutarate. *Nature*, 462(7274):739–744.

Das, B., Bayat-Mokhtari, R., Tsui, M., Lotfi, S., Tsuchida, R., Felsher, D. W., and Yeger, H. (2012). HIF-2α suppresses p53 to enhance the stemness and regenerative potential of human embryonic stem cells. *Stem cells*, 30(8):1685–1695.

Das, U. N. (2011). Influence of polyunsaturated fatty acids and their metabolites on stem cell biology. *Nutrition*, 27(1):21–25.

David, C. J., Chen, M., Assanah, M., Canoll, P., and Manley, J. L. (2010). HnRNP proteins controlled by c-Myc deregulate pyruvate kinase mRNA splicing in cancer. *Nature*, 463(7279):364–368.

De Marchi, U., Santo-Domingo, J., Castelbou, C., Sekler, I., Wiederkehr, A., and Demaurex, N. (2014). NCLX protein, but not LETM1, mediates mitochondrial Ca2+ extrusion, thereby limiting Ca2+-induced NAD(P)H production and modulating matrix redox state. *J. Biol. Chem.*, 289(29):20377–20385.

De Stefani, D., Raffaello, A., Teardo, E., Szabò, I., and Rizzuto, R. (2011). A forty-kilodalton protein of the inner membrane is the mitochondrial calcium uniporter. *Nature*, 476(7360):336–340.

DeFronzo, R. A. and Tripathy, D. (2009). Skeletal muscle insulin resistance is the primary defect in type 2 diabetes. *Diabetes care*, 32 Suppl 2:S157–S163.

del Arco, A. and Satrústegui, J. (1998). Molecular cloning of Aralar, a new member of the mitochondrial carrier superfamily that binds calcium and is present in human muscle and brain. *J. Biol. Chem.*, 273(36):23327–23334.

Di Noia, M. A., Todisco, S., Cirigliano, A., Rinaldi, T., Agrimi, G., Iacobazzi, V., and Palmieri, F. (2014). The human SLC25A33 and SLC25A36 genes of solute carrier family 25 encode two mitochondrial pyrimidine nucleotide transporters. *J. Biol. Chem.*, 289(48):33137–33148.

Diehn, M., Cho, R. W., Lobo, N. A., Kalisky, T., Dorie, M. J., Kulp, A. N., Qian, D., Lam, J. S., Ailles, L. E., Wong, M., Joshua, B., Kaplan, M. J., Wapnir, I., Dirbas, F. M., Somlo, G., Garberoglio, C., Paz, B., Shen, J., Lau, S. K., Quake, S. R., Brown, J. M., Weissman, I. L., and Clarke, M. F. (2009). Association of reactive oxygen species levels and radioresistance in cancer stem cells. *Nature*, 458(7239):780–783.

Dietmair, S., Timmins, N. E., Gray, P. P., Nielsen, L. K., and Krömer, J. O. (2010). Towards quantitative metabolomics of mammalian cells: development of a metabolite extraction protocol. *Analytical biochemistry*, 404(2):155–164.

Divakaruni, A. S. and Brand, M. D. (2011). The regulation and physiology of mitochondrial proton leak. *Physiology*, 26(3):192–205.

Divakaruni, A. S., Wiley, S. E., Rogers, G. W., Andreyev, A. Y., Petrosyan, S., Loviscach, M., Wall, E. A., Yadava, N., Heuck, A. P., Ferrick, D. A., Henry, R. R., McDonald, W. G., Colca, J. R., Simon, M. I., Ciaraldi, T. P., and Murphy, A. N. (2013). Thiazolidinediones are acute, specific inhibitors of the mitochondrial pyruvate carrier. *Proc. Natl. Acad. Sci. U.S.A.*, 110(14):5422–5427.

Dolce, V., Fiermonte, G., and Palmieri, F. (1996). Tissue-specific expression of the two isoforms of the mitochondrial phosphate carrier in bovine tissues. *FEBS Lett.*, 399(1-2):95–98.

Dolce, V., Fiermonte, G., Runswick, M. J., Palmieri, F., and Walker, J. E. (2001). The human mitochondrial deoxynucleotide carrier and its role in the toxicity of nucleoside antivirals. *Proc. Natl. Acad. Sci. U.S.A.*, 98(5):2284–2288.

Dolce, V., Scarcia, P., Iacopetta, D., and Palmieri, F. (2005). A fourth ADP/ATP carrier isoform in man: identification, bacterial expression, functional characterization and tissue distribution. *FEBS Lett.*, 579(3):633–637.

Drago, I., Pizzo, P., and Pozzan, T. (2011). After half a century mitochondrial calcium in- and efflux machineries reveal themselves. *EMBO J.*, 30(20):4119–4125.

Du, J., Cleghorn, W. M., Contreras, L., Lindsay, K., Rountree, A. M., Chertov, A. O., Turner, S. J., Sahaboglu, A., Linton, J., Sadilek, M., Satrústegui, J., Sweet, I. R., Paquet-Durand, F., and Hurley, J. B. (2013). Inhibition of mitochondrial pyruvate transport by zaprinast causes massive accumulation of aspartate at the expense of glutamate in the retina. *The Journal of biological chemistry*, 288(50):36129–36140.

Dzeja, P. P., Bast, P., Ozcan, C., Valverde, A., Holmuhamedov, E. L., Van Wylen, D. G., and Terzic, A. (2003). Targeting nucleotide-requiring enzymes: implications for diazoxide-induced cardioprotection. *Am. J. Physiol. Heart Circ. Physiol.*, 284(4):H1048–1056.

Efferth, T., Fabry, U., Glatte, P., and Osieka, R. (1995). Increased induction of apoptosis in mononuclear cells of a glucose-6-phosphate dehydrogenase deficient patient. *Journal of molecular medicine*, 73(1):47–49.

Elhammali, A., Ippolito, J. E., Collins, L., Crowley, J., Marasa, J., and Piwnica-Worms, D. (2014). A high-throughput fluorimetric assay for 2-hydroxyglutarate identifies zaprinast as a glutaminase inhibitor. *Cancer discovery*, 4(7):828–839.

Enerbäck, S., Jacobsson, A., Simpson, E. M., Guerra, C., Yamashita, H., Harper, M. E., and Kozak, L. P. (1997). Mice lacking mitochondrial uncoupling protein are cold-sensitive but not obese. *Nature*, 387(6628):90–94.

Fan, J., Hitosugi, T., Chung, T. W., Xie, J., Ge, Q., Gu, T. L., Polakiewicz, R. D., Chen, G. Z., Boggon, T. J., Lonial, S., Khuri, F. R., Kang, S., and Chen, J. (2011). Tyrosine phosphorylation of lactate dehydrogenase a is important for NADH/NAD(+) redox homeostasis in cancer cells. *Molecular and cellular biology*, 31(24):4938–4950.

Fan, J., Kamphorst, J. J., Mathew, R., Chung, M. K., White, E., Shlomi, T., and Rabinowitz, J. D. (2012). Glutamine-driven oxidative phosphorylation is a major ATP source in transformed mammalian cells in both normoxia and hypoxia. *Molecular systems biology*, 9.

Favre, C., Zhdanov, A., Leahy, M., Papkovsky, D., and O'Connor, R. (2010). Mitochondrial pyrimidine nucleotide carrier (PNC1) regulates mitochondrial biogenesis and the invasive phenotype of cancer cells. *Oncogene*, 29(27):3964–3976.

Fehér, I. and Gidáli, J. (1974). Prostaglandin e2 as stimulator of haemopoietic stem cell proliferation. *Nature*, 247(5442):550–551.

Fell, V., Pollitt, R. J., Sampson, G. A., and Wright, T. (1974). Ornithinemia, hyperammonemia, and homocitrullinuria. A disease associated with mental retardation and possibly caused by defective mitochondrial transport. *Am. J. Dis. Child.*, 127(5):752–756.

Feng, B., Ng, J. H., Heng, J. C. D., and Ng, H. H. (2009). Molecules that promote or enhance reprogramming of somatic cells to induced pluripotent stem cells. *Cell stem cell*, 4(4):301–312.

Fernandes, T. G., Fernandes-Platzgummer, A. M., da Silva, C. L., Diogo, M. M., and Cabral,

J. M. S. (2010). Kinetic and metabolic analysis of mouse embryonic stem cell expansion under serum-free conditions. *Biotechnology letters*, 32(1):171–179.

Fernandez, C. A., Des Rosiers, C., Previs, S. F., David, F., and Brunengraber, H. (1996). Correction of 13C mass isotopomer distributions for natural stable isotope abundance. *Journal of mass spectrometry*, 31(3):255–262.

Ferranti, R., da Silva, M. M., and Kowaltowski, A. J. (2003). Mitochondrial ATP-sensitive K+ channel opening decreases reactive oxygen species generation. *FEBS Lett.*, 536(1-3):51–55.

Fico, A., Paglialunga, F., Cigliano, L., Abrescia, P., Verde, P., Martini, G., Iaccarino, I., and Filosa, S. (2004). Glucose-6-phosphate dehydrogenase plays a crucial role in protection from redox-stress-induced apoptosis. *Cell death and differentiation*, 11(8):823–831.

Fiermonte, G., De Leonardis, F., Todisco, S., Palmieri, L., Lasorsa, F. M., and Palmieri, F. (2004). Identification of the mitochondrial ATP-Mg/Pi transporter. Bacterial expression, reconstitution, functional characterization, and tissue distribution. *J. Biol. Chem.*, 279(29):30722–30730.

Fiermonte, G., Dolce, V., David, L., Santorelli, F. M., Dionisi-Vici, C., Palmieri, F., and Walker, J. E. (2003). The mitochondrial ornithine transporter. Bacterial expression, reconstitution, functional characterization, and tissue distribution of two human isoforms. *J. Biol. Chem.*, 278(35):32778–32783.

Fiermonte, G., Dolce, V., and Palmieri, F. (1998a). Expression in Escherichia coli, functional characterization, and tissue distribution of isoforms A and B of the phosphate carrier from bovine mitochondria. *J. Biol. Chem.*, 273(35):22782–22787.

Fiermonte, G., Dolce, V., Palmieri, L., Ventura, M., Runswick, M. J., Palmieri, F., and Walker, J. E. (2001). Identification of the human mitochondrial oxodicarboxylate carrier. Bacterial expression, reconstitution, functional characterization, tissue distribution, and chromosomal location. *J. Biol. Chem.*, 276(11):8225–8230.

Fiermonte, G., Palmieri, L., Dolce, V., Lasorsa, F. M., Palmieri, F., Runswick, M. J., and Walker, J. E. (1998b). The sequence, bacterial expression, and functional reconstitution of the rat mitochondrial dicarboxylate transporter cloned via distant homologs in yeast and Caenorhabditis elegans. *J. Biol. Chem.*, 273(38):24754–24759.

Fiermonte, G., Palmieri, L., Todisco, S., Agrimi, G., Palmieri, F., and Walker, J. E. (2002). Identification of the mitochondrial glutamate transporter. Bacterial expression, reconstitution, functional characterization, and tissue distribution of two human isoforms. *J. Biol. Chem.*, 277(22):19289–19294.

Fiermonte, G., Paradies, E., Todisco, S., Marobbio, C. M. T., and Palmieri, F. (2009). A novel member of solute carrier family 25 (SLC25A42) is a transporter of coenzyme A and adenosine 3',5'-diphosphate in human mitochondria. *J. Biol. Chem.*, 284(27):18152–18159.

Fillmore, N. and Lopaschuk, G. D. (2013). Targeting mitochondrial oxidative metabolism as an approach to treat heart failure. *Biochimica et biophysica acta*, 1833(4):857–865.

Fleury, C., Neverova, M., Collins, S., Raimbault, S., Champigny, O., Levi-Meyrueis, C., Bouillaud, F., Seldin, M. F., Surwit, R. S., Ricquier, D., and Warden, C. H. (1997). Uncoupling protein-2: a novel gene linked to obesity and hyperinsulinemia. *Nat. Genet.*, 15(3):269–272.

Floyd, S., Favre, C., Lasorsa, F. M., Leahy, M., Trigiante, G., Stroebel, P., Marx, A., Loughran, G., O'Callaghan, K., Marobbio, C. M. T., Slotboom, D. J., Kunji, E. R., Palmieri, F., and O'Connor, R. (2007). The insulin-like growth factor-I-mTOR signaling pathway induces the mitochondrial pyrimidine nucleotide carrier to promote cell growth. *Mol. Biol. Cell*, 18(9):3545–3555.

Folger, O., Jerby, L., Frezza, C., Gottlieb, E., Ruppin, E., and Shlomi, T. (2011). Predicting selective drug targets in cancer through metabolic networks. *Molecular systems biology*, 7:501.

Folmes, C. D., Nelson, T. J., Martinez-Fernandez, A., Arrell, D. K., Lindor, J. Z., Dzeja, P. P., Ikeda, Y., Perez-Terzic, C., and Terzic, A. (2011). Somatic oxidative bioenergetics transitions into pluripotency-dependent glycolysis to facilitate nuclear reprogramming. *Cell metabolism*, 14(2):264–271.

Forbes, R. A., Steenbergen, C., and Murphy, E. (2001). Diazoxide-induced cardioprotection requires signaling through a redox-sensitive mechanism. *Circ. Res.*, 88(8):802–809.

Foury, F. and Roganti, T. (2002). Deletion of the mitochondrial carrier genes MRS3 and MRS4 suppresses mitochondrial iron accumulation in a yeast frataxin-deficient strain. *J. Biol. Chem.*, 277(27):24475–24483.

Frezza, C., Zheng, L., Folger, O., Rajagopalan, K. N., MacKenzie, E. D., Jerby, L., Micaroni, M., Chaneton, B., Adam, J., Hedley, A., Kalna, G., Tomlinson, I. P., Pollard, P. J., Watson, D. G., Deberardinis, R. J., Shlomi, T., Ruppin, E., and Gottlieb, E. (2011). Haem oxygenase is synthetically lethal with the tumour suppressor fumarate hydratase. *Nature*, 477(7363):225–228.

Gan, B., Hu, J., Jiang, S., Liu, Y., Sahin, E., Zhuang, L., Fletcher-Sananikone, E., Colla, S., Wang, Y. A., Chin, L., and Depinho, R. A. (2010). Lkb1 regulates quiescence and metabolic homeostasis of haematopoietic stem cells. *Nature*, 468(7324):701–704.

Gao, X., Wang, H., Yang, J. J., Liu, X., and Liu, Z. R. (2012). Pyruvate kinase m2 regulates gene transcription by acting as a protein kinase. *Molecular cell*, 45(5):598–609.

Garcia-Gonzalo, F. R. and Belmonte, J. C. I. (2008). Albumin-associated lipids regulate human embryonic stem cell self-renewal. *PloS one*, 3(1):e1384.

Garlid, K. D. (2000). Opening mitochondrial K_{ATP} in the heart - what happens, and what does not happen. *Basic Res. Cardiol.*, 95(4):275–279.

Garlid, K. D., Dos Santos, P., Xie, Z. J., Costa, A. D., and Paucek, P. (2003). Mitochondrial potassium transport: the role of the mitochondrial ATP-sensitive K(+) channel in cardiac function and cardioprotection. *Biochim. Biophys. Acta*, 1606(1-3):1–21.

Garlid, K. D. and Paucek, P. (2003). Mitochondrial potassium transport: the K(+) cycle. *Biochim. Biophys. Acta*, 1606(1-3):23–41.

Ginestier, C., Hur, M. H., Charafe-Jauffret, E., Monville, F., Dutcher, J., Brown, M., Jacquemier, J., Viens, P., Kleer, C. G., Liu, S., Schott, A., Hayes, D., Birnbaum, D., Wicha, M. S., and Dontu, G. (2007). ALDH1 is a marker of normal and malignant human mammary stem cells and a predictor of poor clinical outcome. *Cell stem cell*, 1(5):555–567.

Giorgio, V., von Stockum, S., Antoniel, M., Fabbro, A., Fogolari, F., Forte, M., Glick, G. D., Petronilli, V., Zoratti, M., Szabó, I., Lippe, G., and Bernardi, P. (2013). Dimers of mitochondrial ATP synthase form the permeability transition pore. *Proc. Natl. Acad. Sci. U.S.A.*, 110(15):5887–5892.

Giudetti, A. M., Leo, M., Siculella, L., and Gnoni, G. V. (2006). Hypothyroidism down-regulates mitochondrial citrate carrier activity and expression in rat liver. *Biochim. Biophys. Acta*, 1761(4):484–491.

Goessling, W., North, T. E., Loewer, S., Lord, A. M., Lee, S., Stoick-Cooper, C. L., Weidinger, G., Puder, M., Daley, G. Q., Moon, R. T., and Zon, L. I. (2009). Genetic interaction of PGE2 and wnt signaling regulates developmental specification of stem cells and regeneration. *Cell*, 136(6):1136–1147.

Gordan, J. D., Bertout, J. A., Hu, C. J., Diehl, J. A., and Simon, M. C. (2007a). HIF-2alpha promotes hypoxic cell proliferation by enhancing c-myc transcriptional activity. *Cancer cell*, 11(4):335–347.

Gordan, J. D., Thompson, C. B., and Simon, M. C. (2007b). HIF and c-Myc: sibling rivals for control of cancer cell metabolism and proliferation. *Cancer cell*, 12(2):108–113.

Grassian, A. R., Metallo, C. M., Coloff, J. L., Stephanopoulos, G., and Brugge, J. S. (2011). Erk regulation of pyruvate dehydrogenase flux through PDK4 modulates cell proliferation. *Genes & development*, 25(16):1716–1733.

Grassian, A. R., Parker, S. J., Davidson, S. M., Divakaruni, A. S., Green, C. R., Zhang, X., Slocum, K. L., Pu, M., Lin, F., Vickers, C., Joud-Caldwell, C., Chung, F., Yin, H., Handly, E. D., Straub, C., Growney, J. D., Vander Heiden, M. G., Murphy, A. N., Pagliarini, R., and Metallo, C. M. (2014). IDH1 mutations alter citric acid cycle metabolism and increase dependence on oxidative mitochondrial metabolism. *Cancer research*, 74(12):3317–3331.

Grigorenko, E. V., Small, W. C., Persson, L. O., and Srere, P. A. (1990). Citrate synthase 1 interacts with the citrate transporter of yeast mitochondria. *J. Mol. Recognit.*, 3(5-6):215–219.

Guernsey, D. L., Jiang, H., Campagna, D. R., Evans, S. C., Ferguson, M., Kellogg, M. D., Lachance, M., Matsuoka, M., Nightingale, M., Rideout, A., Saint-Amant, L., Schmidt, P. J., Orr, A., Bottomley, S. S., Fleming, M. D., Ludman, M., Dyack, S., Fernandez, C. V., and Samuels, M. E. (2009). Mutations in mitochondrial carrier family gene SLC25A38 cause non-syndromic autosomal recessive congenital sideroblastic anemia. *Nat. Genet.*, 41(6):651–653.

Gunter, T. E., Yule, D. I., Gunter, K. K., Eliseev, R. A., and Salter, J. D. (2004). Calcium and mitochondria. *FEBS Lett.*, 567(1):96–102.

Guo, Y., Einhorn, L., Kelley, M., Hirota, K., Yodoi, J., Reinbold, R., Scholer, H., Ramsey, H.,

and Hromas, R. (2004). Redox regulation of the embryonic stem cell transcription factor oct-4 by thioredoxin. *Stem cells*, 22(3):259–264.

Gurumurthy, S., Xie, S. Z., Alagesan, B., Kim, J., Yusuf, R. Z., Saez, B., Tzatsos, A., Ozsolak, F., Milos, P., Ferrari, F., Park, P. J., Shirihai, O. S., Scadden, D. T., and Bardeesy, N. (2010). The lkb1 metabolic sensor maintains haematopoietic stem cell survival. *Nature*, 468(7324):659–663.

Gutiérrez-Aguilar, M. and Baines, C. P. (2013). Physiological and pathological roles of mitochondrial SLC25 carriers. *Biochem. J.*, 454(3):371–386.

Guzy, R. D., Hoyos, B., Robin, E., Chen, H., Liu, L., Mansfield, K. D., Simon, M. C., Hammerling, U., and Schumacker, P. T. (2005). Mitochondrial complex III is required for hypoxia-induced ROS production and cellular oxygen sensing. *Cell metabolism*, 1(6):401–408.

Haitina, T., Lindblom, J., Renström, T., and Fredriksson, R. (2006). Fourteen novel human members of mitochondrial solute carrier family 25 (SLC25) widely expressed in the central nervous system. *Genomics*, 88(6):779–790.

Hajnóczky, G., Hager, R., and Thomas, A. P. (1999). Mitochondria suppress local feedback activation of inositol 1,4, 5-trisphosphate receptors by Ca2+. *J. Biol. Chem.*, 274(20):14157–14162.

Halestrap, A. P. (1975). The mitochondrial pyruvate carrier. Kinetics and specificity for substrates and inhibitors. *The Biochemical journal*, 148(1):85–96.

Halestrap, A. P. (2012). The mitochondrial pyruvate carrier: has it been unearthed at last? *Cell metabolism*, 16(2):141–143.

Halestrap, A. P. and Brenner, C. (2003). The adenine nucleotide translocase: a central component of the mitochondrial permeability transition pore and key player in cell death. *Curr. Med. Chem.*, 10(16):1507–1525.

Halestrap, A. P. and Denton, R. M. (1974). Specific inhibition of pyruvate transport in rat liver mitochondria and human erythrocytes by alpha-cyano-4-hydroxycinnamate. *The Biochemical journal*, 138(2):313–316.

Häussinger, D. and Schliess, F. (2007). Glutamine metabolism and signaling in the liver. *Front. Biosci.*, 12:371–391.

He, L. and Lemasters, J. J. (2002). Regulated and unregulated mitochondrial permeability transition pores: a new paradigm of pore structure and function? *FEBS Lett.*, 512(1-3):1–7.

Heaton, G. M., Wagenvoord, R. J., Kemp, A., and Nicholls, D. G. (1978). Brown-adipose-tissue mitochondria: photoaffinity labelling of the regulatory site of energy dissipation. *Eur. J. Biochem.*, 82(2):515–521.

Henry, R. R., Abrams, L., Nikoulina, S., and Ciaraldi, T. P. (1995). Insulin action and glucose metabolism in nondiabetic control and NIDDM subjects. Comparison using human skeletal muscle cell cultures. *Diabetes*, 44(8):936–946.

Hensley, C. T., Wasti, A. T., and DeBerardinis, R. J. (2013). Glutamine and cancer: cell biology, physiology, and clinical opportunities. *J. Clin. Invest.*, 123(9):3678–3684.

Herzig, S., Raemy, E., Montessuit, S., Veuthey, J. L., Zamboni, N., Westermann, B., Kunji, E. R., and Martinou, J. C. (2012). Identification and functional expression of the mitochondrial pyruvate carrier. *Science*, 337(6090):93–96.

Hildyard, J. C., Ammälä, C., Dukes, I. D., Thomson, S. A., and Halestrap, A. P. (2004). Identification and characterisation of a new class of highly specific and potent inhibitors of the mitochondrial pyruvate carrier. *Biochimica et biophysica acta*, 1707(2-3):221–230.

Hoggatt, J., Singh, P., Sampath, J., and Pelus, L. M. (2009). Prostaglandin e2 enhances hematopoietic stem cell homing, survival, and proliferation. *Blood*, 113(22):5444–5455.

Horne, D. W., Holloway, R. S., and Said, H. M. (1992). Uptake of 5-formyltetrahydrofolate in isolated rat liver mitochondria is carrier-mediated. *J. Nutr.*, 122(11):2204–2209.

Horne, D. W., Holloway, R. S., and Wagner, C. (1997). Transport of S-adenosylmethionine in isolated rat liver mitochondria. *Arch. Biochem. Biophys.*, 343(2):201–206.

Horowitz, M. P. and Greenamyre, J. T. (2010). Mitochondrial iron metabolism and its role in neurodegeneration. *J. Alzheimers Dis.*, 20 Suppl 2:S551–568.

Hsu, P. P. and Sabatini, D. M. (2008). Cancer cell metabolism: Warburg and beyond. *Cell*, 134(5):703–707.

Huizing, M., Iacobazzi, V., Ijlst, L., Savelkoul, P., Ruitenbeek, W., van den Heuvel, L., Indiveri, C., Smeitink, J., Trijbels, F., Wanders, R., and Palmieri, F. (1997). Cloning of the human carnitine-acylcarnitine carrier cDNA and identification of the molecular defect in a patient. *Am. J. Hum. Genet.*, 61(6):1239–1245.

Hunter, D. R., Haworth, R. A., and Southard, J. H. (1976). Relationship between configuration, function, and permeability in calcium-treated mitochondria. *J. Biol. Chem.*, 251(16):5069–5077.

Iacobazzi, V., Convertini, P., Infantino, V., Scarcia, P., Todisco, S., and Palmieri, F. (2009). Statins, fibrates and retinoic acid upregulate mitochondrial acylcarnitine carrier gene expression. *Biochem. Biophys. Res. Commun.*, 388(4):643–647.

Iacobazzi, V., Invernizzi, F., Baratta, S., Pons, R., Chung, W., Garavaglia, B., Dionisi-Vici, C., Ribes, A., Parini, R., Huertas, M. D., Roldan, S., Lauria, G., Palmieri, F., and Taroni, F. (2004). Molecular and functional analysis of SLC25A20 mutations causing carnitine-acylcarnitine translocase deficiency. *Hum. Mutat.*, 24(4):312–320.

Indiveri, C., Iacobazzi, V., Giangregorio, N., and Palmieri, F. (1997a). The mitochondrial carnitine carrier protein: cDNA cloning, primary structure and comparison with other mitochondrial transport proteins. *Biochem. J.*, 321 (Pt 3):713–719.

Indiveri, C., Tonazzi, A., and Palmieri, F. (1992). Identification and purification of the ornithine/citrulline carrier from rat liver mitochondria. *Eur. J. Biochem.*, 207(2):449–454.

Indiveri, C., Tonazzi, A., and Palmieri, F. (1994). The reconstituted carnitine carrier from rat liver mitochondria: evidence for a transport mechanism different from that of the other mitochondrial translocators. *Biochim. Biophys. Acta*, 1189(1):65–73.

Indiveri, C., Tonazzi, A., Stipani, I., and Palmieri, F. (1997b). The purified and reconstituted ornithine/citrulline carrier from rat liver mitochondria: electrical nature and coupling of the exchange reaction with H+ translocation. *Biochem. J.*, 327 (Pt 2):349–355.

Infantino, V., Castegna, A., Iacobazzi, F., Spera, I., Scala, I., Andria, G., and Iacobazzi, V. (2011). Impairment of methyl cycle affects mitochondrial methyl availability and glutathione level in Down's syndrome. *Molecular Genetics and Metabolism*, 102(3):378–382.

Infantino, V., Iacobazzi, V., De Santis, F., Mastrapasqua, M., and Palmieri, F. (2007). Transcription of the mitochondrial citrate carrier gene: role of SREBP-1, upregulation by insulin and downregulation by PUFA. *Biochem. Biophys. Res. Commun.*, 356(1):249–254.

Inoue, I., Nagase, H., Kishi, K., and Higuti, T. (1991). ATP-sensitive K+ channel in the mitochondrial inner membrane. *Nature*, 352(6332):244–247.

Ito, K., Hirao, A., Arai, F., Matsuoka, S., Takubo, K., Hamaguchi, I., Nomiyama, K., Hosokawa, K., Sakurada, K., Nakagata, N., Ikeda, Y., Mak, T. W., and Suda, T. (2004). Regulation of oxidative stress by ATM is required for self-renewal of haematopoietic stem cells. *Nature*, 431(7011):997–991002.

Ivan, M., Kondo, K., Yang, H., Kim, W., Valiando, J., Ohh, M., Salic, A., Asara, J. M., Lane, W. S., and Kaelin, W. G. (2001). HIFalpha targeted for VHL-mediated destruction by proline hydroxylation: implications for O2 sensing. *Science*, 292(5516):464–468.

Jaakkola, P., Mole, D. R., Tian, Y. M., Wilson, M. I., Gielbert, J., Gaskell, S. J., von Kriegsheim, A., Hebestreit, H. F., Mukherji, M., Schofield, C. J., Maxwell, P., Pugh, C., and Ratcliffe, P. J. (2001). Targeting of HIF-alpha to the von Hippel-Lindau ubiquitylation complex by O2-regulated prolyl hydroxylation. *Science*, 292(5516):468–472.

Jain, M., Nilsson, R., Sharma, S., Madhusudhan, N., Kitami, T., Souza, A. L., Kafri, R., Kirschner, M. W., Clish, C. B., and Mootha, V. K. (2012). Metabolite profiling identifies a key role for glycine in rapid cancer cell proliferation. *Science*, 336(6084):1040–1044.

Jiang, D., Zhao, L., and Clapham, D. E. (2009). Genome-wide RNAi screen identifies Letm1 as a mitochondrial Ca2+/H+ antiporter. *Science*, 326(5949):144–147.

Jordens, E. Z., Palmieri, L., Huizing, M., van den Heuvel, L. P., Sengers, R. C., Dorner, A., Ruitenbeek, W., Trijbels, F. J., Valsson, J., Sigfusson, G., Palmieri, F., and Smeitink, J. A. (2002). Adenine nucleotide translocator 1 deficiency associated with Sengers syndrome. *Ann. Neurol.*, 52(1):95–99.

Joseph, J. W., Jensen, M. V., Ilkayeva, O., Palmieri, F., Alarcon, C., Rhodes, C. J., and Newgard, C. B. (2006). The mitochondrial citrate/isocitrate carrier plays a regulatory role in glucose-stimulated insulin secretion. *J. Biol. Chem.*, 281(47):35624–35632.

Jurica, M. S., Mesecar, A., Heath, P. J., Shi, W., Nowak, T., and Stoddard, B. L. (1998). The allosteric regulation of pyruvate kinase by fructose-1,6-bisphosphate. *Structure*, 6(2):195–210.

Kaasik, A., Safiulina, D., Zharkovsky, A., and Veksler, V. (2007). Regulation of mitochondrial matrix volume. *Am. J. Physiol., Cell Physiol.*, 292(1):C157–163.

Kabe, Y., Ohmori, M., Shinouchi, K., Tsuboi, Y., Hirao, S., Azuma, M., Watanabe, H., Okura, I., and Handa, H. (2006). Porphyrin accumulation in mitochondria is mediated by 2-oxoglutarate carrier. *J. Biol. Chem.*, 281(42):31729–31735.

Kajimoto, K., Terada, H., Baba, Y., and Shinohara, Y. (2005). Essential role of citrate export from mitochondria at early differentiation stage of 3T3-L1 cells for their effective differentiation into fat cells, as revealed by studies using specific inhibitors of mitochondrial di- and tricarboxylate carriers. *Mol. Genet. Metab.*, 85(1):46–53.

Kamga, C. K., Zhang, S. X., and Wang, Y. (2010). Dicarboxylate carrier-mediated glutathione transport is essential for reactive oxygen species homeostasis and normal respiration in rat brain mitochondria. *Am. J. Physiol., Cell Physiol.*, 299(2):497–505.

Kamphorst, J. J., Cross, J. R., Fan, J., de Stanchina, E., Mathew, R., White, E. P., Thompson, C. B., and Rabinowitz, J. D. (2013). Hypoxic and ras-transformed cells support growth by scavenging unsaturated fatty acids from lysophospholipids. *Proc. Natl. Acad. Sci. U.S.A.*, 110(22):8882–8887.

Kanda, Y., Hinata, T., Kang, S. W., and Watanabe, Y. (2011). Reactive oxygen species mediate adipocyte differentiation in mesenchymal stem cells. *Life Sci.*, 89(7-8):250–258.

Kang, J. and Samuels, D. C. (2008). The evidence that the DNC (SLC25A19) is not the mitochondrial deoxyribonucleotide carrier. *Mitochondrion*, 8(2):103–108.

Kaplan, R. S., Mayor, J. A., Blackwell, R., Maughon, R. H., and Wilson, G. L. (1991a). The effect of insulin supplementation on diabetes-induced alterations in the extractable levels of functional mitochondrial anion transport proteins. *Arch. Biochem. Biophys.*, 287(2):305–311.

Kaplan, R. S., Mayor, J. A., Blackwell, R., Wilson, G. L., and Schaffer, S. W. (1991b). Functional levels of mitochondrial anion transport proteins in non-insulin-dependent diabetes mellitus. *Mol. Cell. Biochem.*, 107(1):79–86.

Kaplan, R. S., Mayor, J. A., and Wood, D. O. (1993). The mitochondrial tricarboxylate transport protein. cDNA cloning, primary structure, and comparison with other mitochondrial transport proteins. *J. Biol. Chem.*, 268(18):13682–13690.

Katz, L. A., Swain, J. A., Portman, M. A., and Balaban, R. S. (1989). Relation between phosphate metabolites and oxygen consumption of heart in vivo. *Am. J. Physiol.*, 256(1 Pt 2):H265–274.

Kelley, R. I., Robinson, D., Puffenberger, E. G., Strauss, K. A., and Morton, D. H. (2002). Amish lethal microcephaly: a new metabolic disorder with severe congenital microcephaly and 2-ketoglutaric aciduria. *Am. J. Med. Genet.*, 112(4):318–326.

Kerr, D. S. (2013). Review of clinical trials for mitochondrial disorders: 1997-2012. *Neurotherapeutics*, 10(2):307–319.

Keung, W., Ussher, J. R., Jaswal, J. S., Raubenheimer, M., Lam, V. H., Wagg, C. S., and Lopaschuk, G. D. (2013). Inhibition of carnitine palmitoyltransferase-1 activity alleviates insulin resistance in diet-induced obese mice. *Diabetes*, 62(3):711–720.

Kharroubi, A. T., Masterson, T. M., Aldaghlas, T. A., Kennedy, K. A., and Kelleher, J. K. (1992). Isotopomer spectral analysis of triglyceride fatty acid synthesis in 3T3-L1 cells. *The American journal of physiology*, 263(4 Pt 1):E667–E675.

Kim, H. S., Park, S. Y., Choi, Y. R., Kang, J. G., Joo, H. J., Moon, W. K., and Cho, J. W. (2009a). Excessive O-GlcNAcylation of proteins suppresses spontaneous cardiogenesis in ES cells. *FEBS letters*, 583(15):2474–2478.

Kim, J. W., Tchernyshyov, I., Semenza, G. L., and Dang, C. V. (2006). HIF-1-mediated expression of pyruvate dehydrogenase kinase: a metabolic switch required for cellular adaptation to hypoxia. *Cell metabolism*, 3(3):177–185.

Kim, M. H., Kim, M. O., Kim, Y. H., Kim, J. S., and Han, H. J. (2009b). Linoleic acid induces mouse embryonic stem cell proliferation via Ca2+/PKC, PI3K/Akt, and MAPKs. *Cellular physiology and biochemistry*, 23(1-3):53–64.

King, J. A. and Miller, W. M. (2007). Bioreactor development for stem cell expansion and controlled differentiation. *Current opinion in chemical biology*, 11(4):394–398.

Kobayashi, K., Sinasac, D. S., Iijima, M., Boright, A. P., Begum, L., Lee, J. R., Yasuda, T., Ikeda, S., Hirano, R., Terazono, H., Crackower, M. A., Kondo, I., Tsui, L. C., Scherer, S. W., and Saheki, T. (1999). The gene mutated in adult-onset type II citrullinaemia encodes a putative mitochondrial carrier protein. *Nat. Genet.*, 22(2):159–163.

Köhler, C., Gahm, A., Noma, T., Nakazawa, A., Orrenius, S., and Zhivotovsky, B. (1999). Release of adenylate kinase 2 from the mitochondrial intermembrane space during apoptosis. *FEBS Lett.*, 447(1):10–12.

Kohn, L. D., Alvarez, F., Marcocci, C., Kohn, A. D., Corda, D., Hoffman, W. E., Tombaccini, D., Valente, W. A., de Luca, M., Santisteban, P., and Grollman, E. F. (1986). Monoclonal antibody studies defining the origin and properties of autoantibodies in Graves' disease. *Ann. N. Y. Acad. Sci.*, 475:157–173.

Kokoszka, J. E., Waymire, K. G., Levy, S. E., Sligh, J. E., Cai, J., Jones, D. P., MacGregor, G. R., and Wallace, D. C. (2004). The ADP/ATP translocator is not essential for the mitochondrial permeability transition pore. *Nature*, 427(6973):461–465.

Kondoh, H., Lleonart, M. E., Gil, J., Wang, J., Degan, P., Peters, G., Martinez, D., Carnero, A., and Beach, D. (2005). Glycolytic enzymes can modulate cellular life span. *Cancer research*, 65(1):177–185.

Kondoh, H., Lleonart, M. E., Nakashima, Y., Yokode, M., Tanaka, M., Bernard, D., Gil, J., and

Beach, D. (2007). A high glycolytic flux supports the proliferative potential of murine embryonic stem cells. *Antioxidants & redox signaling*, 9(3):293–299.

Krämer, R. and Klingenberg, M. (1979). Reconstitution of adenine nucleotide transport from beef heart mitochondria. *Biochemistry*, 18(19):4209–4215.

Krauskopf, A., Eriksson, O., Craigen, W. J., Forte, M. A., and Bernardi, P. (2006). Properties of the permeability transition in VDAC1(-/-) mitochondria. *Biochim. Biophys. Acta*, 1757(5-6):590–595.

Lacey, J. M. and Wilmore, D. W. (1990). Is glutamine a conditionally essential amino acid? *Nutr. Rev.*, 48(8):297–309.

Lamantea, E., Tiranti, V., Bordoni, A., Toscano, A., Bono, F., Servidei, S., Papadimitriou, A., Spelbrink, H., Silvestri, L., Casari, G., Comi, G. P., and Zeviani, M. (2002). Mutations of mitochondrial DNA polymerase gammaA are a frequent cause of autosomal dominant or recessive progressive external ophthalmoplegia. *Ann. Neurol.*, 52(2):211–219.

Lammers, G., Poelkens, F., van Duijnhoven, N. T., Pardoel, E. M., Hoenderop, J. G., Thijssen, D. H., and Hopman, M. T. (2012). Expression of genes involved in fatty acid transport and insulin signaling is altered by physical inactivity and exercise training in human skeletal muscle. *Am. J. Physiol. Endocrinol. Metab.*, 303(10):E1245–1251.

LaNoue, K. F. and Schoolwerth, A. C. (1979). Metabolite Transport in Mitochondria. *Ann. Rev. Biochem.*, 48:871–922.

Lau, K. S., Partridge, E. A., Grigorian, A., Silvescu, C. I., Reinhold, V. N., Demetriou, M., and Dennis, J. W. (2007). Complex n-glycan number and degree of branching cooperate to regulate cell proliferation and differentiation. *Cell*, 129(1):123–134.

Laurenti, E., Wilson, A., and Trumpp, A. (2009). Myc's other life: stem cells and beyond. *Current opinion in cell biology*, 21(6):844–854.

Le, A., Lane, A. N., Hamaker, M., Bose, S., Gouw, A., Barbi, J., Tsukamoto, T., Rojas, C. J., Slusher, B. S., Zhang, H., Zimmerman, L. J., Liebler, D. C., Slebos, R. J., Lorkiewicz, P. K., Higashi, R. M., Fan, T. W., and Dang, C. V. (2012). Glucose-independent glutamine metabolism via TCA cycling for proliferation and survival in b cells. *Cell metabolism*, 15(1):110–121.

Lee, W. K., Bork, U., Gholamrezaei, F., and Thévenod, F. (2005). Cd(2+)-induced cytochrome c release in apoptotic proximal tubule cells: role of mitochondrial permeability transition pore and Ca(2+) uniporter. *Am. J. Physiol. Renal Physiol.*, 288(1):27–39.

Lehmann, J. M., Moore, L. B., Smith-Oliver, T. A., Wilkison, W. O., Willson, T. M., and Kliewer, S. A. (1995). An antidiabetic thiazolidinedione is a high affinity ligand for peroxisome proliferator-activated receptor gamma (PPAR gamma). *J. Biol. Chem.*, 270(22):12953–12956.

Lemasters, J. J., Theruvath, T. P., Zhong, Z., and Nieminen, A. L. (2009). Mitochondrial calcium and the permeability transition in cell death. *Biochim. Biophys. Acta*, 1787(11):1395–1401.

Lemons, J. M., Feng, X. J., Bennett, B. D., Aster, L., Johnson, E. L., Raitman, I., Pollina, E. A., Rabitz, H. A., Rabinowitz, J. D., and Coller, H. A. (2010). Quiescent fibroblasts exhibit high metabolic activity. *PLoS biology*, 8(10):e1000514.

Lewis, C. A., Parker, S. J., Fiske, B. P., McCloskey, D., Gui, D. Y., Green, C. R., Vokes, N. I., Feist, A. M., Vander Heiden, M. G., and Metallo, C. M. (2014). Tracing compartmentalized NADPH metabolism in the cytosol and mitochondria of mammalian cells. *Molecular cell*, 55(2):253–263.

Li, F. Y., Nikali, K., Gregan, J., Leibiger, I., Leibiger, B., Schweyen, R., Larsson, C., and Suomalainen, A. (2001). Characterization of a novel human putative mitochondrial transporter homologous to the yeast mitochondrial RNA splicing proteins 3 and 4. *FEBS Lett.*, 494(1-2):79–84.

Li, Z., Bao, S., Wu, Q., Wang, H., Eyler, C., Sathornsumetee, S., Shi, Q., Cao, Y., Lathia, J., McLendon, R. E., Hjelmeland, A. B., and Rich, J. N. (2009). Hypoxia-inducible factors regulate tumorigenic capacity of glioma stem cells. *Cancer cell*, 15(6):501–513.

Lim, K. H., Javadov, S. A., Das, M., Clarke, S. J., Suleiman, M. S., and Halestrap, A. P. (2002). The effects of ischaemic preconditioning, diazoxide and 5-hydroxydecanoate on rat heart mitochondrial volume and respiration. *J. Physiol.*, 545(Pt 3):961–974.

Lindhurst, M. J., Fiermonte, G., Song, S., Struys, E., De Leonardis, F., Schwartzberg, P. L., Chen, A., Castegna, A., Verhoeven, N., Mathews, C. K., Palmieri, F., and Biesecker, L. G. (2006). Knockout of Slc25a19 causes mitochondrial thiamine pyrophosphate depletion, embryonic lethality, CNS malformations, and anemia. *Proc. Natl. Acad. Sci. U.S.A.*, 103(43):15927–15932.

Liu, D., Lu, C., Wan, R., Auyeung, W. W., and Mattson, M. P. (2002). Activation of mitochondrial ATP-dependent potassium channels protects neurons against ischemia-induced death by a mechanism involving suppression of Bax translocation and cytochrome c release. *J. Cereb. Blood Flow Metab.*, 22(4):431–443.

Liu, J., Cao, L., and Finkel, T. (2011). Oxidants, metabolism, and stem cell biology. *Free radical biology & medicine*, 51(12):2158–2162.

Liu, R., Wang, X., Chen, G. Y., Dalerba, P., Gurney, A., Hoey, T., Sherlock, G., Lewicki, J., Shedden, K., and Clarke, M. F. (2007). The prognostic role of a gene signature from tumorigenic breast-cancer cells. *The New England journal of medicine*, 356(3):217–226.

Locasale, J. W., Grassian, A. R., Melman, T., Lyssiotis, C. A., Mattaini, K. R., Bass, A. J., Heffron, G., Metallo, C. M., Muranen, T., Sharfi, H., Sasaki, A. T., Anastasiou, D., Mullarky, E., Vokes, N. I., Sasaki, M., Beroukhim, R., Stephanopoulos, G., Ligon, A. H., Meyerson, M., Richardson, A. L., Chin, L., Wagner, G., Asara, J. M., Brugge, J. S., Cantley, L. C., and Vander Heiden, M. G. (2011). Phosphoglycerate dehydrogenase diverts glycolytic flux and contributes to oncogenesis. *Nature genetics*, 43(9):869–874.

Locke, R. M., Rial, E., and Nicholls, D. G. (1982). The acute regulation of mitochondrial proton conductance in cells and mitochondria from the brown fat of cold-adapted and warm-adapted

guinea pigs. *Eur. J. Biochem.*, 129(2):381–387.

Lu, C., Ward, P. S., Kapoor, G. S., Rohle, D., Turcan, S., Abdel-Wahab, O., Edwards, C. R., Khanin, R., Figueroa, M. E., Melnick, A., Wellen, K. E., O'Rourke, D. M., Berger, S. L., Chan, T. A., Levine, R. L., Mellinghoff, I. K., and Thompson, C. B. (2012). IDH mutation impairs histone demethylation and results in a block to cell differentiation. *Nature*, 483(7390):474–478.

Maack, C., Cortassa, S., Aon, M. A., Ganesan, A. N., Liu, T., and O'Rourke, B. (2006). Elevated cytosolic Na+ decreases mitochondrial Ca2+ uptake during excitation-contraction coupling and impairs energetic adaptation in cardiac myocytes. *Circ. Res.*, 99(2):172–182.

Maechler, P. and Wollheim, C. B. (1999). Mitochondrial glutamate acts as a messenger in glucose-induced insulin exocytosis. *Nature*, 402(6762):685–689.

Maherali, N. and Hochedlinger, K. (2008). Guidelines and techniques for the generation of induced pluripotent stem cells. *Cell stem cell*, 3(6):595–605.

Mailloux, R. J. and Harper, M. E. (2011). Uncoupling proteins and the control of mitochondrial reactive oxygen species production. *Free Radic. Biol. Med.*, 51(6):1106–1115.

Manganelli, G., Fico, A., Masullo, U., Pizzolongo, F., Cimmino, A., and Filosa, S. (2012). Modulation of the pentose phosphate pathway induces endodermal differentiation in embryonic stem cells. *PloS one*, 7(1):e29321.

Mao, W., Yu, X. X., Zhong, A., Li, W., Brush, J., Sherwood, S. W., Adams, S. H., and Pan, G. (1999). UCP4, a novel brain-specific mitochondrial protein that reduces membrane potential in mammalian cells. *FEBS Lett.*, 443(3):326–330.

Marobbio, C. M. T., Agrimi, G., Lasorsa, F. M., and Palmieri, F. (2003). Identification and functional reconstitution of yeast mitochondrial carrier for S-adenosylmethionine. *EMBO J.*, 22(22):5975–5982.

Marobbio, C. M. T., Di Noia, M. A., and Palmieri, F. (2006). Identification of a mitochondrial transporter for pyrimidine nucleotides in Saccharomyces cerevisiae: bacterial expression, reconstitution and functional characterization. *Biochem. J.*, 393(Pt 2):441–446.

Mathieu, J., Zhang, Z., Zhou, W., Wang, A. J., Heddleston, J. M., Pinna, C. M., Hubaud, A., Stadler, B., Choi, M., Bar, M., Tewari, M., Liu, A., Vessella, R., Rostomily, R., Born, D., Horwitz, M., Ware, C., Blau, C. A., Cleary, M. A., Rich, J. N., and Ruohola-Baker, H. (2011). HIF induces human embryonic stem cell markers in cancer cells. *Cancer research*, 71(13):4640–4652.

Mayr, J. A., Merkel, O., Kohlwein, S. D., Gebhardt, B. R., Böhles, H., Fötschl, U., Koch, J., Jaksch, M., Lochmüller, H., Horváth, R., Freisinger, P., and Sperl, W. (2007). Mitochondrial phosphate-carrier deficiency: a novel disorder of oxidative phosphorylation. *Am. J. Hum. Genet.*, 80(3):478–484.

Mazurek, S., Boschek, C. B., Hugo, F., and Eigenbrodt, E. (2005). Pyruvate kinase type m2 and its role in tumor growth and spreading. *Seminars in cancer biology*, 15(4):300–308.

McCormack, J. G., Halestrap, A. P., and Denton, R. M. (1990). Role of calcium ions in regulation of mammalian intramitochondrial metabolism. *Physiol. Rev.*, 70(2):391–425.

McGarry, J. D., Mills, S. E., Long, C. S., and Foster, D. W. (1983). Observations on the affinity for carnitine, and malonyl-CoA sensitivity, of carnitine palmitoyltransferase I in animal and human tissues. Demonstration of the presence of malonyl-CoA in non-hepatic tissues of the rat. *The Biochemical journal*, 214(1):21–28.

McGivney, B. A., McGettigan, P. A., Browne, J. A., Evans, A. C., Fonseca, R. G., Loftus, B. J., Lohan, A., MacHugh, D. E., Murphy, B. A., Katz, L. M., and Hill, E. W. (2010). Characterization of the equine skeletal muscle transcriptome identifies novel functional responses to exercise training. *BMC Genomics*, 11:398.

Medler, K. and Gleason, E. L. (2002). Mitochondrial Ca(2+) buffering regulates synaptic transmission between retinal amacrine cells. *J. Neurophysiol.*, 87(3):1426–1439.

Meijer, A. J. and Tager, J. M. (1966). Studies on the Permeability of Rat-Liver Mitochondria for Tricarboxylic Acids. *Biochem. J.*, 100:79P.

Metallo, C. M., Gameiro, P. A., Bell, E. L., Mattaini, K. R., Yang, J., Hiller, K., Jewell, C. M., Johnson, Z. R., Irvine, D. J., Guarente, L., Kelleher, J. K., Vander Heiden, M. G., Iliopoulos, O., and Stephanopoulos, G. (2012). Reductive glutamine metabolism by IDH1 mediates lipogenesis under hypoxia. *Nature*, 481(7381):380–384.

Metallo, C. M. and Vander Heiden, M. G. (2013). Understanding metabolic regulation and its influence on cell physiology. *Molecular cell*, 49(3):388–398.

Mitchell, P. (1961). Coupling of phosphorylation to electron and hydrogen transfer by a chemi-osmotic type of mechanism. *Nature*, 191:144–148.

Mo, M. L. and Palsson, B. Ø. (2009). Understanding human metabolic physiology: a genome-to-systems approach. *Trends in biotechnology*, 27(1):37–44.

Mohyeldin, A., Garzón-Muvdi, T., and Quiñones-Hinojosa, A. (2010). Oxygen in stem cell biology: a critical component of the stem cell niche. *Cell stem cell*, 7(2):150–161.

Molinari, F., Kaminska, A., Fiermonte, G., Boddaert, N., Raas-Rothschild, A., Plouin, P., Palmieri, L., Brunelle, F., Palmieri, F., Dulac, O., Munnich, A., and Colleaux, L. (2009). Mutations in the mitochondrial glutamate carrier SLC25A22 in neonatal epileptic encephalopathy with suppression bursts. *Clin. Genet.*, 76(2):188–194.

Molinari, F., Raas-Rothschild, A., Rio, M., Fiermonte, G., Encha-Razavi, F., Palmieri, L., Palmieri, F., Ben-Neriah, Z., Kadhom, N., Vekemans, M., Attie-Bitach, T., Munnich, A., Rustin, P., and Colleaux, L. (2005). Impaired mitochondrial glutamate transport in autosomal recessive neonatal myoclonic epilepsy. *Am. J. Hum. Genet.*, 76(2):334–339.

Mullen, A. R., Wheaton, W. W., Jin, E. S., Chen, P. H., Sullivan, L. B., Cheng, T., Yang, Y., Linehan, W. M., Chandel, N. S., and DeBerardinis, R. J. (2012). Reductive carboxylation supports growth in tumour cells with defective mitochondria. *Nature*, 481(7381):385–388.

Muoio, D. M., Noland, R. C., Kovalik, J. P., Seiler, S. E., Davies, M. N., DeBalsi, K. L., Ilkayeva, O. R., Stevens, R. D., Kheterpal, I., Zhang, J., Covington, J. D., Bajpeyi, S., Ravussin, E., Kraus, W., Koves, T. R., and Mynatt, R. L. (2012). Muscle-specific deletion of carnitine acetyltransferase compromises glucose tolerance and metabolic flexibility. *Cell metabolism*, 15(5):764–777.

Murgia, M., Nagaraj, N., Deshmukh, A. S., Zeiler, M., Cancellara, P., Moretti, I., Reggiani, C., Schiaffino, S., and Mann, M. (2015). Single muscle fiber proteomics reveals unexpected mitochondrial specialization. *EMBO Rep.*, 16(3):387–395.

Murphy, T. A., Dang, C. V., and Young, J. D. (2012). Isotopically nonstationary 13C flux analysis of myc-induced metabolic reprogramming in b-cells. *Metabolic engineering*, 15:206–217.

Nairn, A. V., Kinoshita-Toyoda, A., Toyoda, H., Xie, J., Harris, K., Dalton, S., Kulik, M., Pierce, J., Toida, T., Moremen, K. W., and Linhardt, R. J. (2007). Glycomics of proteoglycan biosynthesis in murine embryonic stem cell differentiation. *Journal of proteome research*, 6(11):4374–4387.

Nakada, D., Saunders, T. L., and Morrison, S. J. (2010). Lkb1 regulates cell cycle and energy metabolism in haematopoietic stem cells. *Nature*, 468(7324):653–658.

Newgard, C. B., An, J., Bain, J. R., Muehlbauer, M. J., Stevens, R. D., Lien, L. F., Haqq, A. M., Shah, S. H., Arlotto, M., Slentz, C. A., Rochon, J., Gallup, D., Ilkayeva, O., Wenner, B. R., Yancy, W. S., Eisenson, H., Musante, G., Surwit, R. S., Millington, D. S., Butler, M. D., and Svetkey, L. P. (2009). A branched-chain amino acid-related metabolic signature that differentiates obese and lean humans and contributes to insulin resistance. *Cell metabolism*, 9(4):311–326.

Nicholls, D. G. (1976). The bioenergetics of brown adipose tissue mitochondria. *FEBS Lett.*, 61(2):103–110.

Odegaard, M. L., Joseph, J. W., Jensen, M. V., Lu, D., Ilkayeva, O., Ronnebaum, S. M., Becker, T. C., and Newgard, C. B. (2010). The mitochondrial 2-oxoglutarate carrier is part of a metabolic pathway that mediates glucose- and glutamine-stimulated insulin secretion. *J. Biol. Chem.*, 285(22):16530–16537.

Ogasawara, M. A. and Zhang, H. (2009). Redox regulation and its emerging roles in stem cells and stem-like cancer cells. *Antioxidants & redox signaling*, 11(5):1107–1122.

O'Rourke, B. (2007). Mitochondrial ion channels. *Annu. Rev. Physiol.*, 69:19–49.

Owusu-Ansah, E. and Banerjee, U. (2009). Reactive oxygen species prime drosophila haematopoietic progenitors for differentiation. *Nature*, 461(7263):537–541.

Ozaki, M., Haga, S., Zhang, H. Q., Irani, K., and Suzuki, S. (2003). Inhibition of hypoxia/reoxygenation-induced oxidative stress in HGF-stimulated antiapoptotic signaling: role of PI3-K and Akt kinase upon rac1. *Cell death and differentiation*, 10(5):508–515.

Palmieri, F. (2013). The mitochondrial transporter family SLC25: identification, properties and physiopathology. *Mol. Aspects Med.*, 34(2-3):465–484.

Palmieri, F., Prezioso, G., Quagliariello, E., and Klingenberg, M. (1971). Kinetic study of the dicarboxylate carrier in rat liver mitochondria. *Eur. J. Biochem.*, 22(1):66–74.

Palmieri, F., Quagliariello, E., and Klingenberger, M. (1972). Kinetics and specificity of the oxoglutarate carrier in rat-liver mitochondria. *Eur. J. Biochem.*, 29(3):408–416.

Palmieri, L., Agrimi, G., Runswick, M. J., Fearnley, I. M., Palmieri, F., and Walker, J. E. (2001a). Identification in Saccharomyces cerevisiae of two isoforms of a novel mitochondrial transporter for 2-oxoadipate and 2-oxoglutarate. *J. Biol. Chem.*, 276(3):1916–1922.

Palmieri, L., De Marco, V., Iacobazzi, V., Palmieri, F., Runswick, M. J., and Walker, J. E. (1997). Identification of the yeast ARG-11 gene as a mitochondrial ornithine carrier involved in arginine biosynthesis. *FEBS Lett.*, 410(2-3):447–451.

Palmieri, L., Palmieri, F., Runswick, M. J., and Walker, J. E. (1996). Identification by bacterial expression and functional reconstitution of the yeast genomic sequence encoding the mitochondrial dicarboxylate carrier protein. *FEBS Lett.*, 399(3):299–302.

Palmieri, L., Pardo, B., Lasorsa, F. M., del Arco, A., Kobayashi, K., Iijima, M., Runswick, M. J., Walker, J. E., Saheki, T., Satrústegui, J., and Palmieri, F. (2001b). Citrin and aralar1 are Ca(2+)-stimulated aspartate/glutamate transporters in mitochondria. *EMBO J.*, 20(18):5060–5069.

Palty, R., Silverman, W. F., Hershfinkel, M., Caporale, T., Sensi, S. L., Parnis, J., Nolte, C., Fishman, D., Shoshan-Barmatz, V., Herrmann, S., Khananshvili, D., and Sekler, I. (2010). NCLX is an essential component of mitochondrial Na+/Ca2+ exchange. *Proc. Natl. Acad. Sci. U.S.A.*, 107(1):436–441.

Panopoulos, A. D., Yanes, O., Ruiz, S., Kida, Y. S., Diep, D., Tautenhahn, R., Herrerías, A., Batchelder, E. M., Plongthongkum, N., Lutz, M., Berggren, W., Zhang, K., Evans, R. M., Siuzdak, G., and Izpisua Belmonte, J. C. (2012). The metabolome of induced pluripotent stem cells reveals metabolic changes occurring in somatic cell reprogramming. *Cell research*, 22(1):168–177.

Papa, S., Francavilla, A., Paradies, G., and Meduri, B. (1971). The transport of pyruvate in rat liver mitochondria. *FEBS letters*, 12(5):285–288.

Papa, S., Lofrumento, N. E., Loglisci, M., and Quagliariello, E. (1969). On the transport of inorganic phosphate and malate in rat-liver mitochondria. *Biochim. Biophys. Acta*, 189(2):311–314.

Papa, S. and Paradies, G. (1974). On the mechanism of translocation of pyruvate and other monocarboxylic acids in rat-liver mitochondria. *European journal of biochemistry*, 49(1):265–274.

Papandreou, I., Cairns, R. A., Fontana, L., Lim, A. L., and Denko, N. C. (2006). HIF-1

mediates adaptation to hypoxia by actively downregulating mitochondrial oxygen consumption. *Cell metabolism*, 3(3):187–197.

Patterson, J. N., Cousteils, K., Lou, J. W., Manning Fox, J. E., MacDonald, P. E., and Joseph, J. W. (2014). Mitochondrial metabolism of pyruvate is essential for regulating glucose-stimulated insulin secretion. *The Journal of biological chemistry*, 289(19):13335–13346.

Pebay-Peyroula, E., Dahout-Gonzalez, C., Kahn, R., Trézéguet, V., Lauquin, G. J., and Brandolin, G. (2003). Structure of mitochondrial ADP/ATP carrier in complex with carboxyatractyloside. *Nature*, 426(6962):39–44.

Perocchi, F., Gohil, V. M., Girgis, H. S., Bao, X. R., McCombs, J. E., Palmer, A. E., and Mootha, V. K. (2010). MICU1 encodes a mitochondrial EF hand protein required for Ca(2+) uptake. *Nature*, 467(7313):291–296.

Pfaff, E., Klingenberg, M., and Heldt, H. W. (1965). Unspecific permeation and specific exchange of adenine nucleotides in liver mitochondria. *Biochim. Biophys. Acta*, 104(1):312–315.

Pivovarova, N. B., Hongpaisan, J., Andrews, S. B., and Friel, D. D. (1999). Depolarization-induced mitochondrial Ca accumulation in sympathetic neurons: spatial and temporal characteristics. *J. Neurosci.*, 19(15):6372–6384.

Plovanich, M., Bogorad, R. L., Sancak, Y., Kamer, K. J., Strittmatter, L., Li, A. A., Girgis, H. S., Kuchimanchi, S., De Groot, J., Speciner, L., Taneja, N., Oshea, J., Koteliansky, V., and Mootha, V. K. (2013). MICU2, a paralog of MICU1, resides within the mitochondrial uniporter complex to regulate calcium handling. *PLoS ONE*, 8(2):e55785.

Pollak, J. K. and Sutton, R. (1980). The transport and accumulation of adenine nucleotides during mitochondrial biogenesis. *Biochem. J.*, 192(1):75–83.

Porcelli, V., Fiermonte, G., Longo, A., and Palmieri, F. (2014). The human gene SLC25A29, of solute carrier family 25, encodes a mitochondrial transporter of basic amino acids. *J. Biol. Chem.*, 289(19):13374–13384.

Possemato, R., Marks, K. M., Shaul, Y. D., Pacold, M. E., Kim, D., Birsoy, K., Sethumadhavan, S., Woo, H. K., Jang, H. G., Jha, A. K., Chen, W. W., Barrett, F. G., Stransky, N., Tsun, Z. Y., Cowley, G. S., Barretina, J., Kalaany, N. Y., Hsu, P. P., Ottina, K., Chan, A. M., Yuan, B., Garraway, L. A., Root, D. E., Mino-Kenudson, M., Brachtel, E. F., Driggers, E. M., and Sabatini, D. M. (2011). Functional genomics reveal that the serine synthesis pathway is essential in breast cancer. *Nature*, 476(7360):346–350.

Prigione, A. and Adjaye, J. (2010). Modulation of mitochondrial biogenesis and bioenergetic metabolism upon in vitro and in vivo differentiation of human ES and iPS cells. *The International journal of developmental biology*, 54(11-12):1729–1741.

Prigione, A., Fauler, B., Lurz, R., Lehrach, H., and Adjaye, J. (2010). The senescence-related mitochondrial/oxidative stress pathway is repressed in human induced pluripotent stem cells. *Stem cells*, 28(4):721–733.

Prigione, A., Lichtner, B., Kuhl, H., Struys, E. A., Wamelink, M., Lehrach, H., Ralser, M., Timmermann, B., and Adjaye, J. (2011). Human induced pluripotent stem cells harbor homoplasmic and heteroplasmic mitochondrial DNA mutations while maintaining human embryonic stem cell-like metabolic reprogramming. *Stem cells*, 29(9):1338–1348.

Prohl, C., Pelzer, W., Diekert, K., Kmita, H., Bedekovics, T., Kispal, G., and Lill, R. (2001). The yeast mitochondrial carrier Leu5p and its human homologue Graves' disease protein are required for accumulation of coenzyme A in the matrix. *Mol. Cell. Biol.*, 21(4):1089–1097.

Puskin, J. S., Gunter, T. E., Gunter, K. K., and Russell, P. R. (1976). Evidence for more than one Ca2+ transport mechanism in mitochondria. *Biochemistry*, 15(17):3834–3842.

Qian, T., Herman, B., and Lemasters, J. J. (1999). The mitochondrial permeability transition mediates both necrotic and apoptotic death of hepatocytes exposed to Br-A23187. *Toxicol. Appl. Pharmacol.*, 154(2):117–125.

Quek, L. E., Dietmair, S., Krömer, J. O., and Nielsen, L. K. (2010). Metabolic flux analysis in mammalian cell culture. *Metabolic engineering*, 12(2):161–171.

Rathmell, J. C., Vander Heiden, M. G., Harris, M. H., Frauwirth, K. A., and Thompson, C. B. (2000). In the absence of extrinsic signals, nutrient utilization by lymphocytes is insufficient to maintain either cell size or viability. *Molecular cell*, 6(3):683–692.

Rizzuto, R., De Stefani, D., Raffaello, A., and Mammucari, C. (2012). Mitochondria as sensors and regulators of calcium signalling. *Nat. Rev. Mol. Cell Biol.*, 13(9):566–578.

Rohatgi, N., Aly, H., Marshall, C. A., McDonald, W. G., Kletzien, R. F., Colca, J. R., and McDaniel, M. L. (2013). Novel insulin sensitizer modulates nutrient sensing pathways and maintains β-cell phenotype in human islets. *PLoS ONE*, 8(5):e62012.

Rosenberg, M. J., Agarwala, R., Bouffard, G., Davis, J., Fiermonte, G., Hilliard, M. S., Koch, T., Kalikin, L. M., Makalowska, I., Morton, D. H., Petty, E. M., Weber, J. L., Palmieri, F., Kelley, R. I., Schäffer, A. A., and Biesecker, L. G. (2002). Mutant deoxynucleotide carrier is associated with congenital microcephaly. *Nat. Genet.*, 32(1):175–179.

Rosenthal, J., Angel, A., and Farkas, J. (1974). Metabolic fate of leucine: a significant sterol precursor in adipose tissue and muscle. *The American journal of physiology*, 226(2):411–418.

Rottenberg, H. and Scarpa, A. (1974). Calcium uptake and membrane potential in mitochondria. *Biochemistry*, 13(23):4811–4817.

Runswick, M. J., Walker, J. E., Bisaccia, F., Iacobazzi, V., and Palmieri, F. (1990). Sequence of the bovine 2-oxoglutarate/malate carrier protein: structural relationship to other mitochondrial transport proteins. *Biochemistry*, 29(50):11033–11040.

Safiulina, D., Veksler, V., Zharkovsky, A., and Kaasik, A. (2006). Loss of mitochondrial membrane potential is associated with increase in mitochondrial volume: physiological role in neurones. *J. Cell. Physiol.*, 206(2):347–353.

Saha, K., Mei, Y., Reisterer, C. M., Pyzocha, N. K., Yang, J., Muffat, J., Davies, M. C.,

Alexander, M. R., Langer, R., Anderson, D. G., and Jaenisch, R. (2011). Surface-engineered substrates for improved human pluripotent stem cell culture under fully defined conditions. *Proc. Natl. Acad. Sci. U.S.A.*, 108(46):18714–18719.

Sales, S. D., Hoggard, P. G., Sunderland, D., Khoo, S., Hart, C. A., and Back, D. J. (2001). Zidovudine phosphorylation and mitochondrial toxicity in vitro. *Toxicol. Appl. Pharmacol.*, 177(1):54–58.

Sancak, Y., Markhard, A. L., Kitami, T., Kovács-Bogdán, E., Kamer, K. J., Udeshi, N. D., Carr, S. A., Chaudhuri, D., Clapham, D. E., Li, A. A., Calvo, S. E., Goldberger, O., and Mootha, V. K. (2013). EMRE is an essential component of the mitochondrial calcium uniporter complex. *Science*, 342(6164):1379–1382.

Sandor, A., Johnson, J. H., and Srere, P. A. (1994). Cooperation between enzyme and transporter in the inner mitochondrial membrane of yeast. Requirement for mitochondrial citrate synthase for citrate and malate transport in Saccharomyces cerevisiae. *J. Biol. Chem.*, 269(47):29609–29612.

Saretzki, G., Armstrong, L., Leake, A., Lako, M., and von Zglinicki, T. (2004). Stress defense in murine embryonic stem cells is superior to that of various differentiated murine cells. *Stem cells*, 22(6):962–971.

Satrústegui, J., Contreras, L., Ramos, M., Marmol, P., del Arco, A., Saheki, T., and Pardo, B. (2007). Role of aralar, the mitochondrial transporter of aspartate-glutamate, in brain N-acetylaspartate formation and Ca(2+) signaling in neuronal mitochondria. *J. Neurosci. Res.*, 85(15):3359–3366.

Sauer, H., Rahimi, G., Hescheler, J., and Wartenberg, M. (2000). Role of reactive oxygen species and phosphatidylinositol 3-kinase in cardiomyocyte differentiation of embryonic stem cells. *FEBS letters*, 476(3):218–223.

Schafer, Z. T., Grassian, A. R., Song, L., Jiang, Z., Gerhart-Hines, Z., Irie, H. Y., Gao, S., Puigserver, P., and Brugge, J. S. (2009). Antioxidant and oncogene rescue of metabolic defects caused by loss of matrix attachment. *Nature*, 461(7260):109–113.

Schell, J. C., Olson, K. A., Jiang, L., Hawkins, A. J., Van Vranken, J. G., Xie, J., Egnatchik, R. A., Earl, E. G., DeBerardinis, R. J., and Rutter, J. (2014). A role for the mitochondrial pyruvate carrier as a repressor of the Warburg effect and colon cancer cell growth. *Mol. Cell*, 56(3):400–413.

Schieke, S. M., Ma, M., Cao, L., McCoy, J. P., Liu, C., Hensel, N. F., Barrett, A., Boehm, M., and Finkel, T. (2008). Mitochondrial metabolism modulates differentiation and teratoma formation capacity in mouse embryonic stem cells. *The Journal of biological chemistry*, 283(42):28506–28512.

Schieke, S. M., Phillips, D., McCoy, J. P., Aponte, A. M., Shen, R. F., Balaban, R. S., and Finkel, T. (2006). The mammalian target of rapamycin (mTOR) pathway regulates mitochondrial oxygen consumption and oxidative capacity. *The Journal of biological chemistry*, 281(37):27643–27652.

Scott, D. A., Richardson, A. D., Filipp, F. V., Knutzen, C. A., Chiang, G. G., Ronai, Z. A., Osterman, A. L., and Smith, J. W. (2011). Comparative metabolic flux profiling of melanoma cell lines: beyond the warburg effect. *The Journal of biological chemistry*, 286(49):42626–42634.

Sekoguchi, E., Sato, N., Yasui, A., Fukada, S., Nimura, Y., Aburatani, H., Ikeda, K., and Matsuura, A. (2003). A novel mitochondrial carnitine-acylcarnitine translocase induced by partial hepatectomy and fasting. *J. Biol. Chem.*, 278(40):38796–38802.

Semenza, G. L. (2009). Regulation of cancer cell metabolism by hypoxia-inducible factor 1. *Semin. Cancer Biol.*, 19(1):12–16.

Sepúlveda, D. E. E., Andrews, B. A., Papoutsakis, E. T., and Asenjo, J. A. (2010). Metabolic flux analysis of embryonic stem cells using three distinct differentiation protocols and comparison to gene expression patterns. *Biotechnology progress*, 26(5):1222–1229.

Shackelford, D. B. and Shaw, R. J. (2009). The LKB1-AMPK pathway: metabolism and growth control in tumour suppression. *Nature reviews. Cancer*, 9(8):563–575.

Shackleton, M., Vaillant, F., Simpson, K. J., Stingl, J., Smyth, G. K., Asselin-Labat, M. L., Wu, L., Lindeman, G. J., and Visvader, J. E. (2006). Generation of a functional mammary gland from a single stem cell. *Nature*, 439(7072):84–88.

Shaw, G. C., Cope, J. J., Li, L., Corson, K., Hersey, C., Ackermann, G. E., Gwynn, B., Lambert, A. J., Wingert, R. A., Traver, D., Trede, N. S., Barut, B. A., Zhou, Y., Minet, E., Donovan, A., Brownlie, A., Balzan, R., Weiss, M. J., Peters, L. L., Kaplan, J., Zon, L. I., and Paw, B. H. (2006). Mitoferrin is essential for erythroid iron assimilation. *Nature*, 440(7080):96–100.

Simsek, T., Kocabas, F., Zheng, J., Deberardinis, R. J., Mahmoud, A. I., Olson, E. N., Schneider, J. W., Zhang, C. C., and Sadek, H. A. (2010). The distinct metabolic profile of hematopoietic stem cells reflects their location in a hypoxic niche. *Cell stem cell*, 7(3):380–390.

Smith, K. N., Lim, J. M., Wells, L., and Dalton, S. (2011). Myc orchestrates a regulatory network required for the establishment and maintenance of pluripotency. *Cell cycle*, 10(4):592–597.

Spaan, A. N., Ijlst, L., van Roermund, C. W., Wijburg, F. A., Wanders, R. J., and Waterham, H. R. (2005). Identification of the human mitochondrial FAD transporter and its potential role in multiple acyl-CoA dehydrogenase deficiency. *Mol. Genet. Metab.*, 86(4):441–447.

Spangrude, G. J., Heimfeld, S., and Weissman, I. L. (1988). Purification and characterization of mouse hematopoietic stem cells. *Science*, 241(4861):58–62.

Sreekumar, A., Poisson, L. M., Rajendiran, T. M., Khan, A. P., Cao, Q., Yu, J., Laxman, B., Mehra, R., Lonigro, R. J., Li, Y., Nyati, M. K., Ahsan, A., Kalyana-Sundaram, S., Han, B., Cao, X., Byun, J., Omenn, G. S., Ghosh, D., Pennathur, S., Alexander, D. C., Berger, A., Shuster, J. R., Wei, J. T., Varambally, S., Beecher, C., and Chinnaiyan, A. M. (2009). Metabolomic profiles delineate potential role for sarcosine in prostate cancer progression. *Nature*, 457(7231):910–914.

Stappen, R. and Krämer, R. (1994). Kinetic mechanism of phosphate/phosphate and phosphate/OH- antiports catalyzed by reconstituted phosphate carrier from beef heart mitochondria. *J. Biol. Chem.*, 269(15):11240–11246.

Stepien, G., Torroni, A., Chung, A. B., Hodge, J. A., and Wallace, D. C. (1992). Differential expression of adenine nucleotide translocator isoforms in mammalian tissues and during muscle cell differentiation. *J. Biol. Chem.*, 267(21):14592–14597.

Stingl, J., Eirew, P., Ricketson, I., Shackleton, M., Vaillant, F., Choi, D., Li, H. I., and Eaves, C. J. (2006). Purification and unique properties of mammary epithelial stem cells. *Nature*, 439(7079):993–997.

Stipani, I., Krämer, R., Palmieri, F., and Klingenberg, M. (1980). Citrate transport in liposomes reconstituted with triton extracts from mitochondria. *Biochem. Biophys. Res. Commun.*, 97(3):1206–1214.

Strauss, K. A., DuBiner, L., Simon, M., Zaragoza, M., Sengupta, P. P., Li, P., Narula, N., Dreike, S., Platt, J., Procaccio, V., Ortiz-González, X. R., Puffenberger, E. G., Kelley, R. I., Morton, D. H., Narula, J., and Wallace, D. C. (2013). Severity of cardiomyopathy associated with adenine nucleotide translocator-1 deficiency correlates with mtDNA haplogroup. *Proc. Natl. Acad. Sci. U.S.A.*, 110(9):3453–3458.

Stuart, J. A., Harper, J. A., Brindle, K. M., Jekabsons, M. B., and Brand, M. D. (2001). Physiological levels of mammalian uncoupling protein 2 do not uncouple yeast mitochondria. *J. Biol. Chem.*, 276(21):18633–18639.

Stumvoll, M., Perriello, G., Meyer, C., and Gerich, J. (1999). Role of glutamine in human carbohydrate metabolism in kidney and other tissues. *Kidney Int.*, 55(3):778–792.

Su, A. I., Wiltshire, T., Batalov, S., Lapp, H., Ching, K. A., Block, D., Zhang, J., Soden, R., Hayakawa, M., Kreiman, G., Cooke, M. P., Walker, J. R., and Hogenesch, J. B. (2004). A gene atlas of the mouse and human protein-encoding transcriptomes. *Proc. Natl. Acad. Sci. U.S.A.*, 101(16):6062–6067.

Sugden, M. C., Zariwala, M. G., and Holness, M. J. (2009). PPARs and the orchestration of metabolic fuel selection. *Pharmacological research*, 60(3):141–150.

Takahashi, K., Tanabe, K., Ohnuki, M., Narita, M., Ichisaka, T., Tomoda, K., and Yamanaka, S. (2007). Induction of pluripotent stem cells from adult human fibroblasts by defined factors. *Cell*, 131(5):861–872.

Takubo, K., Goda, N., Yamada, W., Iriuchishima, H., Ikeda, E., Kubota, Y., Shima, H., Johnson, R. S., Hirao, A., Suematsu, M., and Suda, T. (2010). Regulation of the HIF-1alpha level is essential for hematopoietic stem cells. *Cell stem cell*, 7(3):391–402.

Tennant, D. A., Durán, R. V., and Gottlieb, E. (2010). Targeting metabolic transformation for cancer therapy. *Nature reviews. Cancer*, 10(4):267–277.

Territo, P. R., French, S. A., Dunleavy, M. C., Evans, F. J., and Balaban, R. S. (2001). Calcium

activation of heart mitochondrial oxidative phosphorylation: rapid kinetics of mVO2, NADH, AND light scattering. *J. Biol. Chem.*, 276(4):2586–2599.

Thomson, J. A., Itskovitz-Eldor, J., Shapiro, S. S., Waknitz, M. A., Swiergiel, J. J., Marshall, V. S., and Jones, J. M. (1998). Embryonic stem cell lines derived from human blastocysts. *Science*, 282(5391):1145–1147.

Thornburg, J. M., Nelson, K. K., Clem, B. F., Lane, A. N., Arumugam, S., Simmons, A., Eaton, J. W., Telang, S., and Chesney, J. (2008). Targeting aspartate aminotransferase in breast cancer. *Breast Cancer Res.*, 10(5):R84.

Timón-Gómez, A., Proft, M., and Pascual-Ahuir, A. (2013). Differential regulation of mitochondrial pyruvate carrier genes modulates respiratory capacity and stress tolerance in yeast. *PLoS ONE*, 8(11):e79405.

Titus, S. A. and Moran, R. G. (2000). Retrovirally mediated complementation of the glyB phenotype. Cloning of a human gene encoding the carrier for entry of folates into mitochondria. *J. Biol. Chem.*, 275(47):36811–36817.

Tormos, K. V., Anso, E., Hamanaka, R. B., Eisenbart, J., Joseph, J., Kalyanaraman, B., and Chandel, N. S. (2011). Mitochondrial complex III ROS regulate adipocyte differentiation. *Cell metabolism*, 14(4):537–544.

Tothova, Z., Kollipara, R., Huntly, B. J., Lee, B. H., Castrillon, D. H., Cullen, D. E., McDowell, E. P., Lazo-Kallanian, S., Williams, I. R., Sears, C., Armstrong, S. A., Passegué, E., DePinho, R. A., and Gilliland, D. G. (2007). FoxOs are critical mediators of hematopoietic stem cell resistance to physiologic oxidative stress. *Cell*, 128(2):325–339.

Traba, J., Del Arco, A., Duchen, M. R., Szabadkai, G., and Satrústegui, J. (2012). SCaMC-1 promotes cancer cell survival by desensitizing mitochondrial permeability transition via ATP/ADP-mediated matrix Ca(2+) buffering. *Cell Death Differ.*, 19(4):650–660.

Tritsch, G. L. and Moore, G. E. (1962). Spontaneous decomposition of glutamine in cell culture media. *Experimental cell research*, 28:360–364.

Vacanti, N. M., Divakaruni, A. S., Green, C. R., Parker, S. J., Henry, R. R., Ciaraldi, T. P., Murphy, A. N., and Metallo, C. M. (2014). Regulation of substrate utilization by the mitochondrial pyruvate carrier. *Mol. Cell*, 56(3):425–435.

Vacanti, N. M., Divakaruni, A. S., Murphy, A. N., and Metallo, C. M. (nd). Identification of a mitochondrial glutamine carrier. Unpublished.

van de Poll, M. C., Soeters, P. B., Deutz, N. E., Fearon, K. C., and Dejong, C. H. (2004). Renal metabolism of amino acids: its role in interorgan amino acid exchange. *Am. J. Clin. Nutr.*, 79(2):185–197.

Vander Heiden, M. G., Cantley, L. C., and Thompson, C. B. (2009). Understanding the warburg effect: the metabolic requirements of cell proliferation. *Science*, 324(5930):1029–1033.

Vander Heiden, M. G., Plas, D. R., Rathmell, J. C., Fox, C. J., Harris, M. H., and Thompson,

C. B. (2001). Growth factors can influence cell growth and survival through effects on glucose metabolism. *Molecular and cellular biology*, 21(17):5899–5912.

Varum, S., Rodrigues, A. S., Moura, M. B., Momcilovic, O., Easley, C. A., Ramalho-Santos, J., Van Houten, B., and Schatten, G. (2011). Energy metabolism in human pluripotent stem cells and their differentiated counterparts. *PloS one*, 6(6):e20914.

Vieira, H. L., Alves, P. M., and Vercelli, A. (2011). Modulation of neuronal stem cell differentiation by hypoxia and reactive oxygen species. *Progress in neurobiology*, 93(3):444–455.

Vigueira, P. A., McCommis, K. S., Schweitzer, G. G., Remedi, M. S., Chambers, K. T., Fu, X., McDonald, W. G., Cole, S. L., Colca, J. R., Kletzien, R. F., Burgess, S. C., and Finck, B. N. (2014). Mitochondrial pyruvate carrier 2 hypomorphism in mice leads to defects in glucose-stimulated insulin secretion. *Cell reports*, 7(6):2042–2053.

Vozza, A., Parisi, G., De Leonardis, F., Lasorsa, F. M., Castegna, A., Amorese, D., Marmo, R., Calcagnile, V. M., Palmieri, L., Ricquier, D., Paradies, E., Scarcia, P., Palmieri, F., Bouillaud, F., and Fiermonte, G. (2014). UCP2 transports C4 metabolites out of mitochondria, regulating glucose and glutamine oxidation. *Proc. Natl. Acad. Sci. U.S.A.*, 111(3):960–965.

Wang, J. B., Erickson, J. W., Fuji, R., Ramachandran, S., Gao, P., Dinavahi, R., Wilson, K. F., Ambrosio, A. L., Dias, S. M., Dang, C. V., and Cerione, R. A. (2010). Targeting mitochondrial glutaminase activity inhibits oncogenic transformation. *Cancer Cell*, 18(3):207–219.

Wang, J. C. and Dick, J. E. (2005). Cancer stem cells: lessons from leukemia. *Trends in cell biology*, 15(9):494–501.

Wang, N., Xie, K., Huo, S., Zhao, J., Zhang, S., and Miao, J. (2007). Suppressing phosphatidylcholine-specific phospholipase c and elevating ROS level, NADPH oxidase activity and rb level induced neuronal differentiation in mesenchymal stem cells. *Journal of cellular biochemistry*, 100(6):1548–1557.

Wang, T. J., Larson, M. G., Vasan, R. S., Cheng, S., Rhee, E. P., Elizabeth, M., Lewis, G. D., Fox, C. S., Jacques, P. F., Fernandez, C., O'Donnell, C. J., Carr, S. A., Mootha, V. K., Florez, J. C., Souza, A., Melander, O., Clish, C. B., and Gerszten, R. E. (2011). Metabolite profiles and the risk of developing diabetes. *Nature medicine*, 17(4):448–453.

Ward, P. S., Patel, J., Wise, D. R., Abdel-Wahab, O., Bennett, B. D., Coller, H. A., Cross, J. R., Fantin, V. R., Hedvat, C. V., Perl, A. E., Rabinowitz, J. D., Carroll, M., Su, S. M., Sharp, K. A., Levine, R. L., and Thompson, C. B. (2010). The common feature of leukemia-associated IDH1 and IDH2 mutations is a neomorphic enzyme activity converting alpha-ketoglutarate to 2-hydroxyglutarate. *Cancer cell*, 17(3):225–234.

Weinberg, F., Hamanaka, R., Wheaton, W. W., Weinberg, S., Joseph, J., Lopez, M., Kalyanaraman, B., Mutlu, G. M., Budinger, G. R., and Chandel, N. S. (2010). Mitochondrial metabolism and ROS generation are essential for kras-mediated tumorigenicity. *Proc. Natl. Acad. Sci. U.S.A.*, 107(19):8788–8793.

Wellen, K. E., Hatzivassiliou, G., Sachdeva, U. M., Bui, T. V., Cross, J. R., and Thompson,

C. B. (2009). ATP-citrate lyase links cellular metabolism to histone acetylation. *Science*, 324(5930):1076–1080.

Wellen, K. E., Lu, C., Mancuso, A., Lemons, J. M., Ryczko, M., Dennis, J. W., Rabinowitz, J. D., Coller, H. A., and Thompson, C. B. (2010). The hexosamine biosynthetic pathway couples growth factor-induced glutamine uptake to glucose metabolism. *Genes & development*, 24(24):2784–2799.

West, A. K., Hidalgo, J., Eddins, D., Levin, E. D., and Aschner, M. (2008). Metallothionein in the central nervous system: Roles in protection, regeneration and cognition. *Neurotoxicology*, 29(3):489–503.

Wilkins, H. M., Kirchhof, D., Manning, E., Joseph, J. W., and Linseman, D. A. (2013). Mitochondrial glutathione transport is a key determinant of neuronal susceptibility to oxidative and nitrosative stress. *J. Biol. Chem.*, 288(7):5091–5101.

Wise, D. R. and Thompson, C. B. (2010). Glutamine addiction: a new therapeutic target in cancer. *Trends Biochem. Sci.*, 35(8):427–433.

Wise, D. R., Ward, P. S., Shay, J. E., Cross, J. R., Gruber, J. J., Sachdeva, U. M., Platt, J. M., DeMatteo, R. G., Simon, M. C., and Thompson, C. B. (2011). Hypoxia promotes isocitrate dehydrogenase-dependent carboxylation of α-ketoglutarate to citrate to support cell growth and viability. *Proc. Natl. Acad. Sci. U.S.A.*, 108(49):19611–19616.

Wong, D. J., Liu, H., Ridky, T. W., Cassarino, D., Segal, E., and Chang, H. Y. (2008). Module map of stem cell genes guides creation of epithelial cancer stem cells. *Cell stem cell*, 2(4):333–344.

Wu, C., Orozco, C., Boyer, J., Leglise, M., Goodale, J., Batalov, S., Hodge, C. L., Haase, J., Janes, J., Huss, J. W., and Su, A. I. (2009). BioGPS: an extensible and customizable portal for querying and organizing gene annotation resources. *Genome Biol.*, 10(11):R130.

Yanes, O., Clark, J., Wong, D. M., Patti, G. J., Sánchez-Ruiz, A., Benton, H. P., Trauger, S. A., Desponts, C., Ding, S., and Siuzdak, G. (2010). Metabolic oxidation regulates embryonic stem cell differentiation. *Nature chemical biology*, 6(6):411–417.

Yang, B., Zhao, D., and Verkman, A. S. (2006). Evidence against functionally significant aquaporin expression in mitochondria. *J. Biol. Chem.*, 281(24):16202–16206.

Yang, C., Ko, B., Hensley, C. T., Jiang, L., Wasti, A. T., Kim, J., Sudderth, J., Calvaruso, M. A., Lumata, L., Mitsche, M., Rutter, J., Merritt, M. E., and DeBerardinis, R. J. (2014). Glutamine oxidation maintains the TCA cycle and cell survival during impaired mitochondrial pyruvate transport. *Mol. Cell*, 56(3):414–424.

Yao, J., Rettberg, J. R., Klosinski, L. P., Cadenas, E., and Brinton, R. D. (2011). Shift in brain metabolism in late onset alzheimer's disease: implications for biomarkers and therapeutic interventions. *Molecular aspects of medicine*, 32(4-6):247–257.

Ye, J., Mancuso, A., Tong, X., Ward, P. S., Fan, J., Rabinowitz, J. D., and Thompson, C. B.

(2012). Pyruvate kinase m2 promotes de novo serine synthesis to sustain mTORC1 activity and cell proliferation. *Proc. Natl. Acad. Sci. U.S.A.*, 109(18):6904–6909.

Ye, Y. L., Chan, Y. T., Liu, H. C., Lu, H. T., and Huang, R. F. (2010). Depleted folate pool and dysfunctional mitochondria associated with defective mitochondrial folate proteins sensitize Chinese ovary cell mutants to tert-butylhydroperoxide-induced oxidative stress and apoptosis. *J. Nutr. Biochem.*, 21(9):793–800.

Yoo, H., Antoniewicz, M. R., Stephanopoulos, G., and Kelleher, J. K. (2008). Quantifying reductive carboxylation flux of glutamine to lipid in a brown adipocyte cell line. *The Journal of biological chemistry*, 283(30):20621–20627.

Yoshida, Y., Takahashi, K., Okita, K., Ichisaka, T., and Yamanaka, S. (2009). Hypoxia enhances the generation of induced pluripotent stem cells. *Cell stem cell*, 5(3):237–241.

Young, J. D. (2014). INCA: a computational platform for isotopically non-stationary metabolic flux analysis. *Bioinformatics*, 30(9):1333–1335.

Yu, X. X., Mao, W., Zhong, A., Schow, P., Brush, J., Sherwood, S. W., Adams, S. H., and Pan, G. (2000). Characterization of novel UCP5/BMCP1 isoforms and differential regulation of UCP4 and UCP5 expression through dietary or temperature manipulation. *FASEB J.*, 14(11):1611–1618.

Yun, D. H., Song, H. Y., Lee, M. J., Kim, M. R., Kim, M. Y., Lee, J. S., and Kim, J. H. (2009a). Thromboxane a(2) modulates migration, proliferation, and differentiation of adipose tissue-derived mesenchymal stem cells. *Experimental & molecular medicine*, 41(1):17–24.

Yun, S. P., Lee, M. Y., Ryu, J. M., and Han, H. J. (2009b). Interaction between PGE2 and EGF receptor through MAPKs in mouse embryonic stem cell proliferation. *Cellular and molecular life sciences*, 66(9):1603–1616.

Zamboni, N. (2011). 13C metabolic flux analysis in complex systems. *Current opinion in biotechnology*, 22(1):103–108.

Zamboni, N., Fendt, S. M., Rühl, M., and Sauer, U. (2008). (13)C-based metabolic flux analysis. *Nature protocols*, 4(6):878–892.

Zara, V. and Gnoni, G. V. (1995). Effect of starvation on the activity of the mitochondrial tricarboxylate carrier. *Biochim. Biophys. Acta*, 1239(1):33–38.

Zarrilli, R., Oates, E. L., McBride, O. W., Lerman, M. I., Chan, J. Y., Santisteban, P., Ursini, M. V., Notkins, A. L., and Kohn, L. D. (1989). Sequence and chromosomal assignment of a novel cDNA identified by immunoscreening of a thyroid expression library: similarity to a family of mitochondrial solute carrier proteins. *Mol. Endocrinol.*, 3(9):1498–1505.

Zhang, C. Y., Baffy, G., Perret, P., Krauss, S., Peroni, O., Grujic, D., Hagen, T., Vidal-Puig, A. J., Boss, O., Kim, Y. B., Zheng, X. X., Wheeler, M. B., Shulman, G. I., Chan, C. B., and Lowell, B. B. (2001). Uncoupling protein-2 negatively regulates insulin secretion and is a major link between obesity, beta cell dysfunction, and type 2 diabetes. *Cell*, 105(6):745–755.

Zhang, J., Khvorostov, I., Hong, J. S., Oktay, Y., Vergnes, L., Nuebel, E., Wahjudi, P. N., Setoguchi, K., Wang, G., Do, A., Jung, H. J., McCaffery, J. M., Kurland, I. J., Reue, K., Lee, W. N. P., Koehler, C. M., and Teitell, M. A. (2011). UCP2 regulates energy metabolism and differentiation potential of human pluripotent stem cells. *The EMBO journal*, 30(24):4860–4873.

Zhang, W. C., Shyh-Chang, N., Yang, H., Rai, A., Umashankar, S., Ma, S., Soh, B. S., Sun, L. L., Tai, B. C., Nga, M. E., Bhakoo, K. K., Jayapal, S. R., Nichane, M., Yu, Q., Ahmed, D. A., Tan, C., Sing, W. P., Tam, J., Thirugananam, A., Noghabi, M. S., Pang, Y. H., Ang, H. S., Mitchell, W., Robson, P., Kaldis, P., Soo, R. A., Swarup, S., Lim, E. H., and Lim, B. (2012). Glycine decarboxylase activity drives non-small cell lung cancer tumor-initiating cells and tumorigenesis. *Cell*, 148(1-2):259–272.

Zhou, J., Su, P., Wang, L., Chen, J., Zimmermann, M., Genbacev, O., Afonja, O., Horne, M. C., Tanaka, T., Duan, E., Fisher, S. J., Liao, J., Chen, J., and Wang, F. (2009). mTOR supports long-term self-renewal and suppresses mesoderm and endoderm activities of human embryonic stem cells. *Proc. Natl. Acad. Sci. U.S.A.*, 106(19):7840–7845.

Zhu, S., Li, W., Zhou, H., Wei, W., Ambasudhan, R., Lin, T., Kim, J., Zhang, K., and Ding, S. (2010). Reprogramming of human primary somatic cells by OCT4 and chemical compounds. *Cell stem cell*, 7(6):651–655.

Zotova, L., Aleschko, M., Sponder, G., Baumgartner, R., Reipert, S., Prinz, M., Schweyen, R. J., and Nowikovsky, K. (2010). Novel components of an active mitochondrial K+/H+ exchange. *Journal of Biological Chemistry*, 285(19):14399–14414.